

INFORMATION TO USERS

This manuscript has been reproduced from the microfilm master. UMI films the text directly from the original or copy submitted. Thus, some thesis and dissertation copies are in typewriter face, while others may be from any type of computer printer.

The quality of this reproduction is dependent upon the quality of the copy submitted. Broken or indistinct print, colored or poor quality illustrations and photographs, print bleedthrough, substandard margins, and improper alignment can adversely affect reproduction.

In the unlikely event that the author did not send UMI a complete manuscript and there are missing pages, these will be noted. Also, if unauthorized copyright material had to be removed, a note will indicate the deletion.

Oversize materials (e.g., maps, drawings, charts) are reproduced by sectioning the original, beginning at the upper left-hand corner and continuing from left to right in equal sections with small overlaps. Each original is also photographed in one exposure and is included in reduced form at the back of the book.

Photographs included in the original manuscript have been reproduced xerographically in this copy. Higher quality 6" x 9" black and white photographic prints are available for any photographs or illustrations appearing in this copy for an additional charge. Contact UMI directly to order.

UMI

A Bell & Howell Information Company
300 North Zeeb Road, Ann Arbor MI 48106-1346 USA
313/761-4700 800/521-0600

University of Alberta

Analysis of substrates for DMSO reductase from *Escherichia coli*

by

Pavel Badalov



A thesis submitted to the Faculty of Graduate Studies and Research in partial fulfillment
of the requirements for a degree of Master of Science

Department of Biochemistry

Edmonton, Alberta

Fall 1998



National Library
of Canada

Acquisitions and
Bibliographic Services

395 Wellington Street
Ottawa ON K1A 0N4
Canada

Bibliothèque nationale
du Canada

Acquisitions et
services bibliographiques

395, rue Wellington
Ottawa ON K1A 0N4
Canada

Your file Votre référence

Our file Notre référence

The author has granted a non-exclusive licence allowing the National Library of Canada to reproduce, loan, distribute or sell copies of this thesis in microform, paper or electronic formats.

The author retains ownership of the copyright in this thesis. Neither the thesis nor substantial extracts from it may be printed or otherwise reproduced without the author's permission.

L'auteur a accordé une licence non exclusive permettant à la Bibliothèque nationale du Canada de reproduire, prêter, distribuer ou vendre des copies de cette thèse sous la forme de microfiche/film, de reproduction sur papier ou sur format électronique.

L'auteur conserve la propriété du droit d'auteur qui protège cette thèse. Ni la thèse ni des extraits substantiels de celle-ci ne doivent être imprimés ou autrement reproduits sans son autorisation.

0-612-34332-4

Canada

UNIVERSITY OF ALBERTA

Library Release Form

Name of Author: Pavel R. Badalov
Title of Thesis: Analysis of substrates for DMSO reductase from
Escherichia coli
Degree: Master of Science
Year this Degree Granted: 1998

Permission is hereby granted to the University of Alberta Library to reproduce single copies of this thesis and to lend or sell such copies for private, scholarly, or scientific research purposes only.

The author reserves all other publication and other rights in association with the copyright in the thesis, and except as hereinbefore provided, neither the thesis nor any substantial portion thereof may be printed or otherwise reproduced in any material form whatever without the author's prior written permission.

23 September 1998

Pavel Badalov
517 Michener Park

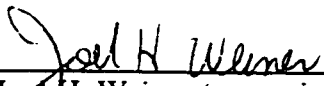
Edmonton, Alberta

T6H 4M5

UNIVERSITY OF ALBERTA

FACULTY OF GRADUATE STUDIES AND RESEARCH

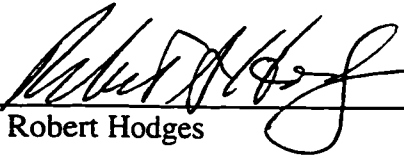
The undersigned certify that they have read, and recommend to the Faculty of Graduate Studies and Research for acceptance, a thesis entitled ANALYSIS OF SUBSTRATES FOR DMSO REDUCTASE FROM *ESCHERICHIA COLI* submitted by PAVEL R. BADALOV in partial fulfillment of the requirements for the degree of MASTER OF SCIENCE.




Dr. Joel H. Weiner (supervisor)



Dr. Carol Cass



Dr. Robert Hodges



Dr. Rakesh Kumar

SEPT. 17, 1998

Abstract

A number of quinones, sulfoxides and amine oxides were chemically synthesized and tested as substrates for or inhibitors of *Escherichia coli* dimethyl sulfoxide (DMSO) reductase.

Methyl *p*-tolyl sulfoxide was reduced by DMSO reductase with a high stereospecificity, the (*R*)-enantiomer being the substrate. The (*S*)-isomer was neither a substrate nor an inhibitor of the enzyme. This specificity distinguishes *E.coli* DMSO reductase from the corresponding enzyme from *Rhodobacter sphaeroides* and suggests a different organization of the molybdenum cofactor in the enzyme active site.

The increase in volume of substituent groups in dialkyl sulfoxides led to the decrease of the binding affinity of a substrate to the enzyme, and dipropyl sulfoxide was not reduced.

When reduced benzyl viologen was used as electron donor, some aliphatic amine oxides, unlike aromatic N-oxides and sulfoxides, did not follow the Michaelis-Menten kinetics.

The reduced form of 3-amino-2-methyl-1,4-naphthoquinone (AMNQH₂) can be easily synthesized and possesses valuable physico-chemical properties such as solubility in water and absorption in the visible range in the oxidized but not the reduced form. The mechanism of the redox reaction between AMNQH₂ and pyridine N-oxide catalyzed by DMSO reductase was shown to have the substituted-enzyme (ping pong) mechanism. The electron transfer from the quinol through the enzyme appeared to have the same mechanism as the oxidation of menaquinol in the bacterial plasma membrane during anaerobic growth. Other *E.coli* redox enzymes, nitrate reductase A and fumarate

reductase, were also shown to use AMNQH₂ as electron donor. Remarkable properties of AMNQH₂ make it a valuable substrate for the study of quinol oxidation by bacterial redox enzymes.

Acknowledgments

I wish to express my deep gratitude and appreciation to my supervisor, Dr. Joel H. Weiner, for his guidance, support, patience and understanding during the course of this project.

I would like to thank Mrs. Gillian Shaw and Mrs. Joanne Simala-Grant for sharing their expertise in protein chemistry and fruitful discussions.

I would also like to thank the members of my supervisory committee, Carol Cass and Robert Hodges, for their helpful comments and advice.

Special thanks are due to Dr. Ronald N. McElhaney for space in his lab for chemical syntheses and help with reagents and to Dr. David A. Mannoek for helpful consultations.

I am very grateful to Dr. Ruthven N.A.H. Lewis for the help with software required for creation of this thesis.

I am also indebted to a number of wonderful people in the Department of Biochemistry whom I have consulted numerous times for advice and information.

Table of Contents

Chapter 1. Introduction.....	1
Role of DMSO reductase in the respiratory chain of <i>E.coli</i>	1
Biogeochemical importance of DMSO respiration	7
Biochemistry of DMSO reductase from <i>E.coli</i>	9
Objective of research.....	12
Basic principles of enzyme kinetics	15
The kinetics of one-substrate reactions	15
The kinetics of two-substrate enzyme-catalyzed reactions	18
Experimental determination of kinetic parameters of enzyme-catalyzed reactions .	23
Determination of kinetic mechanism of two-substrate enzyme-catalyzed reactions	27
Bibliography	30
Chapter 2. Materials and Methods	34
Chemicals	34
Bacterial strains	34
Enzyme preparation.....	35
Preparation of <i>E.coli</i> membranes containing overexpressed DMSO reductase	35
Preparation of solubilized DMSO reductase	35
Preparation of <i>E.coli</i> membranes containing overexpressed fumarate reductase	37
Preparation of <i>E.coli</i> membranes containing overexpressed nitrate reductase A	37
Enzyme assays.....	37
Assay with benzyl viologen as electron donor ("BV assay")	38

Reductase activity assay with AMNQH ₂ as electron donor ("Red Quinone" assay)	38
DMSO reductase assay with AMNQH ₂ as electron donor.....	39
Inhibition assays	39
Chemical synthesis of quinones	40
Synthesis of 2-methyl-3-nitro-1,4-naphthoquinone (MNNQ).....	40
Synthesis of 3-amino-2-methyl-1,4-naphthoquinone (AMNQ)	40
Synthesis of aliphatic amine oxides	40
Isolation of 1-dimethylamino-2-propanol N-oxide	41
Isolation of N,N-dimethylbenzylamine N-oxide monohydrate	42
Isolation of 4-ethylmorpholine N-oxide hydrochloride.....	42
Isolation of N,N-dimethylaniline N-oxide	43
Isolation of triethylamine N-oxide hydrochloride	43
Synthesis of sulfoxides.....	44
Synthesis of alkyl aryl sulfides.....	46
Oxidation of sulfides to sulfoxides	47
Bibliography	48
Chapter 3. Quinone substrates for DMSO reductase	50
Introduction	50
Biochemistry of quinones.....	50
Chemistry of naphthoquinones.....	52
Results	57
Synthesis and properties of 2-methyl-3-nitro-1,4-naphthoquinone.....	57

Synthesis and physical properties of 3-amino-2-methyl-1,4-naphthoquinone (AMNQ) and 2-amino-3-methyl-1,4-dihydroxynaphthalene (AMNQH ₂)	58
The reduced form of 3-amino-2-methyl-1,4-naphthoquinone is a substrate of DMSO reductase from <i>E.coli</i>	60
Kinetic analysis of the two-substrate reaction catalyzed by DMSO reductase	60
Inhibition of DMSO reductase activity by HOQNO	68
AMNQH ₂ as electron donor for nitrate reductase A and fumarate reductase	68
Comparative behavior of DMSO reductase mutants in RQ and BV assays.....	76
Other potential substrates and inhibitors of DMSO reductase	77
Discussion	79
Bibliography	85
Chapter 4. Amine oxides and sulfoxides.....	88
Introduction	88
The chemistry of sulfoxides	88
The chemistry and biochemistry of amine N-oxides.....	90
Results	92
Synthesis of aliphatic amine oxides	92
Reduction of sulfoxides and N-oxides catalyzed by DMSO reductase with reduced benzyl viologen as electron donor.....	93
Discussion	102
Bibliography	107
Chapter 5. Conclusion	108

Bibliography	109
---------------------------	------------

List of Tables

Table 1-1. Midpoint potentials of some redox couples	6
Table 1-2. Definitions of kinetic parameters	22
Table 2-1. Composition of buffers for the preparation of solubilized DMSO reductase ..	36
Table 2-2. Boiling points of alkyl aryl sulfides	46
Table 2-3. Physical properties of sulfoxides	47
Table 3-1. Quinone content of <i>E.coli</i> membranes after aerobic and anaerobic growth on glucose and various electron acceptors	52
Table 3-2. The effect of substituent groups on the potential of 2-substituted 1,4- naphthoquinones.....	54
Table 3-3. Michaelis constants for the substrates of nitrate reductase and fumarate reductase in BV and RQ assays.....	76
Table 3-4. Comparative behavior of wild-type and some DMSO reductase mutants in RQ- and BV-assays	78
Table 3-5. Dissociation constants for some naphthoquinones and their corresponding quinols	82
Table 4-1. Kinetic parameters of sulfoxide and amine oxide substrates of DMSO reductase.....	94

List of Figures

Figure 1-1. Chemical structures of the most abundant quinone molecules synthesized in <i>Escherichia coli</i>	2
Figure 1-2. Possible mechanisms for generation of proton gradient across the bacterial plasma membrane by redox enzymes.....	4
Figure 1-3. Biosynthesis and degradation of 3-dimethylsulphoniopropionate (DMSP) in marine algae	8
Figure 1-4. Molecular organization of DMSO reductase from <i>E.coli</i>	9
Figure 1-5. The structure of an iron-sulfur cluster of DMSO reductase from <i>E.coli</i>	10
Figure 1-6. Chemical structure of 2- <i>n</i> - heptyl-4-hydroxyquinoline N-oxide (HOQNO)..	11
Figure 1-7. The structure of 2,3-dimethyl-1,4-naphthoquinone (DMNQ) and its reduced form, DMNQH ₂	13
Figure 1-8. The structure of benzyl viologen	13
Figure 1-9. UV spectra of methyl phenyl sulfoxide, pyridine N-oxide and products of their reduction	14
Figure 1-10. Two major mechanisms of two-substrate enzyme-catalyzed reactions	20
Figure 1-11. Plot of initial rate <i>v</i> against substrate concentration for a reaction following the Michaelis-Menten kinetics	24
Figure 2-1. Oxidation of tertiary amines to amine oxides.....	41
Figure 2-2. Chemical structures of amine oxides synthesized in this study.....	44
Figure 2-3. Synthesis of sulfoxides	45
Figure 2-4. Chemical structures of sulfoxides synthesized for this study	45

Figure 3-1. Redox and acid-base equilibrium in quinones.....	51
Figure 3-2. The interaction of quinones with mercaptans.....	56
Figure 3-3. Synthesis of 2-methyl-3-nitro-1,4-naphthoquinone.....	57
Figure 3-4. Synthesis of 3-amino-2-methyl-1,4-naphthoquinone (AMNQ) and 2-amino-3-methyl-1,4-dihydroxynaphthalene (AMNQH ₂).....	59
Figure 3-5. The UV/visible spectrum of 3-amino-2-methyl-1,4-naphthoquinone in the oxidized and reduced state	61
Figure 3-6. The reduction of trimethylamine N-oxide (TMAO) catalyzed by DMSO reductase from <i>E.coli</i> with AMNQH ₂ as electron donor.....	63
Figure 3-7. The reduction of pyridine N-oxide (PyNO) catalyzed by <i>E.coli</i> DMSO reductase with AMNQH ₂ as electron donor.....	64
Figure 3-8. The oxidation of AMNQH ₂ catalyzed by <i>E.coli</i> DMSO reductase with TMAO as electron acceptor at enzyme-saturating concentration (14 mM).....	65
Figure 3-9. The relationship between the apparent Michaelis constant for pyridine N-oxide and the concentration of the other substrate, AMNQH ₂	66
Figure 3-10. Analysis of the kinetic mechanism of the redox reaction between AMNQH ₂ and pyridine N-oxide catalyzed by DMSO reductase from <i>E.coli</i>	67
Figure 3-11. Inhibition of DMSO reductase by 2-n-heptyl-4-hydroxyquinoline N-oxide	69
Figure 3-12. Nitrate reduction catalyzed by <i>E.coli</i> nitrate reductase A with AMNQH ₂ as electron donor.....	70
Figure 3-13. The oxidation of AMNQH ₂ catalyzed by <i>E.coli</i> nitrate reductase A at enzyme-saturating concentration of nitrate	71

Figure 3-14. Fumarate reduction catalyzed by <i>E.coli</i> fumarate reductase with AMNQH ₂ as electron donor	72
Figure 3-15. The oxidation of AMNQH ₂ catalyzed by <i>E.coli</i> fumarate reductase at enzyme-saturating concentration of fumarate	73
Figure 3-16. Nitrate reduction catalyzed by <i>E.coli</i> nitrate reductase A with reduced benzyl viologen as electron donor	74
Figure 3-17. Fumarate reduction catalyzed by <i>E.coli</i> fumarate reductase with reduced benzyl viologen as electron donor.....	75
Figure 3-18. Chemical structure of indigo carmine and 2-methyl-1,4-dihydroxynaphthalene diacetate	78
Figure 3-19. Dissociation of the amino group in 2-amino-1,4-naphthoquinone.....	80
Figure 3-20. Chemical structure of 2-hydroxyl-substituted naphthoquinones	82
Figure 4-1. Stereochemistry of sulfoxides and amine oxides.....	89
Figure 4-2. Pyramidal inversion in amines.....	91
Figure 4-3. The reduction of pyridine N-oxide and dimethyl sulfoxide with reduced benzyl viologen as electron donor catalyzed by DMSO reductase from <i>E.coli</i>	96
Figure 4-4. The rate of reduction of some aliphatic amine oxides with reduced benzyl viologen as electron donor catalyzed by DMSO reductase from <i>E.coli</i> is not saturable even at physiologically high concentrations	97
Figure 4-5. The reduction of 4-ethylmorpholine N-oxide and 1-dimethylaminopropanol-2 N-oxide with reduced benzyl viologen as electron donor catalyzed by DMSO reductase from <i>E.coli</i>	98

Figure 4-6. The reduction of TMAO with reduced benzyl viologen as electron donor catalyzed by solubilized <i>E.coli</i> DMSO reductase	99
Figure 4-7. The reduction of TMAO with reduced benzyl viologen as electron donor catalyzed by <i>E.coli</i> membranes containing overexpressed DMSO reductase.....	100
Figure 4-8. The oxidation of benzyl viologen catalyzed by <i>E.coli</i> DMSO reductase with TMAO as electron donor.....	101
Figure 4-9. The structure of the molybdenum cofactor in the active site of DMSO reductase from <i>Rhodobacter sphaeroides</i>	106

Abbreviations

[X]	concentration of reagent X
AMNQ	3-amino-2-methyl-1,4-naphthoquinone
AMNQH₂	2-amino-3-methyl-1,4-dihydroxynaphthalene (reduced form of AMNQ)
BV	benzyl viologen
BV_{red}	reduced form of benzyl viologen, cation-radical
DMNQ	2,3-dimethyl-1,4-naphthoquinone
DMNQH₂	2,3-dimethyl-1,4-dihydroxynaphthalene (reduced form of DMNQ)
DMQ	demethylmenaquinone
DMS	dimethyl sulfide
DMSO	dimethyl sulfoxide
DTT	dithiothreitol
E'₀	standard redox potential at pH 7
EPR	electron paramagnetic resonance
FRD	fumarate reductase
glycerol-3-P	glycerol-3-phosphate
HOQNO	2- <i>n</i> -heptyl-4-hydroxyquinoline N-oxide
IR	infra red
MGD	molybdopterin guanine dinucleotide
MNNQ	2-methyl-3-nitro-1,4-naphthoquinone
Moco	molybdenum cofactor

MOPS	4-morpholinepropanesulfonic acid
MQ	menaquinone
M_r	molecular weight
NADH	reduced form of nicotinamide adenine dinucleotide
NMR	nuclear magnetic resonance
PMSF	phenylmethanesulfonyl fluoride
PyNO	pyridine N-oxide
RDQ	rhodoquinone
RMTSO	(<i>R</i>)-methyl- <i>p</i> -tolyl sulfoxide
RQ	"red quinone", 3-amino-2-methyl-1,4-naphthoquinone
SMTSO	(<i>S</i>)-methyl- <i>p</i> -tolyl sulfoxide
TLC	thin-layer chromatography
TMAO	trimethylamine N-oxide
UQ	ubiquinone
UV	ultraviolet
WT	wild type

Chapter 1. Introduction

Role of DMSO reductase in the respiratory chain of E.coli

Escherichia coli, a facultative anaerobe, is able to grow on various substrates. Expression of proteins constituting its respiratory chains is precisely regulated, and the bacterium can adapt to the presence of a large number of electron donors and acceptors in the growth medium. *E.coli* is able to express 15 primary dehydrogenases and 10 terminal reductases to satisfy its energy needs (Unden and Bongaerts, 1997). Expression of most enzymes highly depends on the growth conditions, so that not all respiratory enzymes are present in the cell simultaneously. Due to intensive genetic studies, nucleotide sequences of all respiratory enzymes are known (Berlyn *et al.*, 1996), and most enzymes are isolated and well-characterized.

Primary dehydrogenases catalyze oxidation of the following electron donors: formate, hydrogen, NADH, glycerol-3-phosphate (glycerol-3-P), pyruvate, D- and L-lactate, amino acids, gluconate and succinate. Terminal reductases serve to reduce oxygen, nitrate, nitrite, DMSO, TMAO and fumarate. Other substrates can also be used if they can be metabolically converted to the above listed substrates. For example, malate can be used because it can be dehydrated to fumarate; glycerol can be phosphorylated to glycerol-3-P. Dehydrogenases and reductases are linked by quinones, so that all these enzymes have two substrates, one of which is either quinone or its reduced form, quinol.

There are three types of quinone molecules (Fig. 1-1) that are synthesized in *E.coli* (Bentley and Meganathan, 1987). Ubiquinone (UQ), a benzoquinone derivative, is the major quinone species during aerobic growth while two naphthoquinones, menaquinone (MQ) and demethylmenaquinone (DMQ), prevail under anaerobic conditions (Table 3-1). The quinones, highly hydrophobic molecules, can freely diffuse within the membrane bilayer transferring electrons from one enzyme to another. Thus, the respiratory enzymes of *E.coli* do not transfer electrons directly to one another.

E.coli, unlike many other organisms, lacks membrane-diffusible electron carriers other than quinones, such as cytochrome *c*, or other potential branching points in electron transfer chain such as the cytochrome *b-c₁* complex.

Dehydrogenases oxidize their oxidizable substrates and reduce quinones to quinols. Quinols donate electrons to terminal reductases that, in turn, reduce an appropriate substrate. Thus, dehydrogenases, quinones, and terminal reductases form a chain that transfers electrons between two chemical compounds present in the growth medium (transport systems responsible for delivering substrates inside the cell are not discussed here).

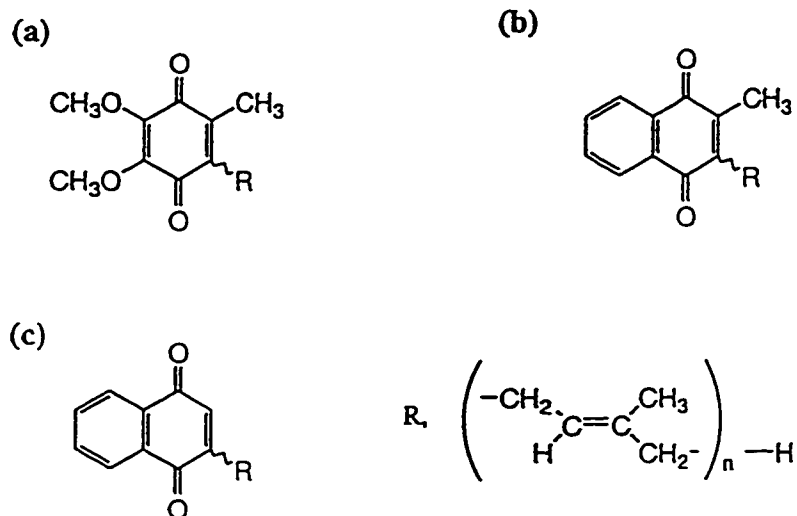


Figure 1-1. Chemical structures of the most abundant quinone molecules synthesized in *Escherichia coli*. a) 2-Methyl-5,6-dimethoxy-3-poly-(3-methylbuten-2-yl)-1,4-benzoquinone (ubiquinone, UQ); b) 2-methyl-3-poly-(3-methylbuten-2-yl)-1,4-naphthoquinone (menaquinone, MQ); c) 2-poly-(3-methylbuten-2-yl)-1,4-naphthoquinone (demethylmenaquinone, DMQ).

The number of isoprenoid units, *n*, attached to the quinonoid ring may vary. The most abundant quinone species in *E.coli* and many other bacteria contain eight isoprenoid units in the molecule as sometimes indicated by an index (UQ₈, MQ₈, DMQ₈). Small amounts of homologues with 5 and 7 isoprenoid units can also be detected (Ramasarma, 1985).

Energy from redox reactions is used to pump protons from cytoplasm to periplasm creating a proton gradient across the bacterial plasma membrane. ATP synthase, a plasma membrane protein, uses the energy of the proton gradient for ATP synthesis.

Protons are translocated across the membrane by respiratory enzymes using several mechanisms (Fig. 1-2). Some enzymes act as proton pumps. Others can generate the proton gradient by arranging their substrate and quinone/quinol binding sites close to the opposite sides of the plasma membrane. With this organization of active sites, protons are consumed on the inner side of the membrane and released on the outside. Coupling of substrate oxidation with quinone reduction is especially important under anaerobic conditions, when oxygen, the electron acceptor with the highest redox potential, is unavailable. Another possibility for increasing energy yield is the arrangement of the quinone reducing site of a dehydrogenase near the cytoplasmic side of the plasma membrane and the reductase's quinol oxidation sites near the periplasmic side of the membrane (Fig. 1-2c). Two-electron reduction of a quinone molecule requires two protons that are taken from the cytoplasm. The resulting quinol diffuses across the membrane and releases the protons into the periplasmic space when oxidized by a terminal reductase. At this time, quinone/quinol binding sites of *E.coli* respiratory enzymes are not well characterized, and whether this principle plays a significant role in bacterial respiration is unclear.

Using quinone as a universal electron mediator allows any dehydrogenase to react with any terminal reductase, at least theoretically. In practice, some interactions do not exist because expression of most respiratory enzymes in *E.coli* is transcriptionally regulated by electron acceptors such as O₂ and nitrate (Gennis and Stewart, 1996). Oxygen, a preferred electron acceptor, inhibits all anaerobic respiratory pathways and fermentation through specialized sensor-regulators proteins Fnr and ArcA/ArcB (Unden and Bongaerts, 1997). Under anaerobic conditions, nitrate is used if it is present in the medium, and in its presence all other anaerobic pathways are repressed by two sensory-regulatory systems, NarX/NarL and NarP/NarQ (Stewart and Rabin, 1995).

DMSO reductase is expressed constitutively under anaerobic conditions. Its mRNA is induced by about 65-fold under anaerobic conditions by Fnr (Eiglmeier *et al.*, 1989). Fnr,

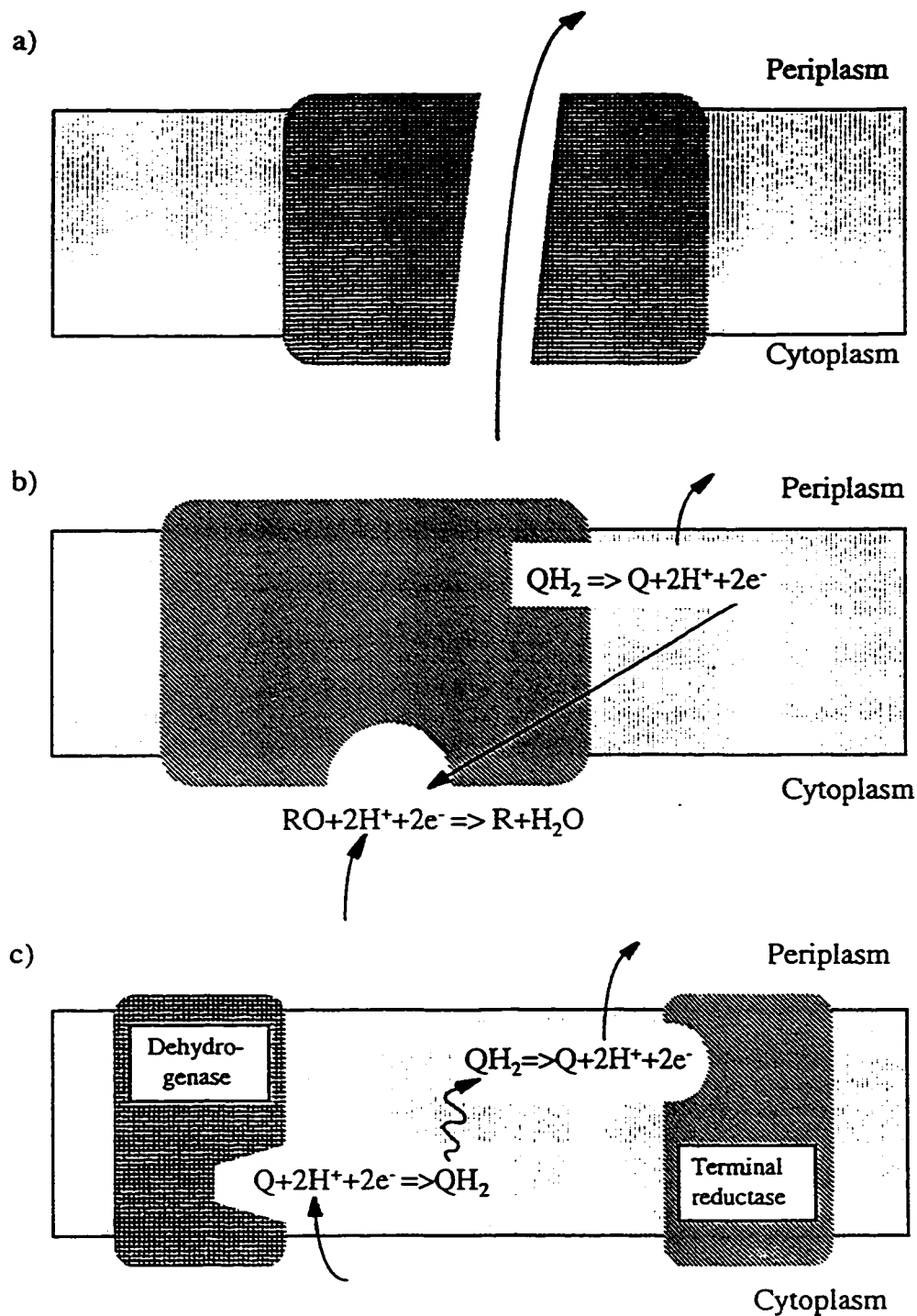


Figure 1-2. Possible mechanisms for generation of proton gradient across the bacterial plasma membrane by redox enzymes. a) Direct pumping of protons; b) arrangement of the enzyme active sites close to the opposite sides of the membrane; c) proton transfer across the membrane by quinone diffusion.

an oxygen sensor protein responsible for activation and repression of a large number of bacterial genes, binds to a specialized site in the DMSO reductase operon.

DMSO reductase sustains bacterial growth on minimal media with a variety of electron acceptors including DMSO, TMAO, methionine sulfoxide or other N- and S-oxides (Sambasivarao and Weiner, 1991b; Simala-Grant and Weiner, 1996). Such substrates provide little energy because of their low midpoint potential (Table 1-1), and the respiratory chain of *E.coli* under these conditions is optimized for maximal energy yield. Predominant dehydrogenases are NADH dehydrogenase I (NDH-I) and anaerobic glycerol-3-phosphate dehydrogenase (G3PDH_N). Expression of noncoupled dehydrogenases is strongly repressed by the Fnr and Arc regulatory systems (Bongaerts *et al.*, 1995, Lin and Iuchi, 1991).

When *E.coli* cells grow on DMSO with glycerol, DMSO reductase is the only active terminal reductase (Sambasivarao and Weiner, 1991b). Bilous and Weiner demonstrated that the anaerobically grown cells acidify the medium upon a DMSO pulse with H⁺/e⁻ ratio of approximately 1.5 (Bilous and Weiner, 1985). Recently, Skulachev with coworkers showed that all work on proton translocation is performed by NDH-I while DMSO reductase does not generate the proton motive force (Bogachev *et al.*, 1996). In the presence of NDH-I inhibitor capsaicine or in mutant cells lacking NDH-I, no medium acidification was detected.

Thus, under anaerobic conditions with DMSO as electron acceptor, DMSO reductase transfers electrons from quinol to DMSO producing dimethyl sulfide and quinone. The latter compound is reduced again by a dehydrogenase that generates a proton electrochemical gradient. The ability of microorganisms to use DMSO as electron "sink" allows them to grow in a variety of natural conditions where this compound is abundant while other electron acceptors such as oxygen and nitrate are unavailable.

Table 1-1. Midpoint potentials of some redox couples

Reaction	E' mV	Reaction	E' mV
$\frac{1}{2} \text{O}_2 + 2\text{H}^+ + 2\text{e}^- \rightarrow \text{H}_2\text{O}$	+820	$\text{UQ} + 2\text{H}^+ + 2\text{e}^- \rightarrow \text{UQH}_2$	+100
$\text{Nitrate} + 2\text{H}^+ + 2\text{e}^- \rightarrow \text{Nitrite} + \text{H}_2\text{O}$	+420	$\text{DMQ} + 2\text{H}^+ + 2\text{e}^- \rightarrow \text{DMQH}_2$	+36
$\text{DMSO} + 2\text{H}^+ + 2\text{e}^- \rightarrow \text{DMS} + \text{H}_2\text{O}$	+160	$\text{MQ} + 2\text{H}^+ + 2\text{e}^- \rightarrow \text{MQH}_2$	-74
$\text{TMAO} + 2\text{H}^+ + 2\text{e}^- \rightarrow$ $\text{Trimethylamine} + \text{H}_2\text{O}$	+130	$\text{RDQ} + 2\text{H}^+ + 2\text{e}^- \rightarrow \text{RDQH}_2$	-63
$\text{Fumarate} + 2\text{H}^+ + 2\text{e}^- \rightarrow \text{Succinate}$	+30	$\text{NAD}^+ + \text{H}^+ + 2\text{e}^- \rightarrow \text{NADH}$	-320

DMSO, dimethyl sulfoxide

DMS, dimethyl sulfide

TMAO, trimethylamine N-oxide

UQ, ubiquinone

UQH₂, ubiquinol

DMQ, demethylmenaquinone

DMQH₂, demethylmenaquinol

MQ, menaquinone

MQH₂, menaquinol

RDQ, rhodoquinone

RDQH₂, rhodoquinol

NAD⁺, nicotinamide adenine dinucleotide

NADH, reduced form of nicotinamide adenine dinucleotide

Biogeochemical importance of DMSO respiration

DMSO and its precursor, DMS, are important components of the atmospheric sulfur cycle (Andreae and Jaeschke, 1992). DMS is a major part of atmospheric sulfur emission from the ocean and land contributing up to 50% to the total biogenic sulfur flux in the atmosphere of estimated $38\text{--}89 \times 10^{12}$ g per year (Andreae, 1992).

Large amounts of DMS, about 1.5×10^{13} g annually, are produced by marine phytoplankton from 3-dimethylsulphonio-*propionate* and, in some organisms, from 4-dimethylsulphonio-2-hydroxybutyrate (Malin, 1996). DMSP is an abundant (about 20 μmol per g fresh weight) osmolyte, cryoprotector, and herbivore repellent in many phytoplankton species and intertidal algae (Gage *et al.*, 1997; Wolfe *et al.*, 1997). It is synthesized from methionine (Fig. 1-3) through the cascade of enzymatic reactions discovered recently (Gage *et al.*, 1997). DMS is released from DMSP by either natural degradation or action of the algal enzyme DMSP lyase (Wolfe *et al.*, 1997). Some aerobic and anaerobic microorganisms degrade DMS in the sea water (Visscher and Taylor, 1993), but much of it escapes from the ocean.

Volatile and barely soluble in water, DMS enters the atmosphere where it plays an important role in cloud formation and other aspects of global climate regulation (Charlson *et al.*, 1987). It can also function as a chemical attractant in trophic cascades of the ocean (Zimmer-Faust *et al.*, 1996). In the atmosphere, DMS is oxidized, among other compounds, to DMSO. The latter compound, water-miscible high-boiling liquid, is washed out from the atmosphere to the surface by rain and thus becomes available to microorganisms living in soil and water. Some industrial processes also supply large amounts of DMSO to the environment, so that study of the mechanism of DMSO reduction is important for our understanding of elaborate interactions affecting global climate, oceanic food chains, and environmental pollution.

The ability to reduce DMSO is widespread among bacteria (Weiner *et al.*, 1992). This fact probably reflects the importance of DMSO respiration for microorganisms. Dimethyl sulfoxide is a stable compound, and possibilities for its chemical or physical

decomposition are very limited, so it can rapidly accumulate in the environment in the absence of biodegradation.

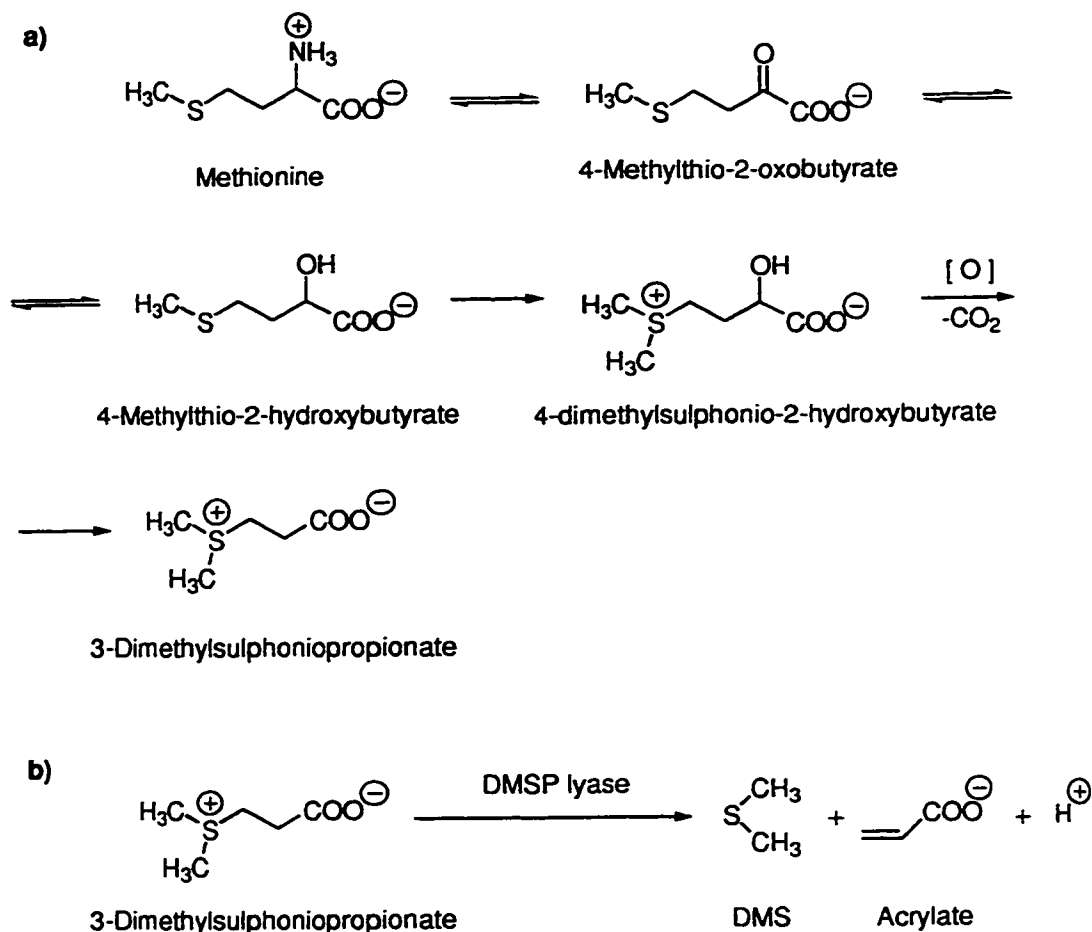


Figure 1-3. Biosynthesis and degradation of 3-dimethylsulphonio-2-hydroxypropionate (DMSP) in marine algae. a) The pathway for DMSP biosynthesis; b) degradation of DMSP by the algal enzyme DMSP lyase leads to the formation of DMS and high local concentrations of acrylate, a potent antimicrobial agent.

Biochemistry of DMSO reductase from E.coli

The DMSO reductase operon has been subcloned and sequenced (Bilous *et al.*, 1988; Bilous and Weiner, 1988). It codes for three polypeptides with M_r 87, 31 and 23 kDa. Overexpression of DMSO reductase in cells transfected with plasmids containing the operon allowed the study of its organization and properties in significant detail. DMSO reductase of *E.coli* is a heterotrimeric membrane protein (Weiner *et al.*, 1992). Two subunits (DmsA and DmsB) are soluble while DmsC is a transmembrane protein that anchors the whole complex to the cytoplasmic membrane (Fig. 1-4).

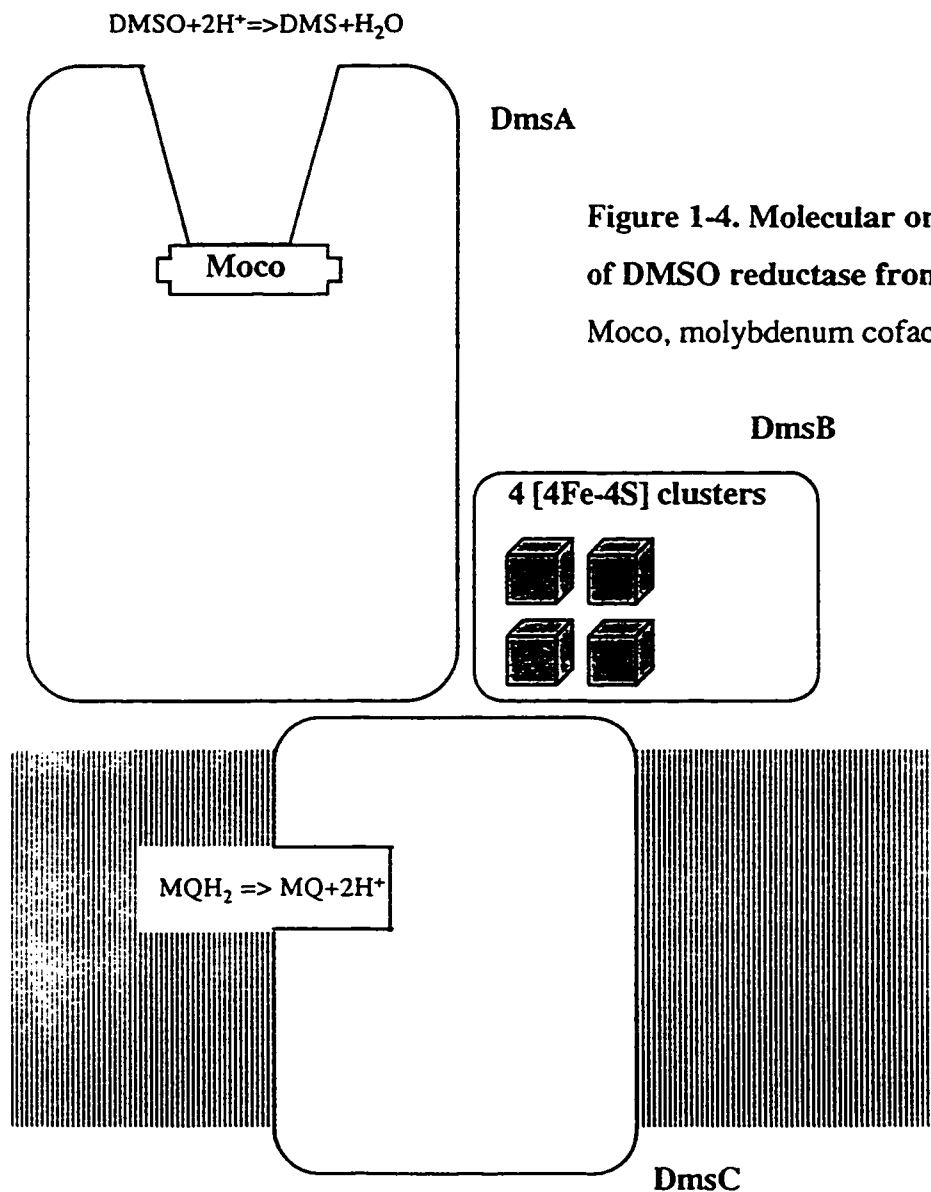


Figure 1-4. Molecular organization of DMSO reductase from *E.coli*.

Moco, molybdenum cofactor

The subunit A (87,350 Da, based on amino acid sequence) contains a molybdenum cofactor (Moco) which is the active site for reduction of sulfoxides and N-oxides. Ability of molybdenum to exist in redox states +4, +5 and +6 allows the enzyme to accumulate electrons and then transfer two electrons to a substrate molecule at once. The structure of Moco will be discussed below.

DmsB (23,070 Da), the smallest subunit of DMSO reductase, has another metal cofactor, four [4Fe-4S] clusters (Fig. 1-5) linked to the polypeptide through cysteine side chains (Rothery *et al.*, 1995). Although roles of particular clusters are not clear yet, they apparently play an important structural role, and some of them may be involved in electron transfer. Midpoint potentials of the clusters are -50, -120, -240, and -330 mV (Cammack and Weiner, 1990); only one of them has a higher potential than menaquinone (-80 mV) and thus is capable of accepting electrons from quinols. Potentials of the other clusters are too low for this purpose.

DmsC (30,789 Da) is the membrane anchor for DmsABC complex. It contains many hydrophobic residues and, according to hydropathy plot analysis, forms eight α -helical segments (Bilous *et al.*, 1988). This subunit serves as a menaquinol oxidation site and is

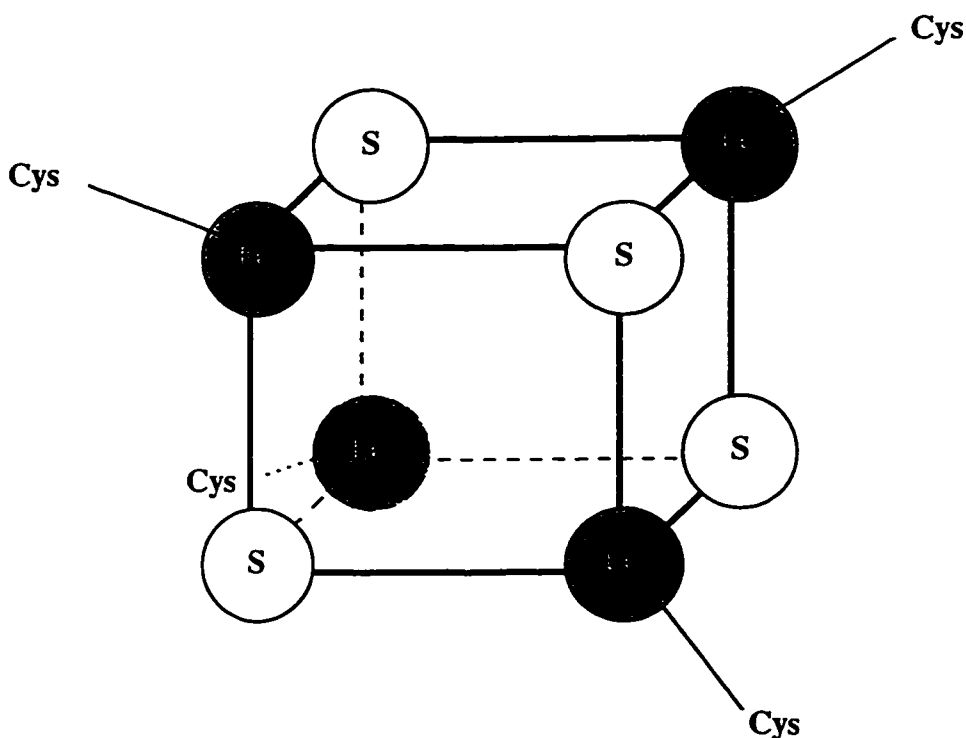


Figure 1-5. The structure of an iron-sulfur cluster of DMSO reductase from *E.coli*.

also required for enzyme stability (Sambasivarao and Weiner, 1991a). The fact that DMSO reductase uses menaquinol as electron donor was established in experiments with *ubi* and *men* mutants of *E.coli* (Cox and Knight, 1981; Meganathan, 1984).

The enzyme can be isolated from bacterial membranes after mild detergent treatment and purified to high degree of homogeneity. The solubilized DMSO reductase retains its activity toward numerous electron donors and acceptors.

The exact electron pathway in DMSO reductase is not known. It has been proposed that electrons donated by menaquinol pass through an iron-sulfur cluster or clusters to the molybdenum cofactor (Weiner *et al.*, 1992). Two important mutations have been characterized that shed some light on the mechanism of electron transfer. Mutation H65R in DmsC abolishes menaquinol oxidation activity and prevents a powerful inhibitor, 2-*n*-heptyl-4-hydroxyquinoline N-oxide (HOQNO) (Fig. 1-6), from binding to the enzyme (Rothery and Weiner, 1996). Analogous mutation in fumarate reductase transmembrane subunit FrdC is known to have the same effect: it blocks bacterial growth on fumarate, and the enzyme is unable to oxidize 2,3-dimethyl-1,4-naphthohydroquinone (DMNQH₂) (Fig. 1-7b on p. 13), an artificial analog of menaquinone (Weiner *et al.*, 1986). Another mutation, replacement of cysteine 102 to serine in DmsB, leads to modification of the iron-sulfur cluster with potential -50 mV ([4Fe-4S] → [3Fe-4S]) and blocks electron transport from DMNQH₂ to DmsA (Rothery and Weiner, 1996).

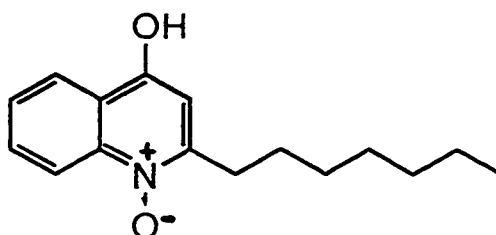


Figure 1-6. Chemical structure of 2-*n*-heptyl-4-hydroxyquinoline N-oxide (HOQNO)

Objective of research

Properties of an enzyme and its mutant forms can be studied through enzymatic assays. There are apparent difficulties with assaying DMSO reductase.

DMSO and analogous aliphatic sulfoxides do not absorb electromagnetic radiation in visible or long ultraviolet range. This does not allow monitoring their reduction by spectroscopy. Aromatic sulfoxides such as methyl phenyl sulfoxide absorb in the ultraviolet region around 254 nm, but products of their reduction, thioethers (sulfides), have very similar spectra, with very close absorption maxima and intensity (Fig. 1-9, p. 14). Accuracy of such assay would be very low.

The same difficulty is observed with amine N-oxides. Aliphatic compounds are transparent both in visible and long UV region, while aromatic N-oxides and their corresponding amines have almost identical UV-spectra. In addition, the number of commercially available sulfides, sulfoxides and N-oxides is very limited. The fact that available electron acceptors reacting with DMSO reductase elude easy detection forces researchers to use the other semireaction, oxidation of electron donors, for monitoring the reaction.

Unfortunately, natural electron donors of DMSO reductase, menaquinols, cannot be used in assays due to extremely low solubility in water. Even simpler naphthoquinone derivatives lacking the isoprenoid tail are very hydrophobic, and their use for kinetic analysis is limited to a very few examples. In addition, UV spectra of naphthoquinones in the oxidized and reduced form are often very similar. In most cases, the quinone is used at one concentration while the concentration of another component or enzyme is varied. Assays of this type allow determination of the enzyme activity at various conditions but do not allow kinetic properties of the quinone itself to be revealed.

One of the most often used compounds is 2,3-dimethyl-1,4-naphthoquinone (DMNQ) (Fig.1-7a). It is routinely used as an electron donor because its reduced form is relatively soluble. But the oxidized form is not, and it precipitates from the solution at higher concentrations. This substrate is not commercially available and must be synthesized.

All these problems with naphthoquinones, S- and N-oxides have led to the fact that the most commonly used assay for oxidoreductases involves the chemically unrelated compound, reduced benzyl viologen (BV_{red}) (Fig. 1-8). This compound is widely used for studies of various redox enzymes because of its high water solubility, low midpoint potential, useful spectral properties, and ability to donate electrons to enzymes in a relatively non-specific manner. Reaction rates of DMSO reductase with BV_{red} are significantly higher than those with quinone substrates that allows smaller amounts of enzymes to be used in the assay. Despite this advantage, application of BV_{red} for analysis of kinetics of DMSO reductase is limited. It has been shown that this substrate donates electrons to enzymes in a non-natural manner. For example, mutants of fumarate

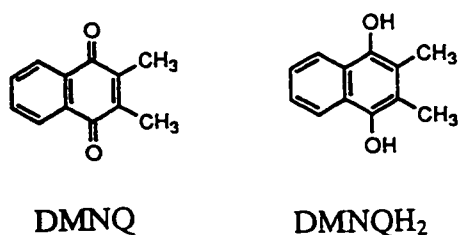


Figure 1-7. The structure of 2,3-dimethyl-1,4-naphthoquinone (DMNQ) and its reduced form, DMNQH₂.

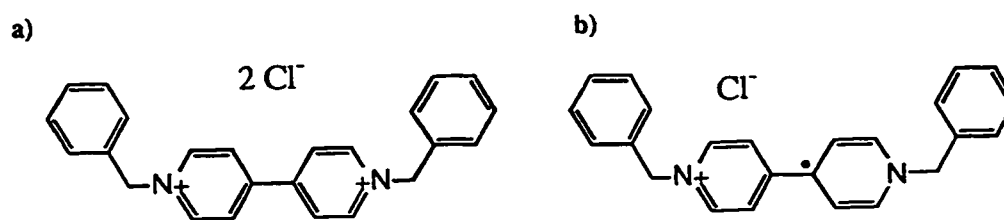


Figure 1-8. The structure of benzyl viologen.

a) The oxidized form, colorless; b) the reduced form, purple (ϵ_{570} 7800 l·mole⁻¹·cm⁻¹).

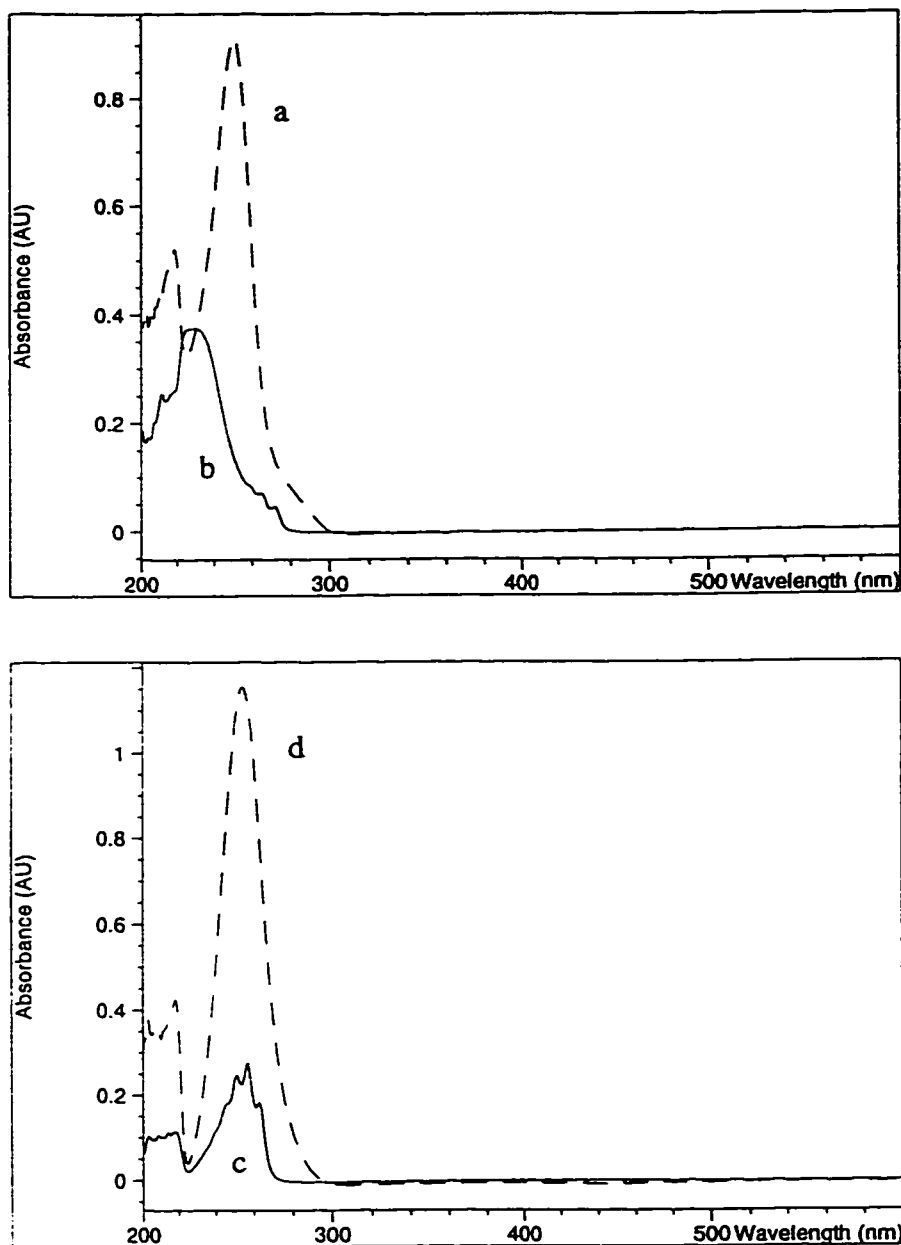


Figure 1-6. UV spectra of methyl phenyl sulfoxide, pyridine N-oxide and products of their reduction. a) Methyl phenyl sulfide; b) methyl phenyl sulfoxide; c) pyridine; d) pyridine N-oxide. All compounds were dissolved in 100 mM MOPS buffer pH 7.0 at the same concentration (0.1 mM).

reductase and DMSO reductase, FrdC:H82R and DmsC:H65R, have similar reductase and BV_{red} -oxidizing activities with their corresponding wild-type counterparts, but their quinol-oxidizing activities are completely blocked. The same effect is observed with catalytic dimers of fumarate reductase and DMSO reductase FrdAB and DmsAB (Sambasivarao and Weiner, 1991a; Weiner *et al.*, 1986). Absence of transmembrane subunits (FrdC and FrdD for fumarate reductase, DmsC for DMSO reductase) abolishes quinol-oxidizing activity but has little effect on BV_{red} oxidation. This suggests that BV_{red} donates electrons to the enzymes through a specialized binding site that is located close to the molybdenum cofactor while quinol is oxidized at a site in the membrane subunit. The objective of this work was to synthesize a number of substrates for DMSO reductase, determine their physical constants and kinetic parameters, and use them for analysis of the structure and function of DMSO reductase from *E.coli*.

Basic principles of enzyme kinetics

The kinetics of one-substrate reactions

The first definitive experiments with an enzyme accompanied by a thorough mathematical analysis of the model was performed by L. Michaelis and M.L. Menten (Michaelis and Menten, 1913). They proposed that the hydrolysis of sucrose (Sucrose + Water \rightarrow Glucose + Fructose) catalyzed by yeast invertase included formation of the enzyme-substrate complex (ES):



where E , S , P are concentrations of the enzyme, substrate and product, respectively, and k_i are rate constants of particular reaction steps in forward (positive index) or reverse (negative index) direction.

To avoid troubles with progressive inactivation of the enzyme, product inhibition, reverse reaction and other experimental variables, they measured *initial rates* of the reaction at different substrate concentrations. The major assumption made by Michaelis and Menten

was that the first step was much faster than the second ($k_{+1} \gg k_{+2}$), and formation of the enzyme-substrate complex can be characterized by the equilibrium constant K_s :

$$K_s = \frac{e \cdot s}{x} \quad (\text{Equation 1-2})$$

where s, x, e are concentrations of the substrate, enzyme-substrate complex, and free enzyme, respectively. The overall reaction rate is defined by the slower second step:

$$v = k_{+2} \cdot x \quad (\text{Equation 1-3})$$

Expression for x can be obtained from the definition of K_s and relationship between the initial concentration of the enzyme e_0 , concentration of the enzyme-substrate complex and concentration of free enzyme ($e_0 = e + x$):

$$x = \frac{(e_0 - x) \cdot s}{K_s} = \frac{e_0 \cdot s}{K_s + s} \quad (\text{Equation 1-4})$$

Finally,

$$v = k_{+2} \cdot \frac{e_0 \cdot s}{K_s + s} \quad \text{or}$$

$$v = \frac{V_{\max} \cdot s}{K_m + s} \quad (\text{Equation 1-5})$$

where V_{\max} , the *maximum velocity*, is the rate of the reaction at indefinitely large substrate concentration ($V_{\max} = k_{+2} \cdot e_0$), and K_m , the *Michaelis constant*, is the dissociation constant of the substrate-enzyme complex, K_s . The Michaelis-Menten equation (Eq. 1-5) accurately describes experimental results with various enzyme systems despite the fact that their assumption about the relative magnitude of rate constants is often unjustified and very difficult to verify in each particular case.

Later, Briggs and Haldane (Briggs and Haldane, 1925) demonstrated that this assumption is unnecessary if the reaction studied has reached a steady state in which the concentration of the enzyme-substrate complex is constant. At steady state

$$\frac{dx}{dt} = k_{+1} \cdot (e_0 - x) \cdot s - k_{-1} \cdot x - k_{+2} \cdot x = 0 \quad (\text{Equation 1-6})$$

After rearrangements,

$$x = \frac{k_{+1} \cdot e_0 \cdot s}{k_{-1} + k_{+2} + k_{+1} \cdot s} \quad \text{(Equation 1-7)}$$

The rate of the reaction is the rate of the product formation:

$$v = k_{+2} \cdot x = \frac{k_{+1} \cdot k_{+2} \cdot e_0 \cdot s}{k_{-1} + k_{+2} + k_{+1} \cdot s} \quad \text{or}$$

$$v = \frac{k_{+2} \cdot e_0 \cdot s}{\frac{k_{-1} + k_{+2}}{k_{+1}} + s} = \frac{V_{\max} \cdot s}{K_m + s} \quad \text{(Equation 1-8)}$$

The final equation proposed by Briggs and Haldane remains the same but the meaning of the Michaelis constant has changed: now this is a combination of all three rate constants that has no special physical meaning ($K_m = (k_{-1} + k_{+2})/k_{+1}$) whereas in the Michaelis-Menten hypothesis K_m was a dissociation constant for the enzyme-substrate complex.

Since there are no reasons to assume that one of the rate constants is much larger than others, the hypothesis of Michaelis and Menten now seems to have only historical value. The assumption of Briggs and Haldane, on the other hand, is often valid, and numerous experiments have demonstrated that for many enzyme systems the steady state is achieved within 5 to 10 msec after beginning of the reaction.

In fact, even the hypothesis of Briggs and Haldane oversimplifies the enzyme kinetics with one substrate because the conversion of the enzyme-substrate complex to free enzyme and the product is considered irreversible. For the most common case, completely reversible chain of reactions (EP is the enzyme-product complex)



the steady-state rate equation can be expressed in either of the two forms:

$$v = \frac{V_{\max 1} \cdot V_{\max 2} \cdot \left(s - \frac{p}{K_{eq}} \right)}{K_{ms} \cdot V_{\max 2} + V_{\max 2} \cdot s + \frac{V_{\max 1} \cdot p}{K_{eq}}} = \frac{V_{\max 1} \cdot \left(s - \frac{p}{K_{eq}} \right)}{K_{ms} \cdot \left(1 + \frac{p}{K_{mp}} \right) + s} \quad \text{(Equation 1-9)}$$

where $V_{\max 1}$ and $V_{\max 2}$ are maximum velocities in forward and reverse directions, K_{ms} and K_{mp} are Michaelis constants for the substrate and product, respectively, K_{eq} is the equilibrium constant, s and p are concentrations of substrate and product (Cleland, 1963). The two forms are related by the *Haldane relationship*:

$$K_{eq} = \frac{V_{\max 1} \cdot K_{mp}}{V_{\max 2} \cdot K_{ms}} \quad \text{(Equation 1-10)}$$

Equation 1-9 is apparently the most general equation for an enzyme-catalyzed reaction with one substrate and one product. For initial conditions ($p=0$), it turns into another form of the Michaelis-Menten equation:

$$v = \frac{V_{\max 1} \cdot s}{K_{ms} + s}$$

Again, the physical meaning of K_m and V_{\max} has changed but the principal relationship between the substrate concentration and the initial rate remains the same. The significance of K_m and V_{\max} is that these parameters can be determined experimentally while the underlying rate constants most often cannot. If the model is thoroughly formulated, measurements of K_m and V_{\max} may allow the determination of rate constants and other reaction parameters such as dissociation constants and inhibition constants.

The kinetics of two-substrate enzyme-catalyzed reactions

The analysis described in the previous chapter demonstrated the complexity of enzyme kinetics even in its simplest case. In fact, one-substrate one-product reactions are rare; they include only some isomerization-type reactions and hydrolysis of various substrates when concentration of water may be considered constant.

Two-substrate reactions account for about 60% of all known enzyme-catalyzed reactions. The detailed analysis of these systems is very complicated: the rate equation for the most

general case has more than 80 terms in numerator and denominator including substrate concentrations squared. To simplify the analysis and rewrite the rate equations in meaningful terms, several approaches have been proposed, the simplest and most useful of them being that of Cleland (Cleland, 1963).

Assumptions about the details of a reaction mechanism allow to greatly reduce the complexity of rate equations for two-substrate reactions. Most reaction mechanisms fall into two major categories: the *substituted-enzyme* mechanism and the *ternary-complex* mechanism (Fig. 1-10). The major difference between the two is the order of substrate binding to the enzyme and product release from the enzyme-product complex.

In the ordinary form of the substituted-enzyme mechanism, the first substrate binds to the enzyme, and the product of the resulting conversion leaves the enzyme before the second substrate can bind. The modified enzyme (with a chemical group transferred to/removed from it or in another redox state) then binds the second substrate and carries out the other semireaction. The general rate equation for this mechanism is given in Eq. 1-11 (Cornish-Bowden, 1979). The meaning of constants and variables in this and the following equations are given in Table 1-2 (page 22) and in the legend to Fig. 1-10.

$$v = \frac{\frac{V^f \cdot a \cdot b}{K_i^A \cdot K_m^B} - \frac{V^r \cdot p \cdot q}{K_i^P \cdot K_m^Q}}{\frac{a}{K_i^A} + \frac{K_m^A \cdot b}{K_i^A \cdot K_m^B} + \frac{p}{K_i^P} + \frac{K_m^P \cdot q}{K_i^P \cdot K_m^Q} + \frac{a \cdot b}{K_i^A \cdot K_m^B} + \frac{a \cdot p}{K_i^A \cdot K_i^P} + \frac{K_m^A \cdot b \cdot q}{K_i^A \cdot K_m^B \cdot K_i^Q} + \frac{p \cdot q}{K_i^P \cdot K_m^Q}}$$

(Equation 1-11)

The ternary-complex mechanism is characterized by the formation of the complex between the enzyme and both substrates, *EAB*. The order of the substrate binding may be strictly determined (first A, then B) (the *compulsory-order* ternary-complex mechanism, Fig. 1-10a, Eq. 1-12) or not (first A, then B or first B, then A) (the *random-order* ternary-complex mechanism, Eq. 1-13).

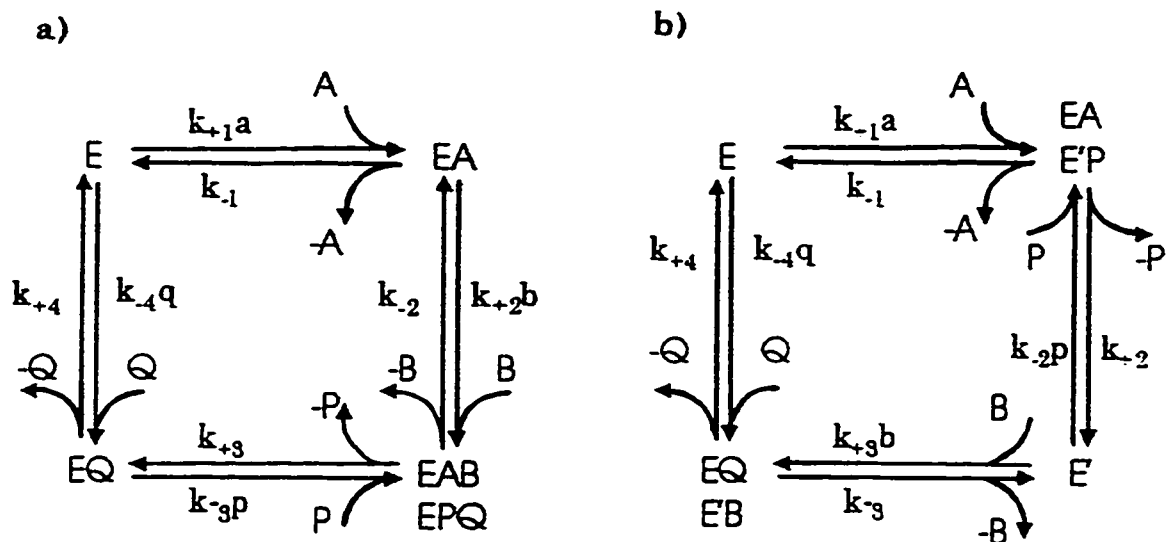


Figure 1-10. Two major mechanisms of two-substrate enzyme-catalyzed reactions.

a) The ternary-complex mechanism; b) the substituted-enzyme mechanism. The rate equations are shown for individual steps.

Abbreviations: E , enzyme; E' , substituted enzyme; A, B , substrates; P, Q , reaction products; a, b, p, q , concentration of the reactant A, B, P, Q . Isomerization of enzyme-substrate or enzyme-product complexes does not change the rate equations.

Modified from (Cornish-Bowden, 1979, p.106)

$$v = \frac{\frac{V^f \cdot a \cdot b}{K_i^A \cdot K_m^B} - \frac{V^r \cdot p \cdot q}{K_m^P \cdot K_i^Q}}{1 + \frac{a}{K_i^A} + \frac{K_m^A \cdot b}{K_i^A \cdot K_m^B} + \frac{K_m^Q \cdot p}{K_m^P \cdot K_i^Q} + \frac{q}{K_i^Q} + \frac{a \cdot b}{K_i^A \cdot K_m^B} + \frac{K_m^Q \cdot a \cdot p}{K_i^A \cdot K_m^P \cdot K_i^Q} + \frac{K_m^A \cdot b \cdot q}{K_i^A \cdot K_m^B \cdot K_i^Q} + \frac{p \cdot q}{K_m^P \cdot K_i^Q} + \frac{a \cdot b \cdot p}{K_i^A \cdot K_m^B \cdot K_i^P} + \frac{b \cdot p \cdot q}{K_i^B \cdot K_m^P \cdot K_i^Q}}$$

(Equation 1-12)

$$v = \frac{\frac{V^f \cdot a \cdot b}{K_i^A \cdot K_m^B} - \frac{V^r \cdot p \cdot q}{K_m^P \cdot K_i^Q}}{1 + \frac{a}{K_i^A} + \frac{b}{K_i^B} + \frac{p}{K_i^P} + \frac{q}{K_i^Q} + \frac{a \cdot b}{K_i^A \cdot K_m^B} + \frac{p \cdot q}{K_m^P \cdot K_i^Q}} \quad (\text{Equation 1-13})$$

Equations 1-11, 1-12 and 1-13 can be simplified if the *initial* velocities are measured. In this case, all terms containing product concentrations p and q turn to zero, and the reverse reaction is absent ($V^r=0$, $V^f=V_{max}$). Thus, for the substituted-enzyme mechanism:

$$v = \frac{V_{max} \cdot a \cdot b}{K_m^B \cdot a + K_m^A \cdot b + a \cdot b} \quad (\text{Equation 1-14})$$

The initial rate for both ternary-complex mechanisms is expressed by the same equation:

$$v = \frac{V_{max} \cdot a \cdot b}{K_i^A \cdot K_m^B + K_m^B \cdot a + K_m^A \cdot b + ab} \quad (\text{Equation 1-15})$$

The principal difference between equations 1-14 and 1-15 is the presence of the constant term in the denominator of Eq. 1-15. As we'll see later, this difference can be exploited for distinguishing the reaction mechanisms.

Table 1-2. Definitions of kinetic parameters

[modified from (Cornish-Bowden, 1979)]

Symbol	Description	Definition	
		Ternary-complex mechanism	Substituted-enzyme mechanism
V^f	Maximum velocity for the forward reaction	$\frac{k_{+3} \cdot k_{+4} \cdot e_0}{k_{+3} + k_{+4}}$	$\frac{k_{+2} \cdot k_{+4} \cdot e_0}{k_{+2} + k_{+4}}$
V^r	Maximum velocity for the reverse reaction	$\frac{k_{-1} \cdot k_{-2} \cdot e_0}{k_{-1} + k_{-2}}$	$\frac{k_{-1} \cdot k_{-3} \cdot e_0}{k_{-1} + k_{-3}}$
K_m^A	Michaelis constant for the substrate A	$\frac{k_{+3} \cdot k_{+4}}{k_{+1} \cdot (k_{+3} + k_{+4})}$	$\frac{(k_{-1} + k_{+2}) \cdot k_{+4}}{k_{+1} \cdot (k_{+2} + k_{+4})}$
K_m^B	Michaelis constant for the substrate B	$\frac{(k_{-2} + k_{+3}) \cdot k_{+4}}{k_{+2} \cdot (k_{+3} + k_{+4})}$	$\frac{k_{+2} \cdot (k_{-3} + k_{+4})}{(k_{+2} + k_{+4}) \cdot k_{+3}}$
K_m^P	Michaelis constant for the product P	$\frac{k_{-1} \cdot (k_{-2} + k_{+3})}{(k_{-1} + k_{-2}) \cdot k_{-3}}$	$\frac{(k_{-1} + k_{+2}) \cdot k_{-3}}{(k_{-1} + k_{-3}) \cdot k_{-2}}$
K_m^Q	Michaelis constant for the product Q	$\frac{k_{-1} \cdot k_{-2}}{(k_{-1} + k_{-2}) \cdot k_{-4}}$	$\frac{k_{-1} \cdot (k_{-3} + k_{+4})}{(k_{-1} + k_{-3}) \cdot k_{-4}}$
K_i^A	Inhibition constant for the substrate A	$\frac{k_{-1}}{k_{+1}}$	$\frac{k_{-1}}{k_{+1}}$
K_i^B	Inhibition constant for the substrate B	$\frac{k_{-1} + k_{-2}}{k_{+2}}$	$\frac{k_{-3}}{k_{+3}}$
K_i^P	Inhibition constant for the product P	$\frac{k_{+3} + k_{+4}}{k_{-3}}$	$\frac{k_{+2}}{k_{-2}}$
K_i^Q	Inhibition constant for the product Q	$\frac{k_{+4}}{k_{-4}}$	$\frac{k_{+4}}{k_{-4}}$

Experimental determination of kinetic parameters of enzyme-catalyzed reactions

The curve defined by the Michaelis-Menten equation is a rectangular hyperbola (Fig. 1-11). The analysis of the equation demonstrates the following features of this curve. The initial reaction rate slowly reaches V_{max} at infinite substrate concentration. The rate is half-maximal ($1/2 V_{max}$) at the substrate concentration equal to K_m . At low concentrations of substrate ($s \ll K_m$) the initial rate increases linearly with the increase of substrate concentration (the slope of the line is V_{max}/K_m).

The Michaelis-Menten equation can be more easily analyzed after rearrangements producing linear relationship between various parameters. This approach allows to determine K_m and V_{max} from the slope of a straight line (obtained from experimental data by the least squares method) and its interceptions with axes rather than using special procedures for fitting the non-linear Michaelis-Menten equation.

The *Lineweaver-Burk* (or *double-reciprocal*) plot is used most often because it was the first example of this kind (Lineweaver and Burk, 1934). The plot of $1/v$ against $1/s$ allows to fit the data with a straight line that intercepts $1/V_{max}$ on the ordinate axis, $-1/K_m$ on the abscissa and with the slope of K_m/V_{max} (Eq. 1-16).

$$\frac{1}{v} = \frac{1}{V_{max}} + \frac{K_m}{V_{max}} \cdot \frac{1}{s} \quad \text{(Equation 1-16)}$$

Later on, several analogous techniques have been invented. Despite their similarity, linear plots produce different results with the same set of experimental data. The reason for this is that experimental errors in v affect these plots differently. For example, at low reaction rates small errors in v lead to enormous errors in $1/v$. Thorough statistical analysis of linear plots with computer-simulated data (with predetermined K_m , V_{max} values and error distribution) demonstrated that the double reciprocal plot was the worst method for determination of K_m and V_{max} (Dowd and Riggs, 1965). The best method that produced K_m and V_{max} close to predetermined values was the Eadie-Hofstee plot (Eadie, 1942; Hofstee, 1952), the plot of v against v/s (Eq. 1-17). The plot gave the lowest deviation

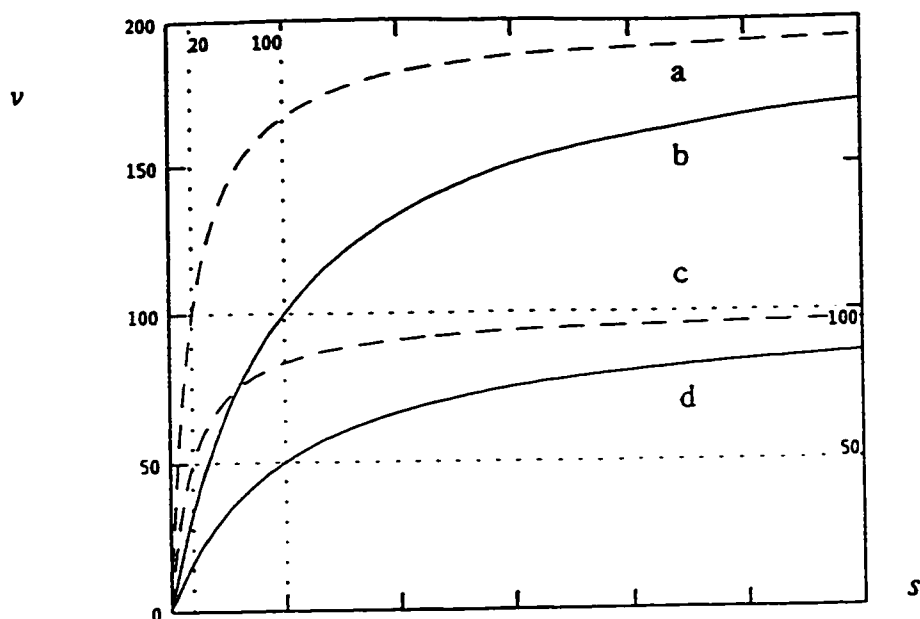


Figure 1-11. Plot of initial rate v against substrate concentration s for a reaction following the Michaelis-Menten kinetics. a) $K_m=20$, $V_{max}=200$; b) $K_m=100$, $V_{max}=200$; c) $K_m=20$, $V_{max}=100$; d) $K_m=100$, $V_{max}=100$. Units of K_m and V_{max} are arbitrary. Values of K_m and half-maximal rate are shown by dotted lines.

from predetermined kinetic parameters for variety of data sets approximating the real laboratory measurements.

$$v = V_{max} - K_m \cdot \frac{v}{s} \quad \text{(Equation 1-17)}$$

Most or all linear plots are usually based on the fitting of experimental data using the linear least-square method without weighting. The simplest technique includes measurements of the initial reaction rate at various concentrations of substrate. The measurements are performed in replicates at each substrate concentration, then results are averaged for each s and fitted with a straight line assuming that all measurements are equally reliable (weight=1.0). The kinetic parameters are determined from the slope of the line, its interceptions with axes or right from the coefficients of the line (especially in the Eadie-Hofstee method). The quality of the results can be roughly estimated by the standard error and the coefficient of determination.

This approach has several serious drawbacks. It does not accurately estimate the reliability of experimental data. When a program fits the data using the least square method, it does not see how good each point is because the averaging of results eliminates the important information about the accuracy of measurements. This problem cannot be eliminated by including all experimental results in calculations because the heart of the technique - the least squares method - is very sensitive to outliers. Each measurement with high deviation from the average (quite often in enzymology) leads to a significant change in the calculated values. Rejecting the outliers on the basis of high deviation only is neither wise nor ethical because points with high deviation could bear important information about the actual values of the kinetic parameters.

The best way to overcome these problems and increase the accuracy of results would be a program that fits experimental data, analyzes the accuracy of measurements at each substrate concentration, detects outliers and reduces their weight in calculations.

All data-fitting programs either incorporate some assumptions about the statistical distribution of experimental error or ask the user to make a choice of predefined models. It should be understood that the least-square solution requires a number of conditions to be satisfied. First, systematic error must be absent. Second, the random errors are not correlated (that is, all errors are independent). Third, the errors have normal (gaussian) distribution. Fourth, only one measured variable is subject to experimental errors. Fifth, the correct model is fitted. Not all of these conditions can be met easily.

It is difficult to prove that the equation fitted is the right equation for the system studied. Most enzyme systems show the linear or almost linear increase in velocity at low substrate concentrations with the following near-saturation at high concentrations but in some systems allosterical regulation of enzyme activity, substrate/product inhibition, loss of enzyme activity in suboptimal assay system cause deviations from the Michaelis-Menten kinetics. These deviations often reveal themselves only under specific conditions so that proving the correctness of a model requires a thorough analysis of experimental data.

There is no (and cannot be) an ultimate proof that a reaction has a particular mechanism. Cornish-Bowden (Cornish-Bowden, 1995, p.6-8) and other researchers have

demonstrated that it is possible to generate many sets of numbers with the same average K_m and V_{max} values and standard errors (most of which containing one or several outliers) and noted the importance of analysis of graphical representation of the experimental data. Interestingly, methods that produce statistically the most reliable results (such as the Eadie-Hofstee plot) are rarely suitable for graphical analysis (Cornish-Bowden, 1979, p. 25).

One of the most convenient and reliable methods of determining whether the experimental results fit the theoretical model is studying the *residual plot* (the plot of the difference between experimental and calculated values of reaction rate against the calculated rate) (Ellis and Duggleby, 1978). If experimental values fit the equation, the points on the graph are scattered randomly, either in a narrow band along the abscissa (if all rates have the same standard deviation) or increasing in magnitude as the calculated rate increases (if the standard deviation of each rate is proportional to its true value). Appearance of any pattern on the residual plot shows that deviation of experimental data from calculated values is not random, and probably requires the modification of the theoretical model.

It is quite difficult to prove that the error distribution follows the normal curve because this requires a very large number of measurements (at least thousands at each substrate concentration under identical conditions). In fact, more thorough considerations could lead to the conclusion that in most experiments the distribution of the experimental error is not normal. For example, a situation when not one but two experimental variables (the reaction rate and the substrate concentration) are subject to experimental error happens very often in enzymology. Sometimes experimental errors are not independent, and so on. Why is it so important? The normal distribution of error guarantees that the arithmetic mean is the best estimate for the data. If the error distribution is not normal, other methods may give a better estimate and can be used (or must be used) instead of the least squares method. Such methods have been developed but most of them were unavailable because the algorithms were written in Fortran, required special computer workstations and covered narrow specialized areas of enzyme kinetics.

Recently, a monograph on application of statistical methods in enzyme kinetics was published by one of the leading researchers in this area, Dr. Athel Cornish-Bowden (Cornish-Bowden, 1995). The book is accompanied by a diskette containing a program called LEONORA that offers a variety of statistical approaches to fitting the data to various equations (Michaelis-Menten, substrate inhibition, two-substrate mechanisms, different types of inhibition, etc.). Automatic generation of residual plots allows to visually verify the correctness of the selected model. The program is easy to use and runs on most IBM PC-compatible computers. Its output contains a valuable statistical information about the relationship of the data and the model and (optionally) a detailed report on the process of the data fitting. Using LEONORA significantly alleviates enzyme kinetics studies.

Determination of kinetic mechanism of two-substrate enzyme-catalyzed reactions

The initial rate equation for the ternary-complex mechanism is given by Eq. 1-15 on p.21. It is interesting to investigate this equation at large concentrations of substrates.

If a and b are very large, $v = V_{max}$.

If only a or b is large, the rate is expressed by Michaelis-Menten-type equations (Eq. 1-18 and Eq. 1-19, correspondingly).

$$v = \frac{V_{max} \cdot b}{K_m^B + b} \quad \text{(Equation 1-18)}$$

$$v = \frac{V_{max} \cdot a}{K_m^A + a} \quad \text{(Equation 1-19)}$$

Thus K_m^A may be defined as the limiting Michaelis constant for the substrate A when the substrate B is saturating. Analogously, K_m^B is the limiting Michaelis constant for B when A is saturating.

If concentration of one of the substrates (*e.g.* b) is kept constant, the Eq. 1-15 can be rearranged to

$$v = \frac{V^{app} \cdot a}{K_m^{app} + a} \quad \text{(Equation 1-20)}$$

which is a kind of the Michaelis-Menten equation in respect to the variable substrate a . Kinetic constants for this equation are

$$V^{app} = \frac{V_{\max} \cdot b}{K_m^B + b} \quad \text{(Equation 1-21)}$$

$$K_m^{app} = \frac{K_i^A \cdot K_m^B + K_m^A \cdot b}{K_m^B + b} \quad \text{(Equation 1-22)}$$

The important conclusion is that when b goes to zero, K_m^{app} approaches K_i^A . The similar (but not identical) equations can be obtained for the substrate b .

The same type of analysis applied to the Eq. 1-14 for the substituted-enzyme mechanism indicates that the reaction follows the Michaelis-Menten equation when one of the substrates is at saturation. When the concentration of one reactant is kept constant (but not very large or very low), the general rate equation is identical to Eq. 1-20 for the ternary-complex mechanism, with the definition of K_m^{app} being different:

$$V^{app} = \frac{V_{\max} \cdot b}{K_m^B + b} \quad \text{(Equation 1-23)}$$

$$K_m^{app} = \frac{K_m^A \cdot b}{K_m^B + b} \quad \text{(Equation 1-24)}$$

As we can see, the apparent Michaelis constant of the substrate a for the substituted-enzyme mechanism decreases to zero when the concentration of the fixed substrate goes to zero. The difference in the behavior of this constant can be used for distinguishing the two kinetic mechanisms.

There are also several graphical methods based on the rearrangements of the ternary-complex and the substituted enzyme equations. For example, they both can be

represented in the form similar to the Lineweaver-Burk equation (Eq. 1-25 for the ternary-complex mechanism and Eq. 1-26 for the substituted-enzyme mechanism at fixed concentrations of reactant b).

$$\frac{1}{v} = \frac{K_i^A \cdot K_m^B + K_m^A \cdot b}{V_{\max} \cdot b} \cdot \frac{1}{a} + \frac{K_m^B + b}{V_{\max} \cdot b} \quad \text{(Equation 1-25)}$$

$$\frac{1}{v} = \frac{K_m^A}{V_{\max}} \cdot \frac{1}{a} + \frac{K_m^B + b}{V_{\max} \cdot b} \quad \text{(Equation 1-26)}$$

It can be easily seen from these equations that both of them are straight lines in coordinates $1/v$ against $1/a$. The big difference is that the slopes of the lines depend on the concentration of the fixed substrate b for the ternary-complex- but not for the substituted-enzyme mechanism. As a result, the straight lines will be parallel (or nearly parallel due to experimental errors) for the latter mechanism while the lines will not be parallel if the reaction has the ternary-complex mechanism.

Other mathematical representations of equations 1-14 and 1-15 can also be used to determine the mechanism of the two-substrate enzyme-catalyzed reactions (Cornish-Bowden, 1979).

Certainly, none of these methods can give the clear answer because experimental errors cause deviations from the ideal case. The best way to obtain a reliable result is to use several independent analytical methods.

Bibliography

- Andreae, M.O. and W.A. Jaeschke. (1992). Exchange of sulphur between biosphere and atmosphere over temperate and tropical regions. *In* Sulphur Cycling on the Continents, R. W. Howarth, J. W. B. Stewart and M. V. Ivanov, eds. (New York: Wiley), pp. 27-61.
- Andreae, M.O. (1992). The global biochemical sulfur cycle: a review. *In* Trace Gases and the Biosphere, B. Moor and D. Schimel, eds. (Boulder, Colorado: UCAR Office for Interdisciplinary Earth Studies).
- Bentley, R. and R. Meganathan. (1987). Biosynthesis of the isoprenoid quinones ubiquinone and menaquinone. *In* *Escherichia coli* and *Salmonella typhimurium*, F. C. Neidhardt, J. L. Ingraham, K. B. Low, B. Magasanik, M. Schaechter and H. E. Umbarger, eds. (Washington, DC: American Society for Microbiology), pp. 512-520.
- Berlyn, M.K.B., K.B. Low and K.E. Rudd. (1996). Linkage map of *Escherichia coli* K-12, Edition 9. *In* *Escherichia coli* and *Salmonella typhimurium*, F. C. Neidhardt, ed. (Washington, DC: ASM Press), pp. 1715-1902.
- Bilous, P.T. and J.H. Weiner (1985). Proton translocation coupled to dimethyl sulfoxide reduction in anaerobically grown *Escherichia coli* HB101. *J. Bacteriol.* **163**, 369-375.
- Bilous, P.T., S.T. Cole, W.F. Anderson and J.H. Weiner (1988). Nucleotide sequence of the dmsABC operon encoding the anaerobic dimethylsulphoxide reductase of *Escherichia coli*. *Mol. Microbiol.* **2**, 785-795.
- Bilous, P.T. and J.H. Weiner (1988). Molecular cloning and expression of the *Escherichia coli* dimethyl sulfoxide reductase operon. *J. Bacteriol.* **170**, 1511-1518.
- Bogachev, A.V., R.A. Murtazina and V.P. Skulachev (1996). H^+/e^- Stoichiometry for NADH dehydrogenase I and dimethyl sulfoxide reductase in anaerobically grown *Escherichia coli* cells. *J. Bacteriol.* **178**, 6233-6237.
- Bongaerts, J., S. Zoske, U. Weidner and G. Uden (1995). Transcriptional regulation of the proton translocating NADH dehydrogenase genes (nuoA-N) of *Escherichia coli* by electron acceptors, electron donors and gene regulators. *Mol. Microbiol.* **16**, 521-534.
- Briggs, G.E. and J.B.S. Haldane (1925) A note on the kinetics of enzyme action. *Biochem. J.* **19**, 338-339.

- Cammack, R. and J.H. Weiner (1990). Electron paramagnetic resonance spectroscopic characterization of dimethyl sulfoxide reductase of *Escherichia coli*. *Biochemistry* **29**, 8410-8416.
- Charlson, R.J., J.E. Lovelock, M.O. Andreae and S.G. Warren (1987). Oceanic phytoplankton, atmospheric sulphur, cloud albedo and climate. *Nature* **326**, 655-661.
- Cleland, W.W. (1963) The kinetics of enzyme-catalyzed reactions with two or more substrates or products. *Biochim. Biophys. Acta* **67**, 104-137.
- Cornish-Bowden, A. (1995). Analysis of enzyme kinetic data (New York: Oxford University Press Inc.).
- Cox, J.C. and R. Knight (1981). Trimethylamine N-oxide (TMAO) reductase activity in chlorate-resistant or respiration-deficient mutants of *Escherichia coli*. *FEMS Microbiol. Lett.* **12**, 249-252.
- Dowd, J.E. and D.S. Riggs (1965) A comparison of estimates of Michaelis-Menten kinetic constants from various linear transformations. *J. Biol. Chem.* **240**, 863-869.
- Eadie, G.S. (1942) The inhibition of cholinesterase by physostigmine and prostigmine. *J. Biol. Chem.* **146**, 85-93.
- Eiglmeier, K., N. Honore, S. Iuchi, E.C.C. Lin and S.T. Cole (1989). Molecular genetic analysis of FNR-dependent promoters. *Mol. Microbiol.* **3**, 869-878.
- Ellis, K.J. and R.G. Duggleby (1978) What happens when data are fitted to the wrong equation? *Biochem. J.* **171**, 513-517.
- Gage, D.A., D. Rhodes, K.D. Nolte, W.A. Hicks, T. Leustek, A.J.L. Cooper and A.D. Hanson (1997). A new route for synthesis of dimethylsulphoniopropionate in marine algae. *Nature* **387**, 891-894.
- Hofstee, B.H.J. (1952) Specificity of esterases. I. Identification of two pancreatic aliesterases. *J. Biol. Chem.* **199**, 357-364.
- Gennis, R.P. and V. Stewart. (1996). Respiration. In *Escherichia coli* and *Salmonella typhimurium*, F. C. Neidhardt, ed. (Washington, DC: ASM Press), pp. 217-261.
- Lin, E.C.C. and S. Iuchi (1991). Regulation of gene expression in fermentative and respiratory systems in *Escherichia coli* and related bacteria. *Annu. Rev. Genet.* **25**, 361-387.

- Lineweaver, H. and D. Burk (1934) The determination of enzyme dissociation constants. *J. Amer. Chem. Soc.* **56**, 658-666.
- Malin, G. (1996). *In* Biological and Environmental Chemistry of DMSP and Related Sulfonium Compounds, R. P. Kiene, P. T. Visscher, M. D. Keller and G. O. Kirst, eds. (New York: Plenum), pp. 177-189.
- Meganathan, R. (1984). Inability of *men* mutants of *Escherichia coli* to use trimethylamine N-oxide as an electron acceptor. *FEMS Microbiol. Lett.* **24**, 57-62.
- Michaelis, L. and M.L.Menten (1913) *Biochemisches Zeitschrift* **49**, 333-369.
- Rothery, R.A., J.L. Simala Grant, J.L. Johnson, K.V. Rajagopalan and J.H. Weiner (1995). Association of molybdopterin guanine dinucleotide with *Escherichia coli* dimethyl sulfoxide reductase: effect of tungstate and a mob mutation. *J. Bacteriol.* **177**, 2057-2063.
- Rothery, R.A. and J.H. Weiner (1996). Interaction of an engineered [3Fe-4S] cluster with a menaquinol binding site of *Escherichia coli* DMSO reductase. *Biochemistry* **35**, 3247-3257.
- Sambasivarao, D. and J.H. Weiner (1991a). Dimethyl sulfoxide reductase of *Escherichia coli*: an investigation of function and assembly by use of in vivo complementation. *J. Bacteriol.* **173**, 5935-5943.
- Sambasivarao, D. and J.H. Weiner (1991b). Differentiation of the multiple S- and N-oxide reducing activities of *Escherichia coli*. *Curr. Microbiol.* **23**, 105-110.
- Simala-Grant, J.L. and J.H. Weiner (1996). Kinetic analysis and substrate specificity of *Escherichia coli* dimethyl sulfoxide reductase. *Microbiology* **142**, 3231-3239.
- Stewart, V. and R.S. Rabin. (1995). Dual sensors and dual response regulators interact to control nitrate- and nitrite-responsive gene expression in *Escherichia coli*. *In* Two-component Signal Transduction, J. A. Hoch and T. J. Silhavy, eds. (Washington, DC: ASM Press), pp. 233-252.
- Uden, G. and J. Bongaerts (1997). Alternative respiratory pathways of *Escherichia coli*: energetics and transcriptional regulation in response to electron acceptors. *Biochim. Biophys. Acta* **1320**, 217-234.

- Visscher, P.T. and B.F. Taylor (1993). A new mechanism for the aerobic catabolism of dimethyl sulfide. *Appl. Environ. Microbiol.* **59**, 3784-3789.
- Weiner, J.H., R. Cammack, S.T. Cole, C. Condon, N. Honore, B.D. Lemire and G. Shaw (1986). A mutant of *Escherichia coli* fumarate reductase decoupled from electron transport. *Proc. Natl. Acad. Sci. USA* **83**, 2056-2060.
- Weiner, J.H., R.A. Rothery, D. Sambasivarao and C.A. Trieber (1992). Molecular analysis of dimethylsulfoxide reductase: a complex iron-sulfur molybdoenzyme of *Escherichia coli*. *Biochim. Biophys. Acta* **1102**, 1-18.
- Wolfe, G.V., M. Steinke and G.O. Kirst (1997). Grazing-activated chemical defense in a unicellular marine alga. *Nature* **387**, 894-897.
- Zimmer-Faust, R.K., M.P. de Souza and D.C. Yoch (1996). Bacterial chemotaxis and its potential role in marine dimethylsulfide production and biogeochemical sulfur cycling. *Limnol. Oceanogr.* **41**, 1330-1334.

Chapter 2. Materials and Methods

Chemicals

Chemical reagents of the highest purity available for the synthesis of potential DMSO reductase substrates and inhibitors were purchased from Aldrich. Solvents and 30% hydrogen peroxide were obtained from Fisher Scientific Co. 2-Methyl-1,4-naphthoquinone (menadione) and trimethylamine N-oxide (TMAO) dihydrate was from Eastman Kodak, DMSO from Fisher Scientific. 4-Methylmorpholine N-oxide, (*R*)- and (*S*)-methyl *p*-tolyl sulfoxides, and other commercially available DMSO reductase substrates were purchased from Aldrich. HOQNO was purchased from Sigma. All commercially available compounds were used without additional purification except pyridine N-oxide which was doubly distilled in vacuum. Benzyl viologen dichloride hydrate was from Aldrich.

Bacto tryptone, Bacto peptone and Bacto yeast extract were from Difco. Salts for growth media were from BDH and Sigma. Triton X-100 was from Sigma.

Thin-layer chromatography (TLC) was performed on silica gel-coated aluminum plates with a 254 nm fluorescent indicator (Fluka 60778). Proton magnetic resonance spectra were recorded on a Bruker AM-300 spectrometer with tetramethylsilane as internal standard.

Bacterial strains

E.coli strain HB101 (*F⁻ hsdR hsdM pro leu gal lac thi recA rpsL*) (Boyer and Roulland-Dussoix, 1969) was from the lab collection. Strain DSS401 is a chromosomal *dms* deletion mutant (Sambasivarao and Weiner, 1991).

All manipulations with plasmids and bacterial strains were performed as described by Sambrook *et al.* (Sambrook, *et al.*, 1989).

Enzyme preparation

Preparation of *E.coli* membranes containing overexpressed DMSO reductase

E.coli HB101 transformed with pDMS160 (Rothery and Weiner, 1991) was grown anaerobically in a 4-liter carboy for 48 h on glycerol-fumarate medium with ampicillin (Weiner *et al.*, 1988). Cells were concentrated using a Pellicone membrane system, harvested by centrifugation, resuspended in buffer and French-pressed three times (Bilous and Weiner, 1985; Rothery and Weiner, 1991). This procedure produces small vesicles with the inside-out orientation of the membrane. The unbroken cells and cell debris was removed by low-speed centrifugation (10 min. at 3000 g, twice). The membrane fraction was separated by high-speed centrifugation (2 hours at 140,000g) of the supernatant from the previous step and thoroughly washed by homogenization/high-speed centrifugation.

Preparation of solubilized DMSO reductase

E.coli membrane fractions obtained as described above from four 19-litre carboys were extracted with 10% Triton X-100 (Cammack and Weiner, 1990) and purified by chromatography on DEAE-Sepharose CL-6B as described in (Simala-Grant and Weiner, 1996), except that 80-150 mM NaCl was used (the enzyme elutes at approximately 120 mM salt) and glycerol was excluded from chromatographic buffers. The enzyme activity was monitored by TMAO reduction assay (60 mM TMAO) with BV_{red} as electron donor. TMAO was used as a substrate because of its high reduction rate as compared with other substrates that allows to assay even highly diluted DMSO reductase samples.

All enzyme purification steps were performed at 5°C. The membranes were resuspended in the Buffer A (Table 2-1), and the total amount of protein in membranes was determined by the modified Lowry procedure as recommended by Markwell (Markwell *et al.*, 1978) with bovine serum albumin as a standard. After addition of 0.8 mg Triton X-100 per 1 mg total protein the mixture was gently shaken for 45 min., then centrifuged for 1 h at 140,000 g. The white pellet was discarded, the supernatant was analyzed for TMAO reductase activity and total protein and loaded onto chromatographic column (42 x 3.2 cm) equilibrated with the Buffer B (Table 2-1) containing 80 mM NaCl. After the enzyme was loaded onto the column, the column was washed with 500 ml of Buffer B

(80 mM NaCl), then a linear gradient of NaCl in Buffer B was applied (1 l of 80 mM and 1 l of 150 mM NaCl). Sixty 20 ml fractions were collected. Fractions 35-54 containing a dark-brown pigment were analyzed for TMAO reductase activity and total protein. Eight most active fractions containing 150-300 units/ml were pooled (total volume 164 ml), 16 ml glycerol was added, and the solution was concentrated to 5.8 ml using the Amicon cell with PM30 membrane.

The resulting enzyme stock solution was aliquoted into Eppendorf tubes (200 μ l per tube), rapidly frozen in liquid nitrogen and stored in the freezer at -70°C.

The final buffer contains 10% glycerol, 20 mM histidine, 0.5 mM EDTA, 1 mM DTT, 2 mM PMSF, about 2% Triton X-100 and 20 mM DMSO. The latter is added to chromatographic buffers to prevent the loss of DMSO reductase activity.

Table 2-1. Composition of buffers for the preparation of solubilized DMSO reductase

Buffer (purpose)	Solute	Final concentration
Buffer A (preparation of membrane suspension, enzyme solubilization)	MOPS, pH 7.0	50 mM
	TMAO	70 mM
	DTT	1 mM
	PMSF	2 mM
Buffer B (chromatography)	Histidine, pH 6.8	20 mM
	EDTA	0.5 mM
	DTT	1 mM
	PMSF	2 mM
	Triton X-100	10% (w/v)
	DMSO	20 mM
Buffer C (enzyme assay)	MOPS, pH 7.0, degassed	100 mM

Preparation of *E.coli* membranes containing overexpressed fumarate reductase

E.coli HB101 was transformed with pFRD84 plasmid (Lemire *et al.*, 1982) and grown anaerobically on glycerol-fumarate medium with ampicillin. Everted vesicles were made as described above for DMSO reductase.

Preparation of *E.coli* membranes containing overexpressed nitrate reductase A

E.coli HB101 was transformed with pVA700 plasmid (Guigliarelli *et al.*, 1996) and grown anaerobically on glycerol-fumarate medium with ampicillin. Everted membrane vesicles were made as described above for DMSO reductase.

Enzyme assays

All types of enzyme assays were performed under anaerobic conditions. Glass cuvettes with a hollow polytetrafluoroethylene stopper were used for spectroscopic measurements. Ordered addition of reagents to the cuvette was performed using Hamilton syringes through the hole in the stopper to prevent access of oxygen into the cuvette. Assay buffer was 100 mM MOPS, pH 7.0, thoroughly degassed in vacuum and then bubbled with nitrogen gas for 30-60 min.

Assays were performed on a Gilford 250 UV/visible spectrophotometer at 25°C. The initial rates were determined from the slope of reaction curves. Between two and five assays were performed for each substrate concentration. The kinetic analysis was accomplished using IBM PC program LEONORA (Cornish-Bowden, 1995) which assesses the appropriate weighting scheme from internal evidence of the data and minimizes the effect of outliers by use of the biweight method. Least squares method with weights calculated with adjustable σ/σ (default program settings) were used for calculations. The values analyzed were results of separate experiments, they were not averaged before analysis to allow the program to estimate pure experimental error.

The validity of the applied kinetic model was verified by studying the residual plot of the reaction rate. Appearance of any kind of pattern on the residual plot was considered as either a deviation from the proposed mechanism or a systematic experimental error.

Assay with benzyl viologen as electron donor ("BV assay")

All reagents were dissolved in the assay buffer. The cuvette was completely filled with the buffer and tightly stoppered so that excess of the buffer leaks out through the hole in the stopper. Benzyl viologen dichloride solution was added first to the final concentration of 200 μM , followed by the solution of a substrate-electron acceptor. A solution of sodium dithionite was added to give absorbance of 1.3-1.6 at 570 nm, and the stable baseline was recorded.

Reactions were started by addition of freshly diluted DMSO reductase solution. The course of a reaction was monitored by decrease in absorbance at 570 nm with the extinction coefficient of BV_{red} 7800 $\text{l}\cdot\text{mole}^{-1}\cdot\text{cm}^{-1}$. One unit of enzyme activity corresponds to 1 μmole BV_{red} oxidized per minute. Reduction of one mole of amine oxide or sulfoxide requires two moles of BV_{red} , according to the stoichiometry of the reactions. With some easily oxidizable substrates, the absorbance was slowly decreasing in the absence of the enzyme reflecting non-catalyzed chemical reaction between BV_{red} and the electron acceptor. In such cases, the rate of the non-catalyzed reaction was subtracted from the total rate achieved after addition of DMSO reductase to the cuvette.

The amount of DMSO reductase added was kept constant or varied insignificantly for the entire set of experiments with each substrate. In the control, the reaction rate in the absence of added electron acceptor was estimated, and this value was subtracted from the total rate.

Reductase activity assay with AMNQH₂ as electron donor ("Red Quinone" assay)

A solution of AMNQ in acetonitrile (40 mM) and aqueous solution of sodium dithionite (20 mg/ml) were mixed in the cuvette so that optical density of the resulting mixture at 465 nm was about 0.005-0.010 thus avoiding large excess of dithionite. After addition of a reducible substrate solution the baseline was confirmed. The reaction was started by the addition of an enzyme, and its course was monitored by the increase of absorbance at 465 nm using $\Delta\epsilon$ (AMNQ/AMNQH₂) of 2100. One unit of enzyme activity corresponds to 1 μmole AMNQH₂ oxidized per minute. Reduction of 1 molecule of AMNQH₂

requires two electrons and corresponds to oxidation of one molecule of a sulfoxide or amine oxide.

This procedure was used with bacterial membranes containing overexpressed nitrate reductase, fumarate reductase, and DMSO reductase.

DMSO reductase assay with AMNQH₂ as electron donor

Preliminary experiments showed that the rate of reduction of most substrates catalyzed by DMSO reductase was about two orders of magnitude lower when AMNQH₂ was used instead of BV_{red} as electron donor. As a result, small amount of DMSO in the enzyme stock solution interfered with the measurements.

In order to avoid such interference, the enzyme was added to the reaction mixture lacking the substrate-electron acceptor, and the reaction was allowed to run until all DMSO was reduced. Then an additional amount of sodium dithionite was added in order to reduce AMNQ back to AMNQH₂, solution of N-oxide or sulfoxide was injected, and the reaction curve was recorded.

The following is the RQ assay protocol used in this study with solubilized DMSO reductase.

The required amount of 40 mM AMNQ in acetonitrile was mixed with the buffer in the cuvette and the solution of sodium dithionite was added to reduce absorbance at 465 nm to almost zero (excess of dithionite should be avoided). After DMSO reductase stock solution was added, absorbance was allowed to increase until its maximal value. Several microliters of sodium dithionite solution were added to bring absorbance back to 0.005-0.010, and stable baseline was recorded. After addition of a reducible substrate, the reaction curve was recorded, and the rate of AMNQH₂ oxidation was determined from the slope at time zero using $\Delta\epsilon_{465}$ of AMNQ/AMNQH₂ of 2100.

Inhibition assays

DMSO reductase inhibition assays were performed as regular activity assays except that a substance-inhibitor or potential inhibitor was added to the cuvette together with or immediately before a substrate for DMSO reductase.

Chemical synthesis of quinones

Synthesis of 2-methyl-3-nitro-1,4-naphthoquinone (MNNQ)

The reaction scheme for this synthesis is outlined in Fig. 3-3, p. 57.

2-Methyl-1,4-hydroxynaphthalene diacetate (10 g, 38.7 mmole) was dissolved in 100 ml glacial acetic acid and the cold mixture of 30 ml concentrated sulfuric acid and 15 ml 70% nitric acid was added at once. The mixture was stirred at room temperature overnight and another 50 ml of nitric acid was added. The course of the reaction was controlled by TLC in hexane-ethyl ether (4:1). R_f of 2-methyl-1,4-hydroxynaphthalene diacetate is 0.20, R_f of MNNQ 0.34. After 5-6 hours the reaction mixture was poured in 1 l water and stirred for 15 min. The yellow precipitate was collected by filtration, thoroughly washed with water on the filter, and recrystallized from acetic acid-methanol (1:1). The yield of MNNQ is 7.1 g (85%), mp 124°C is consistent with the literature data (Baker *et al.*, 1942).

Synthesis of 3-amino-2-methyl-1,4-naphthoquinone (AMNQ)

The reaction scheme for this synthesis is given on Fig. 3-4, p. 59.

A solution of 3.5 g (54 mmole) of sodium azide in 10 ml of water was slowly added to the solution of 5 g (29 mmole) of menadione in 50 ml of glacial acetic acid at 40°C. After stirring overnight at 40°C, the reaction mixture was diluted with 100 ml cold water with ice and the dark red crystalline material was collected by filtration, washed with cold water on the filter and recrystallized from aqueous ethanol. The light golden-red substance forms tiny wool-like crystals that, unlike other quinones, are easy to handle.

The uncorrected melting point of 161°C is consistent with the literature data of 162-162.5°C (Baker *et al.*, 1942). The yield was 4 g (74%). $^1\text{H-NMR}$ (DMSO-d_6) δ 1.92 (s, 3H, CH_3), 6.67 (s, 2H, NH_2), 7.67 and 7.77 (m, 1H each, H-6,7), 7.92 (m, 2H, H-5,8).

Synthesis of aliphatic amine oxides

Oxidation of tertiary amines to N-oxides was performed with 30% hydrogen peroxide in methanol (Fig. 2-1) as reported (Cope and Ciganec, 1963a; Cope and Ciganec, 1963b).

0.3 mole amine was added to 45 ml methanol and cooled on ice bath. Initial pH of this mixture was measured with indicator strips (Merck ColorpHast, Cat. 9558) and found to be higher than 10 for all amines. The first portion of 30% hydrogen peroxide (34 ml, 0.3 mole) was added slowly with vigorous stirring, and the reaction mixture was stirred for 2 hours. The second portion of hydrogen peroxide (34 ml, 0.3 mole) was added slowly, and the reaction was stirred for another 4 hours. The third portion of hydrogen peroxide (34 ml, 0.3 mole) was added at once at room temperature, and the mixture was left overnight. The reaction was complete when the indicator strip shows pH to be about 7-8. This corresponds to the disappearance of the strongly basic tertiary amine and its conversion to almost neutral amine oxide.

A small amount of platinum black (1-2 mg) was added to 1 ml water in a test tube and the resulting suspension was added to the reaction mixture. The mixture was stirred until emergence of oxygen bubbles ceased, filtered and concentrated in vacuum. The thick syrup was dissolved in chloroform. Further purification steps were performed individually for each compound as described below. Chemical structures of the synthesized aliphatic amines are given on Fig. 2-2, p. 44.

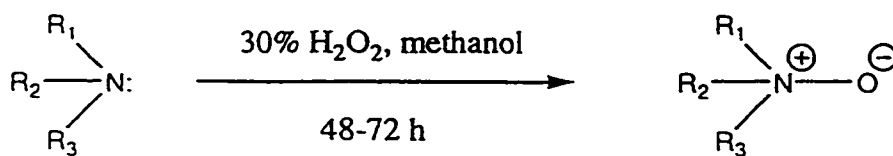


Figure 2-1. Oxidation of tertiary amines to amine oxides.

Isolation of 1-dimethylamino-2-propanol N-oxide

The solution of the N-oxide in chloroform was dried over barium oxide, the solvent was removed in vacuum. The resulting semi-solid was dissolved in the mixture of 400 ml benzene and 50 ml methanol. After addition of 300 ml hexane the mixture was cooled on

an ice bath and slightly concentrated in vacuum. White precipitate formed was filtered and dried in a dessiccator. The yield was 26.6 g (74%), mp 158-160°C.

Elemental analysis	%C	%H	%N
Calculated	50.40	11.00	11.75
Found	49.92	11.07	11.31

Isolation of N,N-dimethylbenzylamine N-oxide monohydrate

The solution of the N-oxide in chloroform was dried over anhydrous sodium sulfate, filtered and evaporated. The residue was dissolved in acetone, filtered and chilled on an ice bath. Hexane was slowly added until the solution became opalescent. After cooling of the mixture on ethanol-dry ice bath a heavy yellow liquid has formed. Vigorous shaking of the flask led to formation of white crystalline substance which was filtered and dried in a dessiccator. The yield was 35.5 g (70%), mp 54-55°C.

Elemental analysis	%C	%H	%N
Calculated for C ₉ H ₁₃ NO	71.49	8.67	9.26
Calculated for monohydrate	63.88	8.93	8.28
Found	63.71	8.64	8.33

Isolation of 4-ethylmorpholine N-oxide hydrochloride

When the reaction of 0.3 mole amine with hydrogen peroxide was complete, the mixture was evaporated in vacuum and the residue was treated with excess of concentrated hydrochloric acid. The solution was evaporated in vacuum, dissolved in minimal amount of ethyl acetate-isopropanol mixture (1:1) and dried over sodium sulfate. After addition of hexane the mixture was slightly evaporated in vacuum, and white precipitate was collected by filtration and dried in a dessiccator. The yield was 37.6 g (75%), mp 95°C.

Elemental analysis	%C	%H	%N	%Cl
Calculated for C ₆ H ₁₃ NO ₂	54.94	9.99	10.68	-
Calculated for hydrochloride	42.99	8.42	8.36	21.15
Found	42.72	8.48	8.19	22.56

Isolation of N,N-dimethylaniline N-oxide

Evaporation of the chloroformic solution of this N-oxide in high vacuum led to crystallization and formation of dark brown crystals. The substance was crystallized twice from ethyl acetate - hexane. Brownish-white crystals were dried in a dessiccator over phosphorus pentoxide. The yield was 15.2 g (37%), mp 124-125°C.

Elemental analysis	%C	%H	%N
Calculated	70.04	8.08	10.21
Found	68.46	8.11	9.86

Isolation of triethylamine N-oxide hydrochloride

When the reaction of 0.3 mole amine with hydrogen peroxide was complete, the mixture was evaporated in vacuum and the residue was treated with excess of concentrated hydrochloric acid. The solvent was evaporated in vacuum, the resulting thick syrup was dissolved in chloroform and dried over sodium sulfate. Precipitation started after evaporation of chloroform in vacuum. Snow-white crystals were collected by filtration and dried in a vacuum dessiccator over phosphorus pentoxide. The yield was 20.3 g (44%), mp 98-99°C. IR (chloroform cast): 790, 945, 992, 1158, 1365, 1389, 1465, 1509, 1528, 2559, 2687, 2736, 2854, 2982, 3395 cm^{-1} . $^1\text{H-NMR}$ (DMSO-d_6) δ , ppm: 1.25 (t, 9H, CH_3), 3.65 (d, 6H, CH_2), 12.32 (s, 1H, HCl).

Elemental analysis	%C	%H	%N	%Cl
Calculated for $\text{C}_6\text{H}_{15}\text{NO}$	61.49	12.90	11.95	-
Calculated for hydrochloride	46.90	10.50	9.12	23.07
Found	46.22	12.09	8.78	23.00

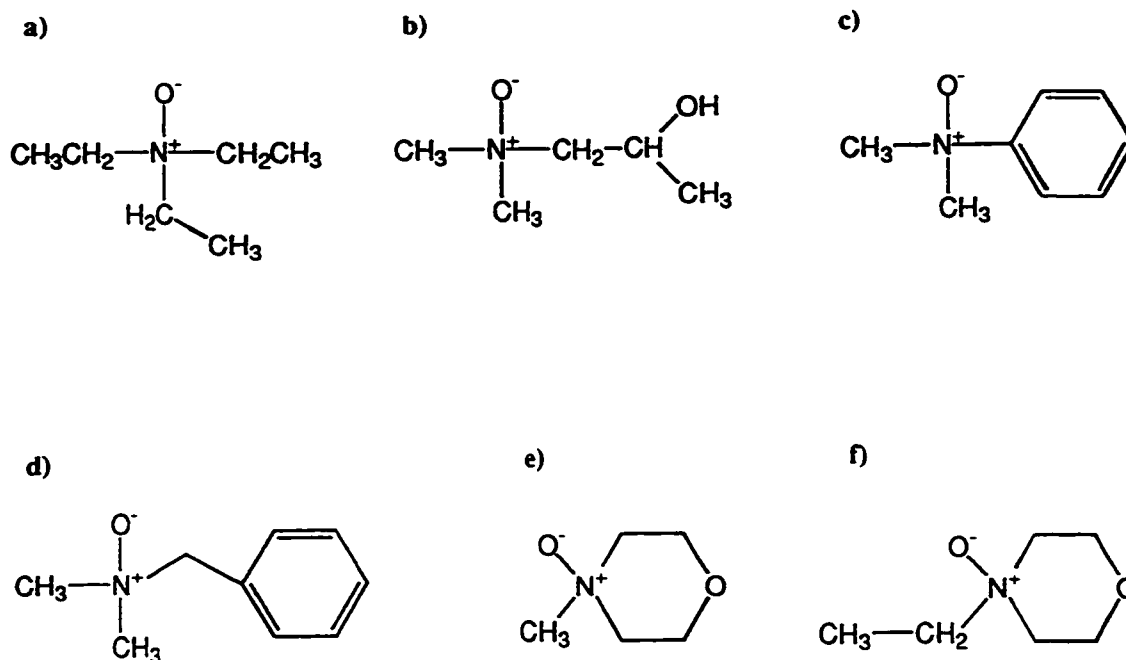


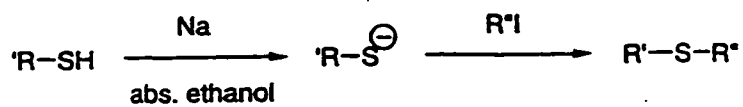
Figure 2-2. Chemical structures of amine oxides synthesized in this study.
a) triethylamine N-oxide; b) 1-dimethylaminopropanol-2 N-oxide; c) N,N-dimethylaniline N-oxide; d) N,N-dimethylbenzylamine N-oxide; e) 4-methylmorpholine N-oxide; f) 4-ethylmorpholine N-oxide.

Synthesis of sulfoxides

Synthesis of dialkyl- and alkyl aryl sulfoxides was performed by oxidation of the corresponding sulfides by 30% hydrogen peroxide in acetone as shown on Fig. 2-3, step 2 (Gazdar and Smiles, 1908). Ethyl sulfide and propyl sulfide were purchased from Aldrich while other sulfides were synthesized by alkylation of the corresponding mercaptans (Fig. 2-3, step 1) with methyl or ethyl iodide (Lewis and Archer, 1951). Resulting sulfoxides were purified by high-vacuum distillation. There is a significant difference in boiling temperature between sulfoxides and the corresponding sulfides that allows to effectively separate these compounds by distillation.

Boiling points after second distillation of all sulfoxides synthesized were in good agreement with published values.

Step 1



Step 2

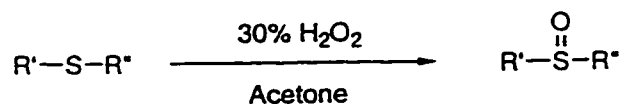
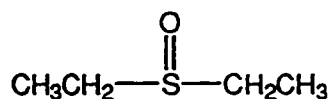
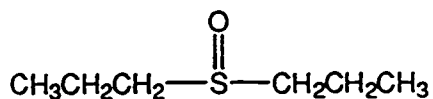


Figure 2-3. Synthesis of sulfoxides.

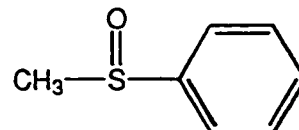
a)



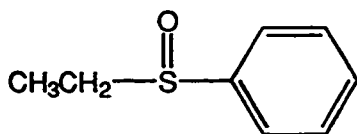
b)



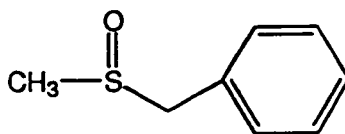
c)



d)



e)



f)

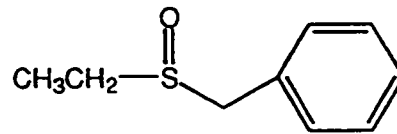


Figure 2-4. Chemical structures of sulfoxides synthesized for this study. a) Ethyl sulfoxide; b) propyl sulfoxide; c) methyl phenyl sulfoxide; d) ethyl phenyl sulfoxide; e) methyl benzyl sulfoxide; f) ethyl benzyl sulfoxide.

Synthesis of alkyl aryl sulfides

A solution of 0.47 mole of mercaptan (benzyl mercaptan, 36.4 ml or thioanisole, 32 ml) and 4.6 g (0.3 mole) sodium in 200 ml anhydrous ethanol was cooled on ice bath and kept at this temperature during the dropwise addition of a solution of 0.35 mole alkyl iodide (methyl iodide, 14 ml or ethyl iodide, 18.4 ml) in 70 ml anhydrous ethanol. The mixture was stirred for 3 hours, then the ice bath was removed and the mixture was allowed to warm to room temperature. The reaction was stirred overnight at room temperature.

The condenser set for downward distillation was attached to the flask and, after about 200 ml of ethanol had distilled, the emulsion was poured into 100 ml water with ice. The organic layer was separated and aqueous phase was washed twice with 100 ml benzene. The combined organic fractions were washed with 100 ml water, dilute sodium hydroxide and again with water. The benzene was distilled under normal pressure, and the residue was purified by vacuum distillation.

In the following table the boiling temperatures of alkyl aryl sulfides synthesized are compared with previously published data (Table 2-2). Since these compounds have been synthesized and characterized more than a century ago, the references are given to the Beilstein Handbook of Organic Chemistry where the data from various publications of that time are summarized.

Table 2-2. Boiling points of alkyl aryl sulfides

Substance	Boiling point, °C (mm Hg)	Published boiling point, °C (mm Hg)	Reference
Methyl phenyl sulfide	29-31 (0.8)	193, 74.2 (12)	Beilstein 6, IV 1466
Ethyl phenyl sulfide	39-40 (0.8)	204.5-205.5, 83-84 (10)	Beilstein 6, IV 1468
Methyl benzyl sulfide	62-63 (4)	195-198, 91-92 (12)	Beilstein 6, IV 2633
Ethyl benzyl sulfide	48-50 (0.4)	218-224, 102-104 (15)	Beilstein 6, IV 2635

Oxidation of sulfides to sulfoxides

Sulfoxides were synthesized from sulfides by oxidation with 30% hydrogen peroxide in acetone (Gazdar and Smiles, 1908).

A sulfide (140 mmole) was dissolved in 60 ml acetone and cooled on ice bath. A solution of 140 mmole (16 ml) 30% hydrogen peroxide in 10 ml acetone was slowly added, and the reaction was stirred overnight at room temperature. After addition of 250 ml water the mixture was extracted with ether (2x200 ml). The combined organic fractions were washed with 250 ml water, dried over anhydrous sodium sulfate and evaporated in vacuum. The main fraction was redistilled in vacuum. Yields of sulfoxides vary from 10% to 45% because significant amount of the sulfides remained intact under these conditions. The yields could be increased by using larger amounts of hydrogen peroxide and higher temperature, but the concurrent reaction of the formation of sulfone from sulfoxide and excess of hydrogen peroxide would have made the purification of sulfoxides more complicated.

Boiling points or melting points of the synthesized sulfoxides are given in Table 2-3.

Table 2-3. Physical properties of sulfoxides

Substance	bp, °C (mm Hg) or mp, °C ^{a)}	Published data	Reference
Methyl phenyl sulfoxide	bp 125 (4)	264, 115 (2)	Beilstein 6, IV 1467
Ethyl phenyl sulfoxide	bp 88-90 (0.8)	146 (13), 124 (2)	Beilstein 6, IV 1469
Methyl benzyl sulfoxide	bp 132 (2)	116-118 (0.8)	Beilstein 6, IV 2634
Ethyl benzyl sulfoxide	mp 45-46	49	Beilstein 6, III 1575b
Ethyl sulfoxide	bp 85 (13)	87 (14)	Beilstein 1, IV 1395
Propyl sulfoxide	bp 84-86 (4)	115 (16), 80 (2)	Beilstein 1, IV 1453

^{a)} bp, boiling point
mp, melting point

Bibliography

- Anderson, R.J. and M.S. Newman (1933). The chemistry of the lipids of tubercle bacilli. XXXVII. The synthesis of phtiocol, the pigment of the human Tubercle bacillus. *J. Chem. Soc.* , 405-412.
- Baker, B.R., T.H. Davies, L. McElroy and G.H. Carlson (1942). The antihemorrhagic activity of sulfonated derivatives of 2-methylnaphthalene. *J. Amer. Chem. Soc.* **64**, 1096-1101.
- Bilous, P.T. and J.H. Weiner (1985). Dimethyl sulfoxide reductase activity by anaerobically grown *Escherichia coli*. *J. Bacteriol.* **162**, 1151-1155.
- Boyer, H.W. and D. Roulland-Dussoix (1969). A complementary analysis of the restriction and modification of DNA in *Escherichia coli*. *J. Mol. Biol.* **41**, 459-472.
- Cammack, R. and J.H. Weiner (1990). Electron paramagnetic resonance spectroscopic characterization of dimethyl sulfoxide reductase of *Escherichia coli*. *Biochemistry* **29**, 8410-8416.
- Cope, A.C. and E. Ciganec (1963a). Methylenecyclohexane and N,N-dimethylhydroxylamine hydrochloride. *Org. Syn., Coll. Vol.* **4**, 612-615.
- Cope, A.C. and E. Ciganec (1963b). N,N-Dimethylcyclohexylmethylamine. *Org. Syn., Coll. Vol.* **4**, 339-344.
- Cornish-Bowden, A. (1995). Analysis of enzyme kinetic data (New York: Oxford University Press Inc.).
- Fieser, L.F. and J.L. Hartwell (1935). The reaction of hydrazoic acid with the naphthoquinones. *J. Amer. Chem. Soc.* **57**, 1482.
- Gazdar, M. and S. Smiles (1908). *J. Chem. Soc.* **93**, 1833.
- Guigliarelli, B., A. Magalon, M. Asso, P. Bertrand, C. Frixon, G. Giordano and F. Blasco (1996). Complete coordination of the four Fe-S centers of the beta subunit from *Escherichia coli* nitrate reductase. Physiological, biochemical, and EPR characterization of site-directed mutants lacking the highest or lowest potential [4Fe-4S] clusters. *Biochemistry* **35**, 4828-4836.

- Leandri, G., A. Mangini and R. Passerini (1957). Absorption spectra of some sulfoxides in the near ultraviolet region. *J. Chem. Soc.* , 1386-1395.
- Lemire, B.D., J.J. Robinson and J.H. Weiner (1982). Identification of membrane anchor polypeptides of *Escherichia coli* fumarate reductase. *J. Bacteriol.* **152**, 1126-1131.
- Lewis, T.R. and S. Archer (1951). Alkyl phenyl-(2-pyridyl)-methyl sulfones. Sulfonium salts as alkylating agents. *J. Amer. Chem. Soc.* **73**, 2109-2113.
- Markwell, M.A.K., S.M. Haas, L.L. Bieber and N.E. Tolbert (1978). A modification of the Lowry procedure to simplify protein determination in membrane and lipoprotein samples. *Anal. Biochem.* **87**, 206-210.
- Rothery, R.A. and J.H. Weiner (1991). Alteration of the iron-sulfur cluster composition of *Escherichia coli* dimethyl sulfoxide reductase by site-specific mutagenesis. *Biochemistry* **30**, 8296-8305.
- Sambasivarao, D. and J.H. Weiner (1991). Differentiation of the multiple S- and N-oxide reducing activities of *Escherichia coli*. *Curr. Microbiol.* **23**, 105-110.
- Sambrook, J., E.F. Fritsch and T. Maniatis. (1989). *Molecular Cloning: a Laboratory Manual* (Cold Spring Harbor, NY: Cold Spring Harbor Laboratory).
- Simala-Grant, J.L and J.H. Weiner (1996). Kinetic analysis and substrate specificity of *Escherichia coli* dimethyl sulfoxide reductase. *Microbiology* **142**, 3231-3239.
- Weiner, J.H., D.P. MacIsaac, R.E. Bishop and P.T. Bilous (1988). Purification and properties of *Escherichia coli* dimethyl sulfoxide reductase, an iron-sulfur molybdoenzyme with broad substrate specificity. *J. Bacteriol.* **170**, 1505-1510.

Chapter 3. Quinone substrates for DMSO reductase

Introduction

Biochemistry of quinones

Quinones synthesized by *E.coli* are very hydrophobic molecules with a slightly polar head group and a long polyisoprenoid tail (Fig. 1-1, p. 2). The apparent reason for the high hydrophobicity of quinone molecules is to prevent their diffusion from the membrane bilayer to the surrounding aqueous environment. The long hydrophobic tail containing forty atoms of carbon is more than sufficient to keep quinone molecules in the membrane; their solubility in water does not exceed 10^{-4} - 10^{-5} M. Quinols, on the other hand, are able to form much stronger hydrogen bonds with water, and their partition coefficients are much less favorable for the lipid phase (Rich and Harper, 1990). This can explain the presence of the hydrocarbon tail in all naturally occurring quinones involved in electron transport.

The high hydrophobicity of natural quinones and even their synthetic analogs lacking the hydrophobic tail makes enzymatic assays very difficult. There are only a few papers on enzyme kinetics where quinones are used as substrates and measured directly because low solubility does not allow the use of a wide enough range of substrate concentrations (Kröger *et al.*, 1979; Weiner *et al.*, 1986). More often, reaction of an enzyme with quinones is monitored by the change in adsorption of the other substrate such as a cytochrome (Estornell *et al.*, 1996), NADH (Marcinkeviciene and Blanchard, 1995), or an intermediate electron carrier such as dithionite (Sambasivarao and Weiner, 1991). As mentioned above, spectroscopic properties of amine oxides and sulfoxides do not allow monitoring of the course of their reduction. Recently, it has been discovered that excess of dithionite greatly affects the apparent K_m for TMAO (Simala-Grant and Weiner, 1996), so that the assay in which quinol oxidation is measured by the change in dithionite concentration probably cannot provide reliable kinetic data.

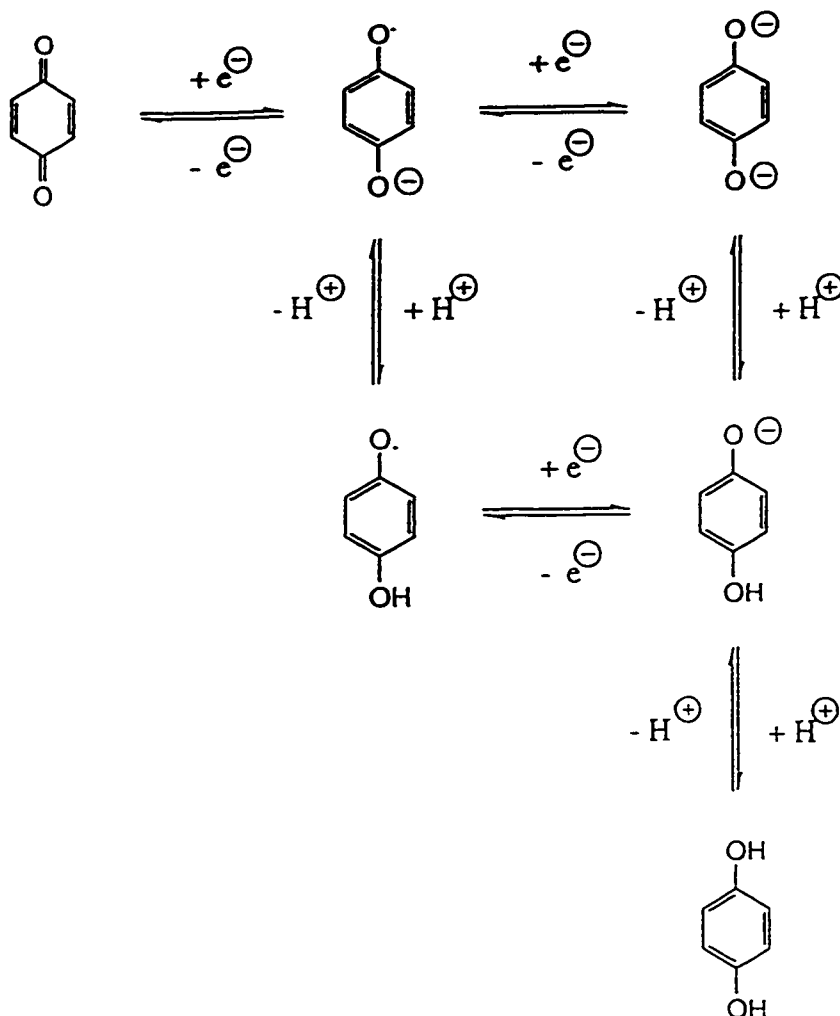


Figure 3-1. Redox and acid-base equilibrium in quinones. Substituents are not shown for clarity.

Although *E.coli* is able to express three chemically distinct quinones, only two of them, menaquinone and demethylmenaquinone, are present under anaerobic conditions (Table 3-1). DMQ predominates when bacteria grow anaerobically in the presence of nitrate, so that MQ represents the major quinone molecule when DMSO reductase is expressed. Experiments with *E.coli* quinone biosynthesis mutants *men* and *ubi* demonstrated that MQ is required for anaerobic growth on DMSO while UQ does not support growth (Weiner *et al.*, 1992).

Table 3-1. Quinone content of *E.coli* membranes after aerobic and anaerobic growth on glucose and various electron acceptors

(modified from Unden, G. and J. Bongaerts (1997))

Quinone	Content, μmol quinone per g dry weight (% total)		
	O ₂	Nitrate	Fumarate or DMSO
Ubiquinone (UQ)	0.36 (60%)	undetectable	0.09 (10%)
Demethylmenaquinone (DMQ)	0.22 (37%)	0.69 (70%)	0.14 (16%)
Menaquinone (MQ)	0.02 (3%)	0.29 (30%)	0.66 (74%)

The preference for a quinone is probably dictated by its redox potential rather than its structural features. Ubiquinone is a benzoquinone derivative and has a high redox potential, +100 mV. Menaquinone has a naphthoquinone nucleus and a lower potential of -74 mV. DMSO reductase is also capable of using several quinone analogs as electron acceptors. Reduced forms of 2,3-dimethyl-1,4-naphthoquinone, DMNQH₂, and duroquinone (2,3,5,6-tetramethyl-1,4-benzoquinone), DQH₂, can serve as electron donors for DMSO reductase despite their structural difference. Their midpoint redox potentials at pH 7.0 for the first step of reduction ($Q + e^- \rightarrow Q^-$) are very close, -240 mV and -235 mV, respectively (Ilan *et al.*, 1976; Meisel and Czapski, 1975) although two-electron redox potentials are quite different, (-70 mV and +50 mV, correspondingly) (Patel and Willson, 1973). This raises a possibility that the preferred reduced quinone molecule for DMSO reductase may be semiquinone produced by a dehydrogenase. It is not known so far whether this is correct.

Chemistry of naphthoquinones

The most remarkable property of quinones is their rapid and reversible reduction. It can occur in two steps in which a quinone molecule accepts one electron and one proton with formation of semiquinone radical (Fig. 3-1). In the second step, semiquinone combines with one more electron and proton producing the molecule of the corresponding quinol. Although semiquinones can be detected in membranes, these particles are unstable and

rapidly undergo either redox conversion (oxidation or reduction) or disproportionation (interaction of two semiquinone molecules resulting in one quinone and one quinol molecule). Oxidation of the quinol is also a two-step process.

The chemistry of quinone reduction is not often as simple as described above. There are several side reactions that could make a quinone assay much more complicated. First of all, many quinones and quinols can form *quinhydrons*, weak charge-transfer complexes consisting of one quinone and one quinol molecule. Despite the fact that most quinhydrone molecules can easily dissociate in solution, they absorb visible and UV radiation much more strongly than their components alone. So far, the significance of this phenomenon has not been studied. It is not known whether or not quinones form quinhydrons in membranes, but they certainly can in the assay cuvette. As a result, the spectrum of quinone-quinol mixture may not always be represented as a sum of quinone and quinol spectra.

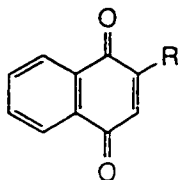
The ability of a quinone to form quinhydrone depends on its structure and electrochemical properties. Bulky substituents in the quinone ring prevent the interaction of the oxidized and reduced forms; this can explain the fact that duroquinone does not form quinhydrone. DMNQ, a widely used quinone analog, does form quinhydrone, and isolation of pure DMNQH₂ proved to be very difficult even in the atmosphere of nitrogen due to its easy oxidation and formation of intensely colored quinhydrone (Crawford, 1935). Apparently, two methyl groups in this naphthoquinone do not sterically block formation of the charge transfer complex.

Quinones with very high or very low midpoint potentials do not form quinhydrons with their corresponding quinols because in the first case the quinol is not electronegative enough to interact with highly electropositive quinone; in the second case, both oxidized and reduced forms of quinone are too electronegative. Due to thermodynamic considerations, the latter quinone would be preferred since low midpoint potential of the quinone favors the reaction flow in the direction of DMSO reduction.

The redox potential of quinones is defined by the structure of its ring (potential of naphthoquinones is about 200 mV more negative than potential of the corresponding

Table 3-2. The effect of substituent groups on the potential of 2-substituted 1,4-naphthoquinones

(modified from Fieser, L.F. and J.L. Hartwell (1935))



Substituent,R	Effect, mV	Substituent,R	Effect, mV	Substituent,R	Effect, mV
-NHCH ₃	-252	-OH	-127	-OCOCH ₃	-9
-NH ₂	-210	-CH ₃	-76	-Cl	+24
-NHC ₆ H ₅	-198	-NHCOCH ₃	-67	-SO ₃ Na	+69
-N(CH ₃) ₂	-181	-CH(C ₆ H ₅) ₂	-51	-SO ₂ C ₆ H ₄ CH ₃	+121
-OCH ₃	-131	-C ₆ H ₅	-32		

benzoquinones) and the nature of substituents (Table 3-2). As expected, *ortho-para*-directing substituents decrease the potential while *meta*-directing groups increase it by affecting the overall electron density of the ring.

Summarizing these data, one can conclude that the potential quinone candidate for enzymatic assay should be a naphthoquinone or heavily substituted benzoquinone bearing some electron-donating substituents such as amino-, methoxy-, hydroxy-, methyl groups. On the other hand, if such compounds will not show appropriate spectroscopic properties, an electron-withdrawing substituent (sulfo-, nitro-) may be the reporter group of choice. Despite their higher redox potentials, these derivatives may have valuable spectroscopic properties such as intensive absorption in the visible range that depends on the quinone redox state.

Absorption of naphthoquinones in the UV and visible spectral regions is caused by the presence of two chromophors: carbonyl group (λ_{max} 280 nm, ϵ 20) and a cyclic system of highly conjugated (separated by a single ordinary bond) double bonds (λ_{max} 265 nm, ϵ about 3000). Since these two chromophors in turn are conjugated, the overall spectrum

has new very intensive absorption peaks (Fig. 3-5, peaks at 250-280 nm with ϵ 10,000-12,000). Unfortunately, this region of spectrum is overcrowded because every aromatic ring absorbs at 254-280 nm. As a result, the difference in spectrum between oxidized and reduced form of quinone is very small.

Addition of so-called auxochromes (groups like thiol -SH, hydroxyl -OH, amino group -NH₂, that do not absorb light themselves but cause a red shift and increase in intensity of existing spectral lines) can lead to quinones with absorption in the visible region of spectrum. Potential quinone substrates can also be obtained by addition to the quinone ring of another chromophore such as the nitro group (λ_{\max} 280 nm, ϵ 20) or iodine (λ_{\max} 260 nm, ϵ 400). The latter two groups will cause an increase in the redox potential of the naphthoquinone derivatives but if these compounds have distinctive spectra, their use may be justified even if reaction rates are slower.

The ability of quinones to easily react with thiols represent another possible complication (Fieser and Turner, 1947). Thiols, e.g. dithiothreitol or 2-mercaptoethanol, are often added to assay mixtures and enzyme stock solutions to prevent oxidation of enzyme cysteine residues. Quinones having free positions in the ring can react with these thiols and even with exposed cysteine groups of proteins with formation of corresponding adducts (Fig. 3-2). The ability of quinones to react with proteins quickly and irreversibly has been widely exploited, and such quinones as lawsone and lapachol are still used as industrial dyes (Natural Orange 6 and Natural Yellow 16, respectively). The modification of proteins by quinones has been also noted as a complication in the treatment of hemorrhagical patients with derivatives of vitamin K₁ (Fieser and Turner, 1947 and references therein).

To prevent this side reaction, the potential quinone substrate of DMSO reductase should have all positions in the quinonoid ring blocked by substituents.

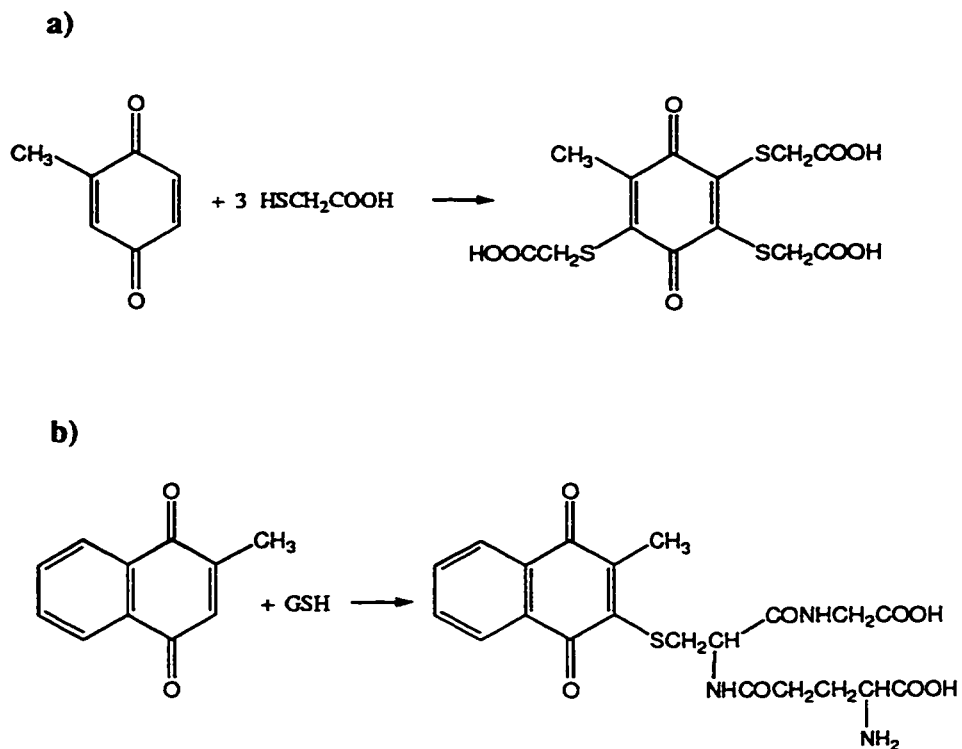


Figure 3-2. The interaction of quinones with mercaptans. a) All free positions of the quinonoid ring can be substituted by thiols. Sulfhydryl groups of cysteine in proteins readily form conjugates with quinones in the same way. b) In naphthoquinones, the benzenoid ring is not affected. GSH, reduced glutathione.

Results

Synthesis and properties of 2-methyl-3-nitro-1,4-naphthoquinone

The synthesis was performed in two steps (Fig. 3-3). 2-Methyl-1,4-hydroxynaphthalene diacetate was synthesized by reductive acetylation of 2-methyl-1,4-naphthoquinone (menadione) with acetic anhydride and zinc as described in the literature with 90-95% yield (Anderson and Newman, 1933). The nitro group was introduced using protocol modified from (Baker *et al.*, 1942) in which chlorosulfonic acid was replaced with sulfuric acid and the yield of the final product was increased from about 30% to 85-90%. MNNQ is a yellow solid barely soluble in water. The corresponding hydroquinone (MNNQH₂) has not been obtained. Attempts to reduce MNNQ to MNNQH₂ with a mild reductant N,N-diethylhydroxylamine that has been reported to be capable of reducing quinones without affecting other easily reducible groups (Fujita and Sano, 1975) was unsuccessful when carried out in benzene, toluene or ethyl acetate; MNNQ was unaffected by N,N-diethylhydroxylamine according to TLC.

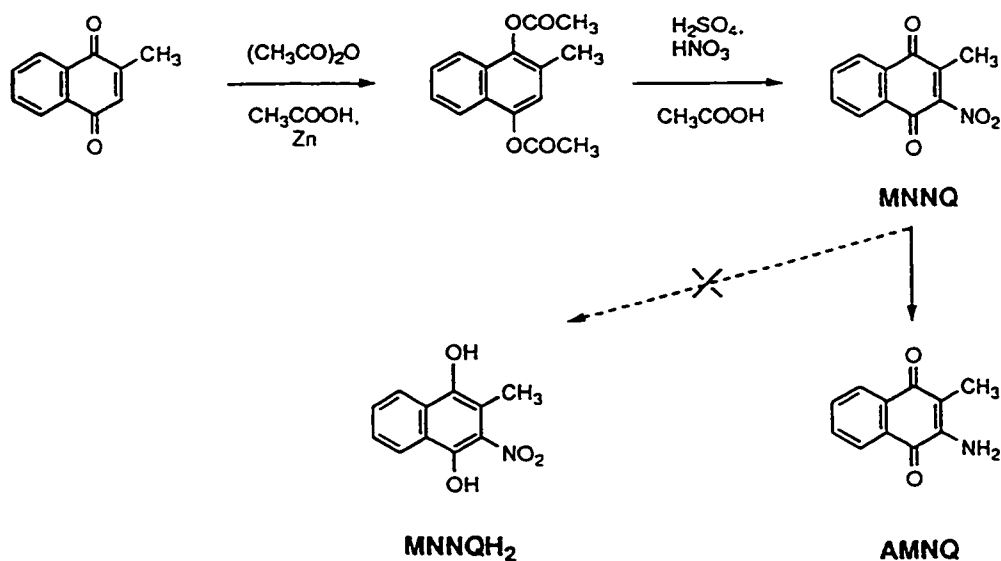


Figure 3-3. Synthesis of 2-methyl-3-nitro-1,4-naphthoquinone.

Reduction of MNNQ with stronger reductants such as zinc/hydrochloric acid, sodium dithionite, sodium borohydride gave a dark red solution. Successive oxidation of the resulting substance with FeCl_3 or hydrogen peroxide did not lead back to MNNQ. Apparently, the red substance represents the product of reduction of the nitro group in MNNQ to amino group with the formation of 3-amino-2-methyl-1,4-naphthoquinone (AMNQ). This conclusion was later confirmed by comparison of chromatographic mobility of this sample and purified AMNQ. Treatment with large excess of reductant leads to disappearance of the red color and formation of colorless solution. It was suggested that the hydroquinone of AMNQ is colorless, unlike its oxidized form.

Synthesis and physical properties of 3-amino-2-methyl-1,4-naphthoquinone (AMNQ) and 2-amino-3-methyl-1,4-dihydroxynaphthalene (AMNQH₂)

Synthesis of AMNQ by hydrogenation of MNNQ with platinum catalyst was reported a long time ago (Baker *et al.*, 1942). The product, a red crystalline substance, was obtained in different forms including neutral compound, triacetate and hydroquinone. The color and solubility of the hydroquinone in water were not reported.

Since AMNQ is not commercially available, it was synthesized in this study from menadione using a one-step protocol analogous to the method reported by L.F. Fieser (Fieser and Hartwell, 1935) for 2-aminonaphthoquinone (Fig. 3-4). This method is faster and simpler than the method proposed by Baker, although it was found that interaction of menadione with sodium azide requires more time than reported by L.F. Fieser (overnight instead of 2 hours).

Reduction of MNNQ to AMNQ with sodium dithionite or other reducing agents (sodium borohydride, stannous chloride, zinc/hydrochloric acid) leads to formation of AMNQ that can be isolated by organic solvent extraction and recrystallization, although the yield is very low in most cases.

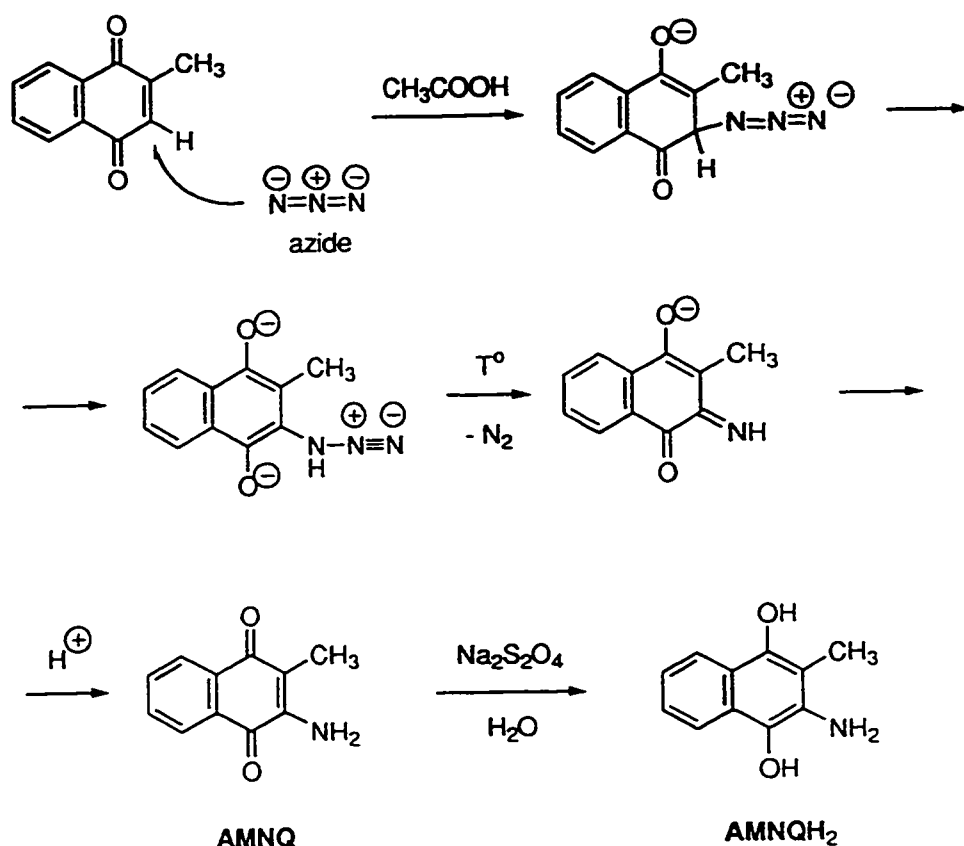
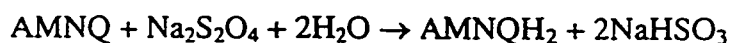


Figure 3-4. Synthesis of 3-amino-2-methyl-1,4-naphthoquinone (AMNQ) and 2-amino-3-methyl-1,4-dihydroxynaphthalene (AMNQH₂).

Further reduction of AMNQ brings about colorless (slightly yellow in organic solvents) hydroquinone (AMNQH₂). The red color of AMNQ disappears gradually upon the addition of reductant, no formation of any highly-colored molecular species such as quinhydron has been observed. Reoxidation of AMNQH₂ by air, ferrous chloride or hydrogen peroxide regenerates the original quinone.

Since AMNQH₂ is not stable in the presence of oxygen, it was synthesized for enzyme assays using *in situ* reduction of equimolar amount of AMNQ by sodium dithionite:



UV/visible spectra of the oxidized and reduced form of AMNQ show significant difference in the region 440-520 nm where quinone absorption reaches maximum at 465 nm with extinction coefficient (ϵ) of $2100 \text{ M}^{-1}\text{cm}^{-1}$ while absorption of the reduced form is more than ten times less (Fig.3-5).

AMNQ is appreciably soluble in water, up to 0.26 mM (determined spectrophotometrically). Its reduced form is at least twice more soluble. Solubility of AMNQ is higher in organic solvents: 1 mM in 20% aqueous ethanol, 30 mM in isopropanol, 40 mM in ethanol (determined by dissolving AMNQ in the corresponding solvent). Solubility of AMNQ in chloroform, acetone and especially acetonitrile is very high and was not determined. Solubility of AMNQ in acidic solutions (including concentrated hydrochloric acid) is not significantly increased in comparison with water.

The reduced form of 3-amino-2-methyl-1,4-naphthoquinone is a substrate of DMSO reductase from *E.coli*

AMNQH₂ can serve as the terminal electron donor in DMSO reductase-catalyzed reduction of various N- and S-oxides. Steady-state analysis of reactions demonstrated that both oxidant and reductant follow Michaelis-Menten kinetics when concentration of the other substrate is kept constant (Fig. 3-6-3-8).

Apparent K_m for TMAO at 0.5 mM AMNQH₂ (almost saturating concentration in water) is $11 \pm 2 \text{ } \mu\text{M}$, for PyNO $26 \pm 12 \text{ } \mu\text{M}$. Apparent K_m for AMNQ at enzyme-saturating concentration of TMAO (14 mM) is $1.16 \pm 0.14 \text{ mM}$. Michaelis constant for DMSO was not determined because the reaction rate remained practically constant even at the lowest concentration of DMSO tested, 2 μM .

Kinetic analysis of the two-substrate reaction catalyzed by DMSO reductase

Since the enzyme-saturating concentration of AMNQ cannot be achieved due to insufficient solubility of this compound and its high Michaelis constant, a series of measurements at various concentrations of AMNQ and PyNO was carried out to extrapolate K_m for PyNO to enzyme-saturating concentration of AMNQ and estimate the effect of increase in AMNQ concentration on apparent kinetic parameters of PyNO.

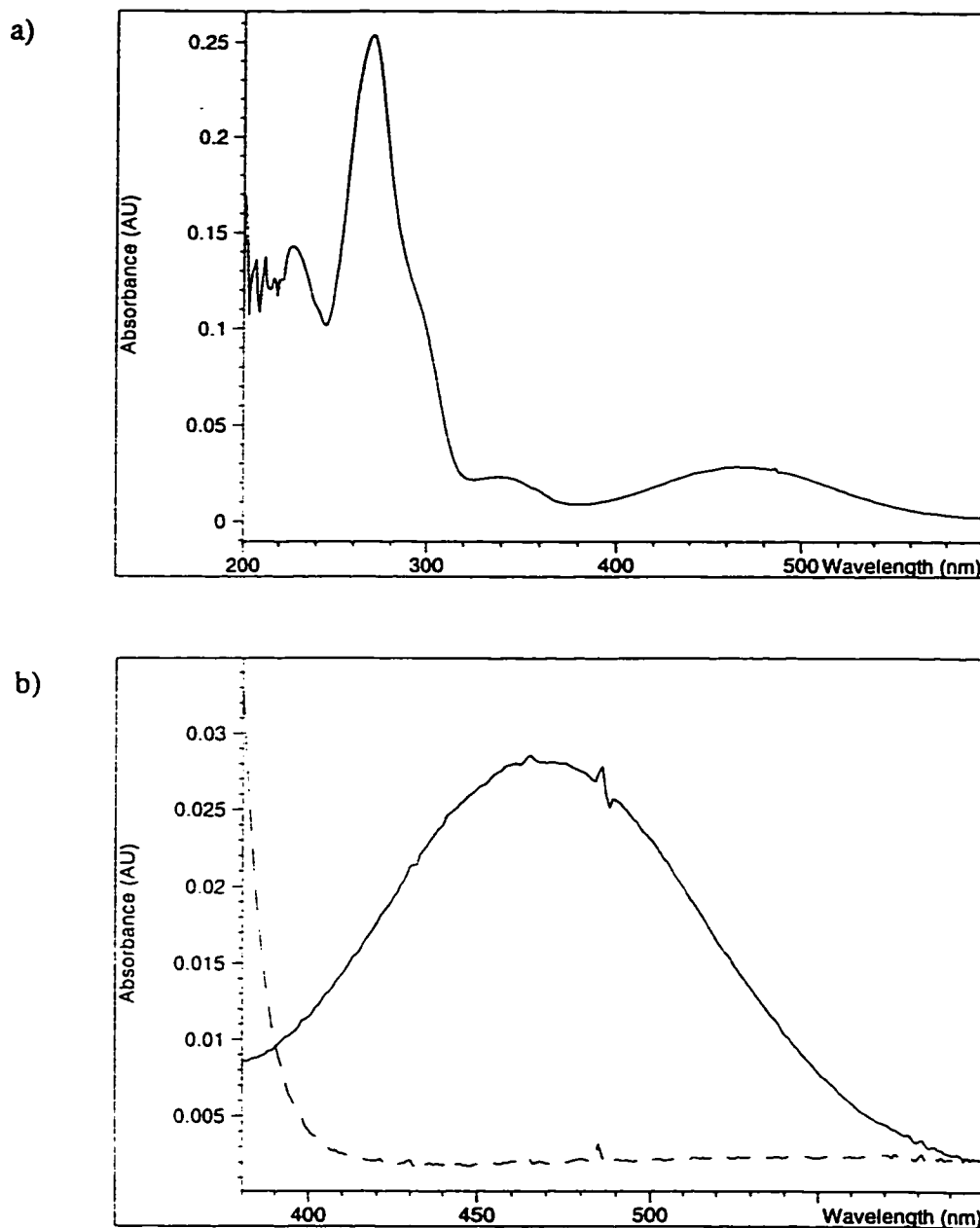


Figure 3-5. The UV/visible spectrum of 3-amino-2-methyl-1,4-naphthoquinone in the oxidized and reduced state. a) The absorption spectrum of 12.5 μM AMNQ in 100 mM MOPS buffer pH 7.0 at 30°C; b) the disappearance of the long-wave maximum at 465 nm upon the reduction of AMNQ (solid line) to AMNQH₂ (broken line) by sodium dithionite.

Reaction rate was measured at six concentrations of AMNQ and six concentrations of PyNO that varied around the K_m values determined in the previous experiment. Results were analyzed with LEONORA using equations for several possible reaction mechanisms: the ping-pong (substituted enzyme) mechanism, the ternary complex mechanism, and two ordered equilibrium mechanisms. The latter two gave unsatisfactory fit and were rejected. In order to distinguish the substituted-enzyme and the ternary-complex mechanisms, the analysis of Cleland (Cleland, 1963) was applied based on the variation of apparent Michaelis constant of one substrate with concentration of the other substrate.

Calculations of K_m^{PyNO} at different concentrations of AMNQH₂ gave a linear relationship between the apparent K_m and the quinone concentration, and the Michaelis constant decreases to zero when concentration of AMNQH₂ goes to zero (Fig. 3-9, p. 66), in full compliance with the Eq. 1-24 (p. 28) for bireactant ping-pong mechanism.

To further test the kinetic mechanism of the reaction, its double reciprocal plots were analyzed as described by A.Kröger for formate dehydrogenase from *Vibrio succinogenes* (Kröger *et al.*, 1979). This method is based on the dependence of the reciprocal initial reaction rate on the reciprocal substrate concentration when the concentration of the second substrate is kept constant (Eq. 1-25, p. 29 and 1-26, p. 29).

The plot of reciprocal enzyme activity vs. reciprocal concentration of PyNO at different concentrations of AMNQH₂ gave a set of nearly parallel straight lines (Fig. 3-10a, p. 67). Ordinate interceptions of these lines were plotted against reciprocal concentrations of AMNQ and, again, a straight line was obtained (Fig. 3-10b).

From this, one can conclude that reduction of PyNO catalyzed by DMSO reductase with AMNQH₂ as electron donor has the ping-pong mechanism. Kinetic parameters calculated from the entire set of data are the following:

V_{\max}	14.1±2.2 units per mg enzyme
K^{PyNO}	39.3±7.0 µM
K^{AMNQH_2}	1.80±0.30 mM

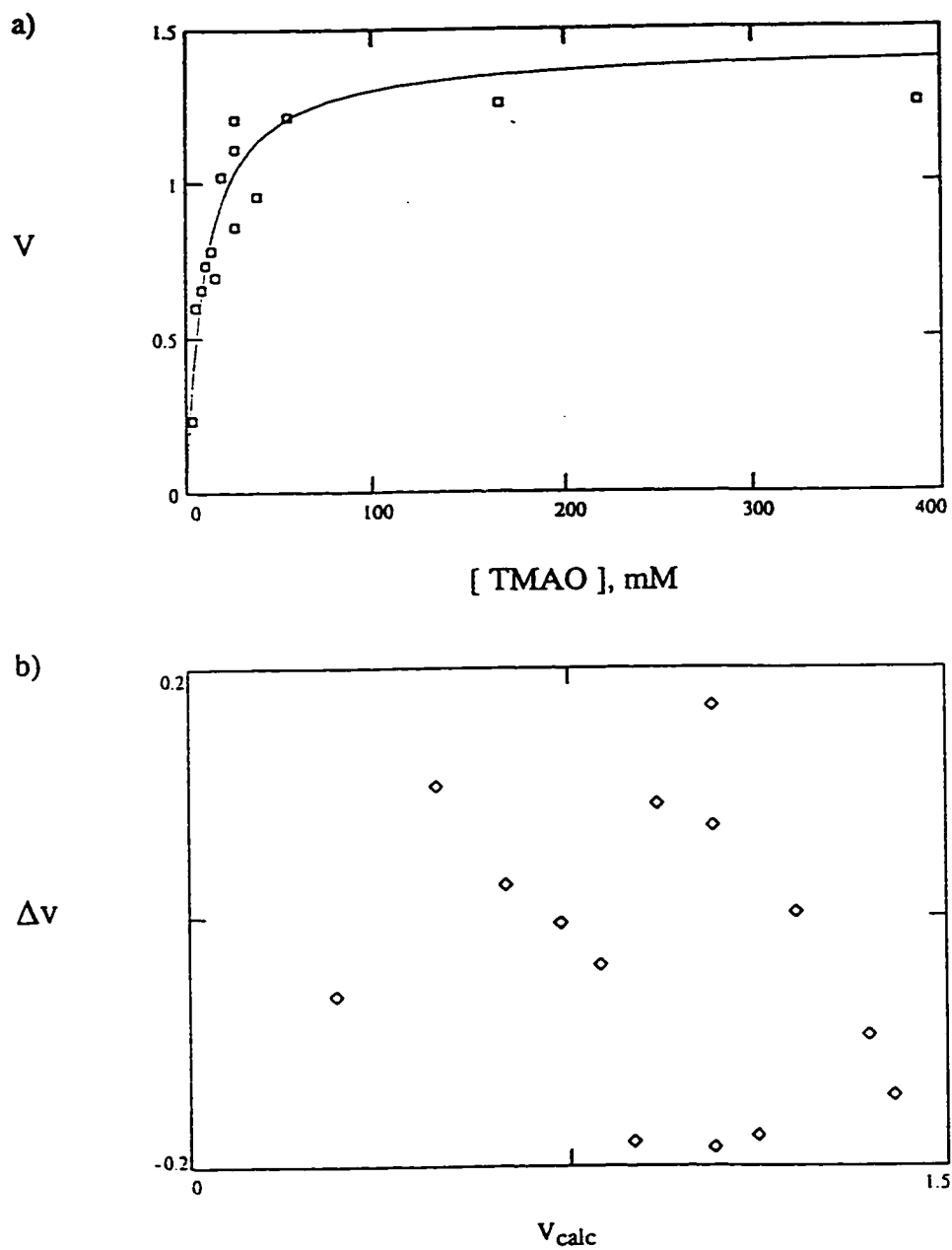


Figure 3-6. The reduction of trimethylamine N-oxide (TMAO) catalyzed by DMSO reductase from *E.coli* with AMNQH₂ as electron donor. a) Plot of enzyme activity (in $\mu\text{mole AMNQH}_2/\text{min per mg protein}$) vs. the concentration of TMAO; b) the residual plot.

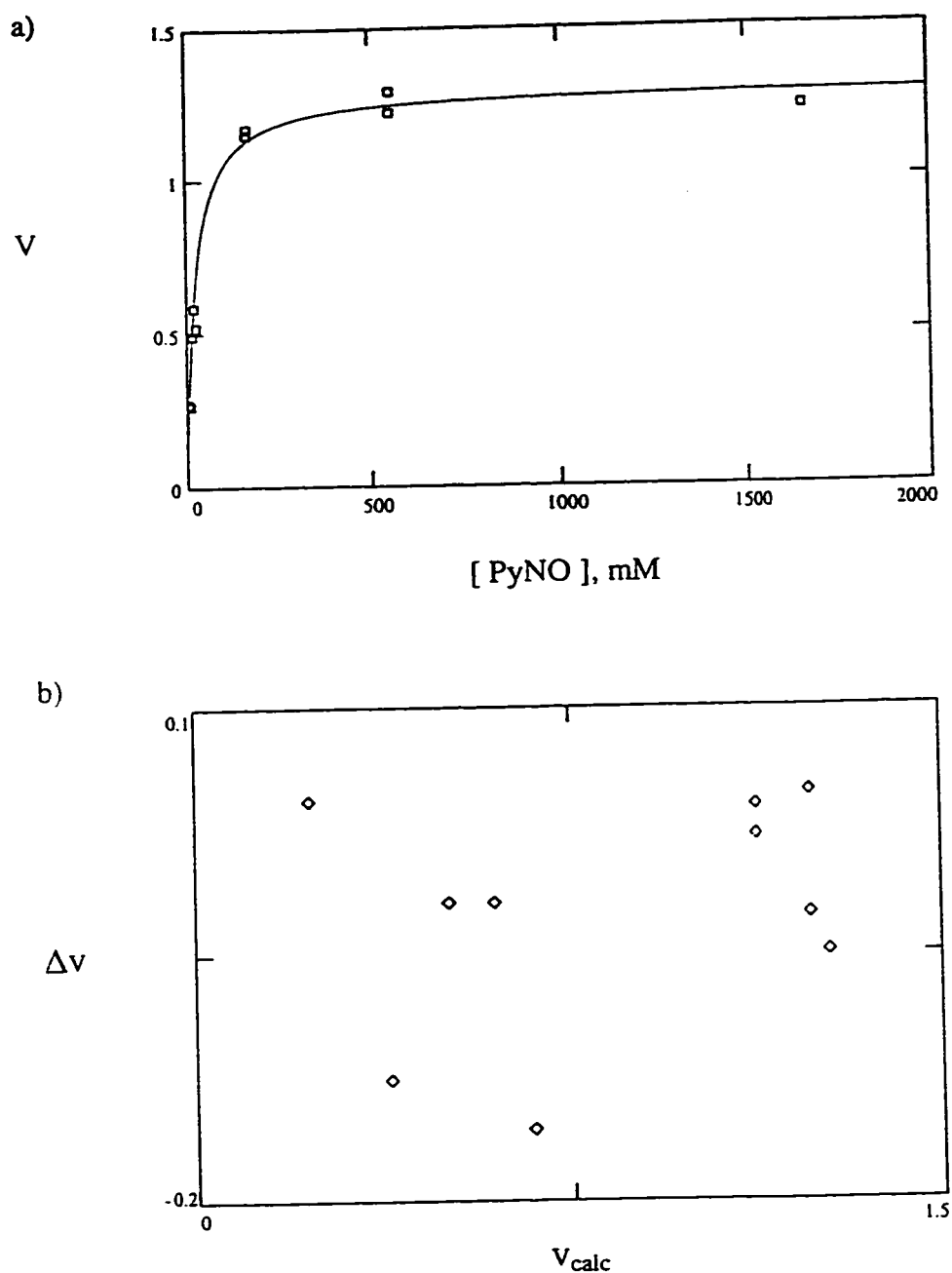


Figure 3-7. The reduction of pyridine N-oxide (PyNO) catalyzed by *E. coli* DMSO reductase with AMNQH₂ as electron donor. a) The plot of enzyme activity (in $\mu\text{mole AMNQH}_2/\text{min per mg protein}$) vs. the concentration of PyNO; b) the residual plot. Points of highest concentration are omitted from the residual plot to make the picture more illustrative.

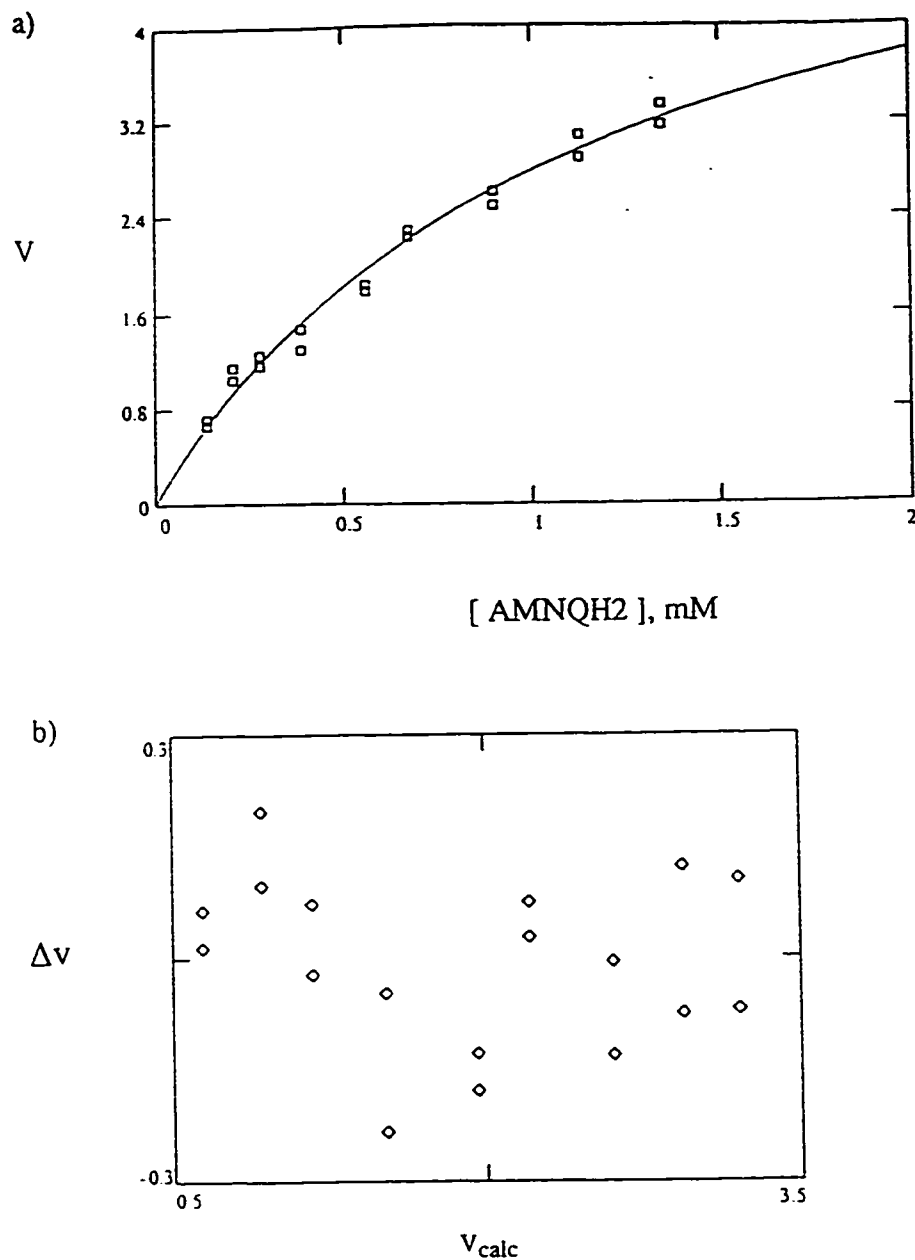


Figure 3-8. The oxidation of AMNQH_2 catalyzed by *E.coli* DMSO reductase with TMAO as electron acceptor at enzyme-saturating concentration (14 mM). a) The plot of enzyme activity (in $\mu\text{mole AMNQH}_2/\text{min per mg protein}$) vs. the substrate concentration. b) the residual plot.

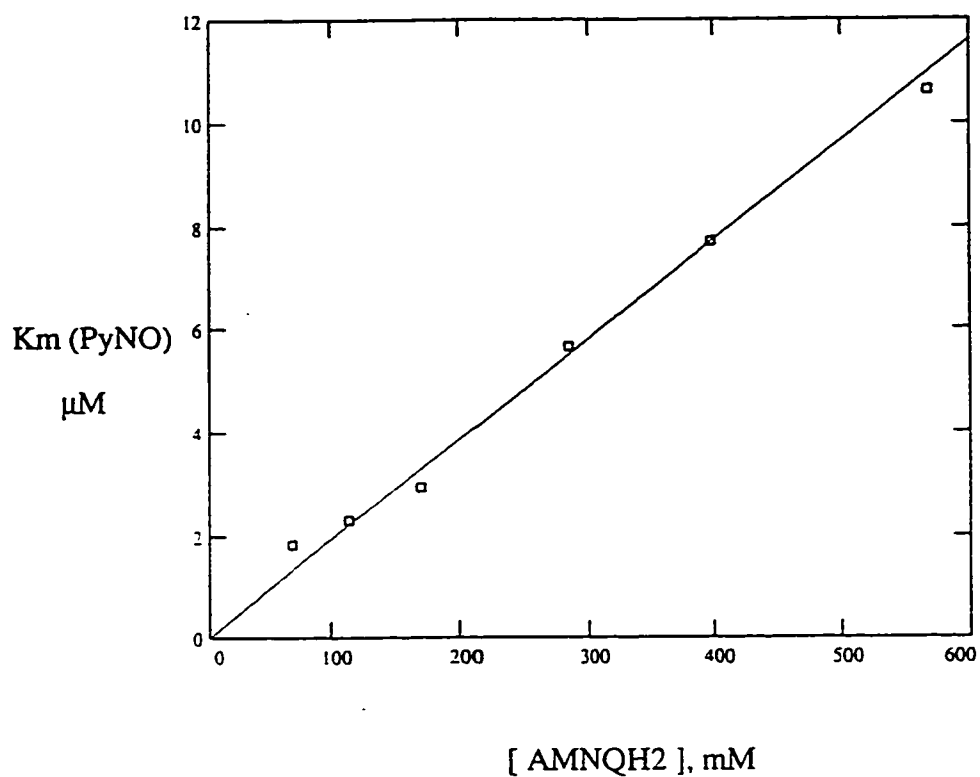


Figure 3-9. The relationship between the apparent Michaelis constant for pyridine N-oxide and the concentration of the other substrate, AMNQH_2 .

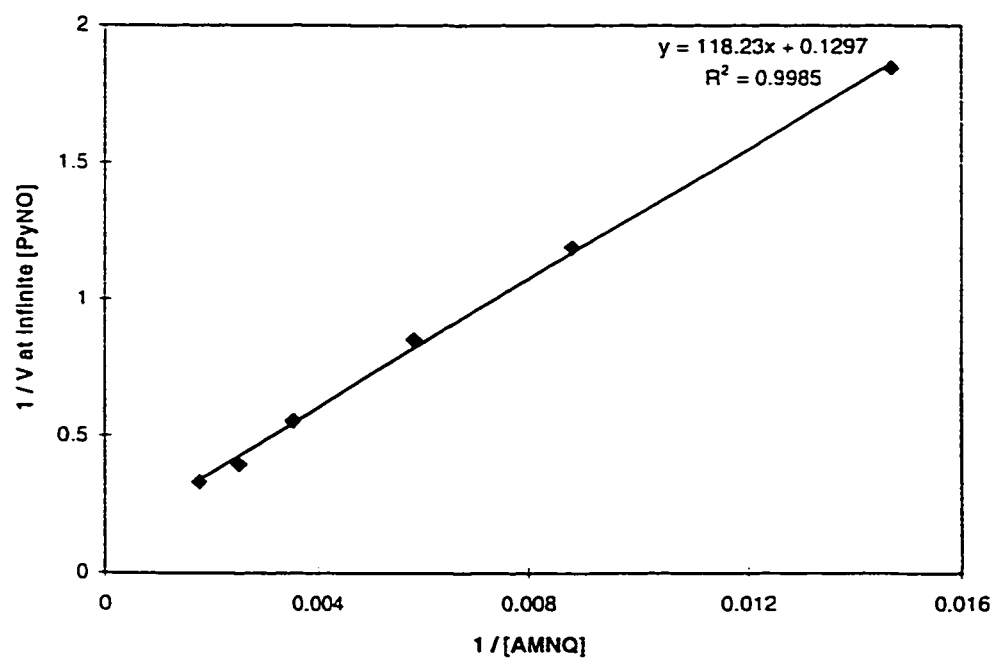
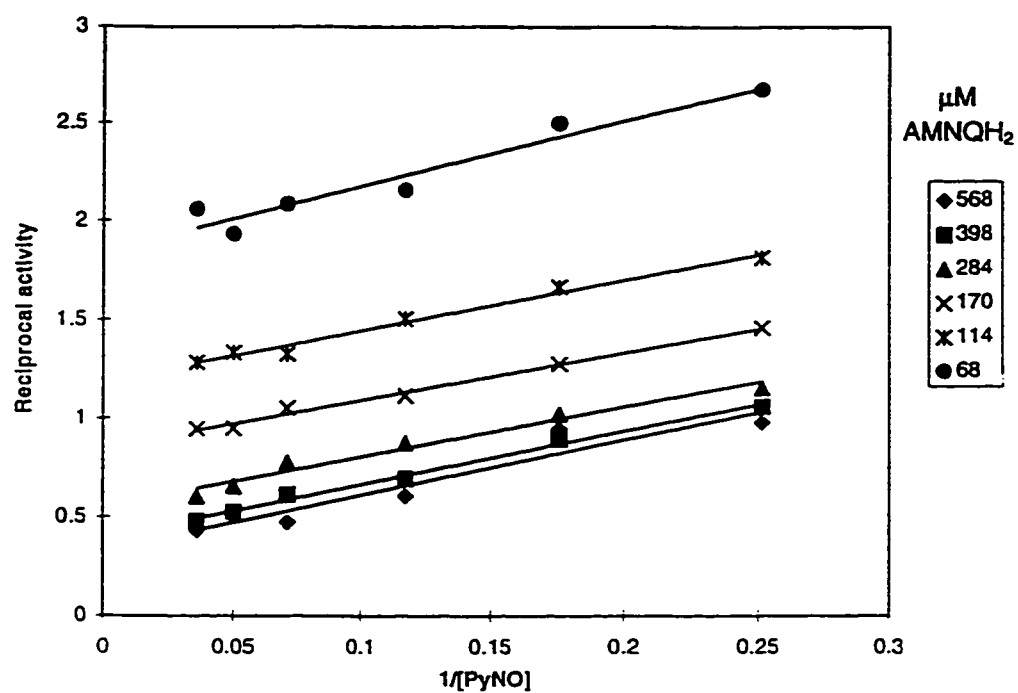


Figure 3-10. Analysis of the kinetic mechanism of the redox reaction between AMNQH_2 and pyridine N-oxide catalyzed by DMSO reductase from *E.coli*.

Inhibition of DMSO reductase activity by HOQNO

HOQNO, 2-*n*-heptyl-4-hydroxyquinoline N-oxide (Cornforth and James, 1956), is known as a powerful inhibitor of quinol oxidation and quinone reduction. Many enzymes including cytochromes *b* (Jones and Garland, 1982), succinate dehydrogenase (Lemma *et al.*, 1991), DMSO reductases from *E.coli* (Rothery and Weiner, 1996) and *Wolinella succinogenes* (Lorenzen *et al.*, 1994), fumarate reductase (Cole *et al.*, 1985) are sensitive to this compound at as low as 10^{-5} M concentrations.

To determine inhibitory parameters of HOQNO with purified solubilized DMSO reductase and AMNQH₂ as electron donor, the RQ assay was performed as described above except that various amounts of ethanolic solution of HOQNO were added to the reaction right before the addition of the substrate, DMSO.

The results demonstrate that solubilized DMSO reductase is extremely susceptible to the inhibition by HOQNO when AMNQH₂ is used as electron donor, the half-inhibiting concentration of HOQNO being about 5 nM (Fig. 3-11).

On the other hand, the inhibition was not so pronounced when BV_{red} was used as electron donor. Twenty times higher concentrations of HOQNO had little effect on the reaction rate (data not shown).

AMNQH₂ as electron donor for nitrate reductase A and fumarate reductase

To determine the ability of reduced AMNQ to serve as a substrate for other redox enzymes such as nitrate reductase A and fumarate reductase from *E.coli*, bacterial membranes containing the overexpressed enzymes were used in the standard RQ assay.

Both enzymes appeared to react with AMNQH₂ reducing nitrate to nitrite and fumarate to succinate, respectively. The reactions follow Michaelis-Menten mechanism in regard to both substrates (Fig. 3-12 - 3-15).

Kinetic parameters of the reactions were determined by varying concentrations of one substrate at saturated concentration of the other. Since the enzyme content of the membrane was not determined, specific reaction rates were not calculated and only Michaelis constants are given (Table 3-3). For comparison, K_m of nitrate and fumarate were determined with reduced benzyl viologen as electron donor (Fig. 3-16, 3-17).

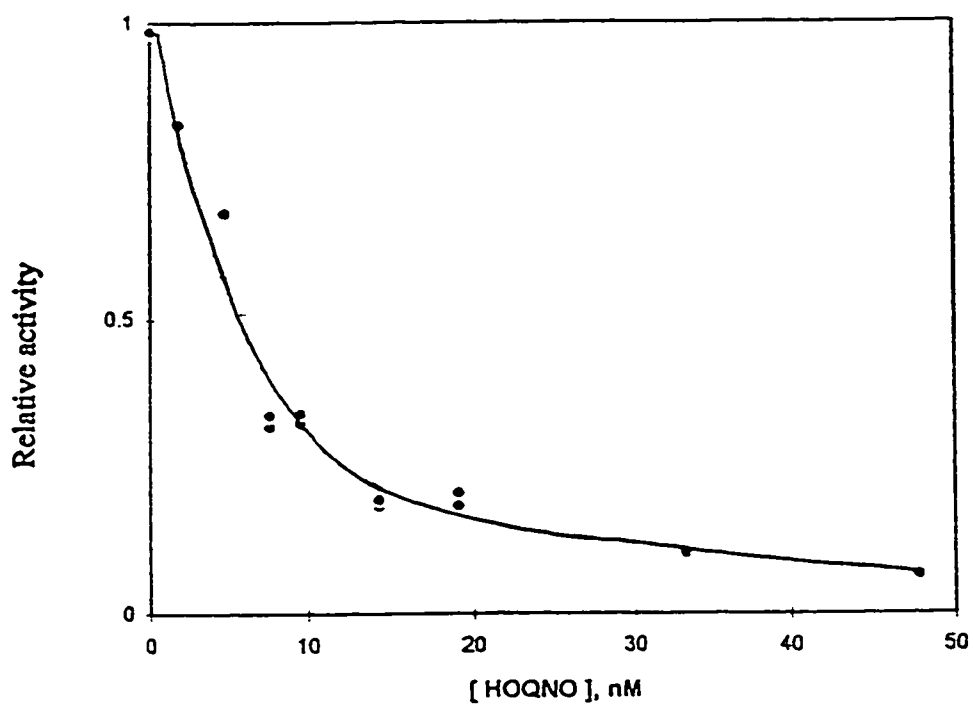


Figure 3-11. Inhibition of DMSO reductase by 2-n-heptyl-4-hydroxyquinoline N-oxide. 10 mM DMSO and 0.5 mM AMNQH₂ were used as substrates. Enzyme activity is in μ mole AMNQH₂/min per mg protein.

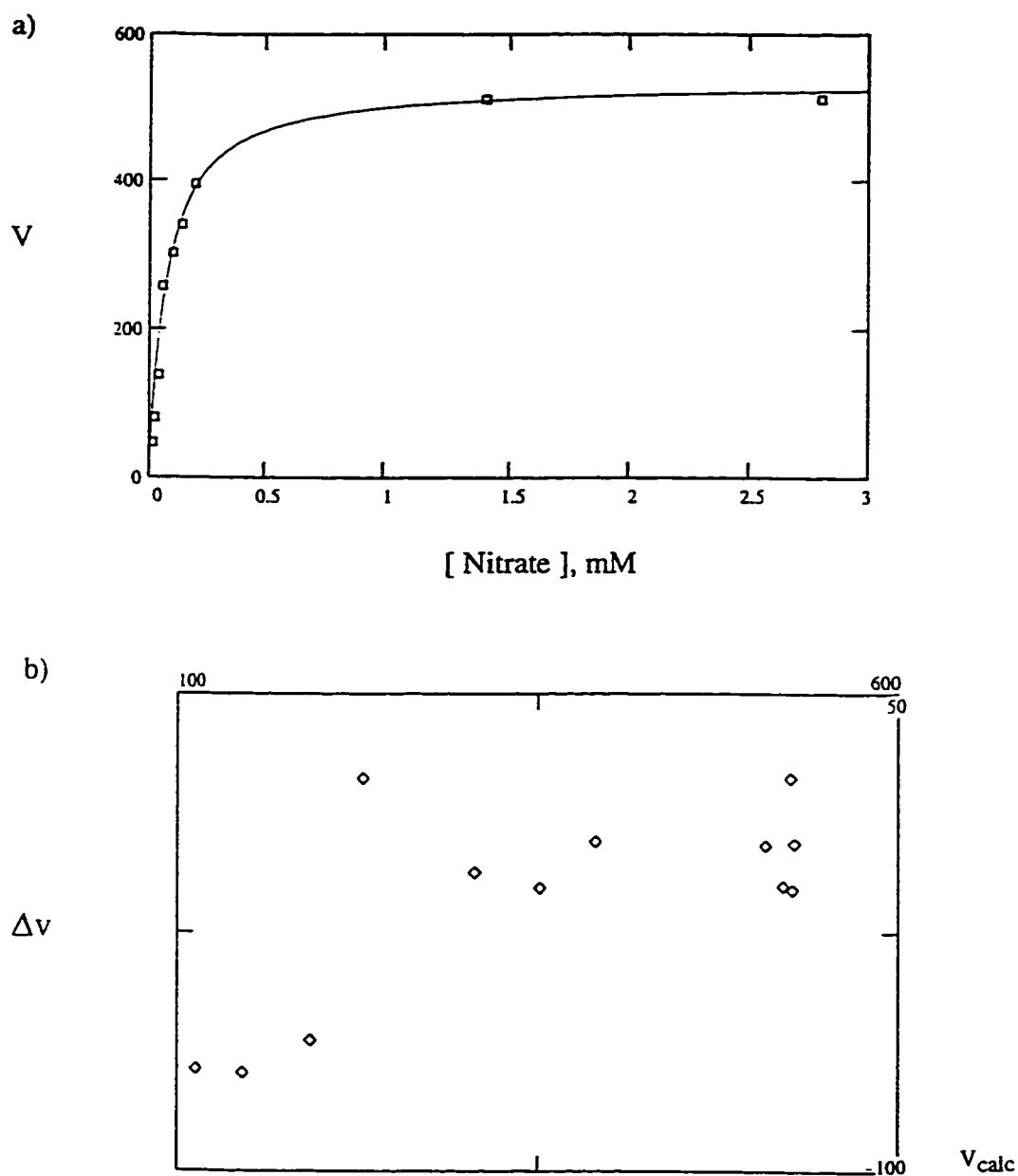


Figure 3-12. Nitrate reduction catalyzed by *E.coli* nitrate reductase A with AMNQH_2 as electron donor. a) The plot of enzyme activity (in $\mu\text{mole AMNQH}_2/\text{min per mg protein}$) vs. the substrate concentration; b) the residual plot. Points of highest concentrations are omitted from both plots for clarity.

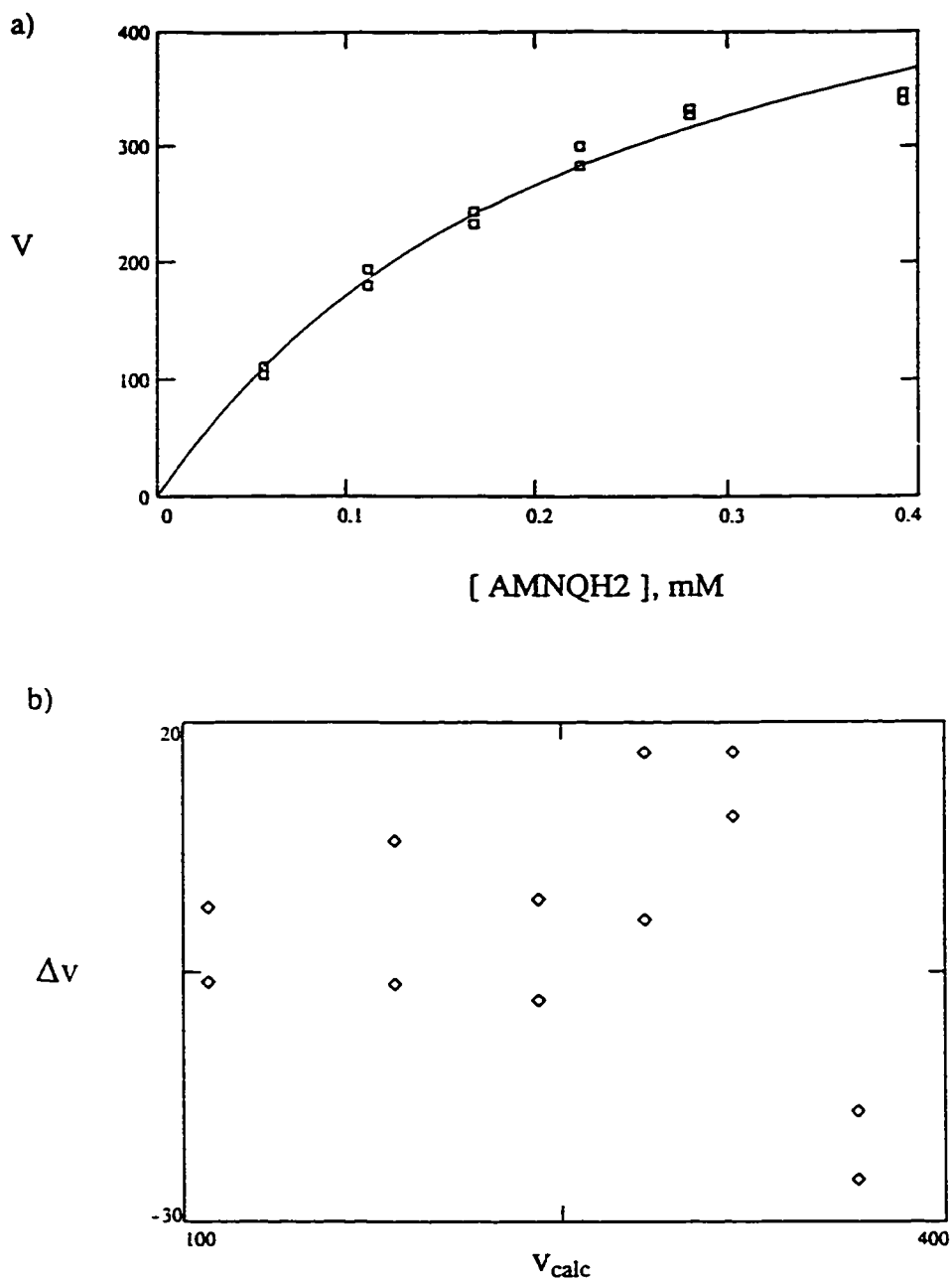


Figure 3-13. The oxidation of AMNQH₂ catalyzed by *E.coli* nitrate reductase A at the enzyme-saturating concentration of nitrate. a) The plot of enzyme activity (in $\mu\text{mole AMNQH}_2/\text{min per mg protein}$) vs. the concentration of AMNQH₂; b) the residual plot.

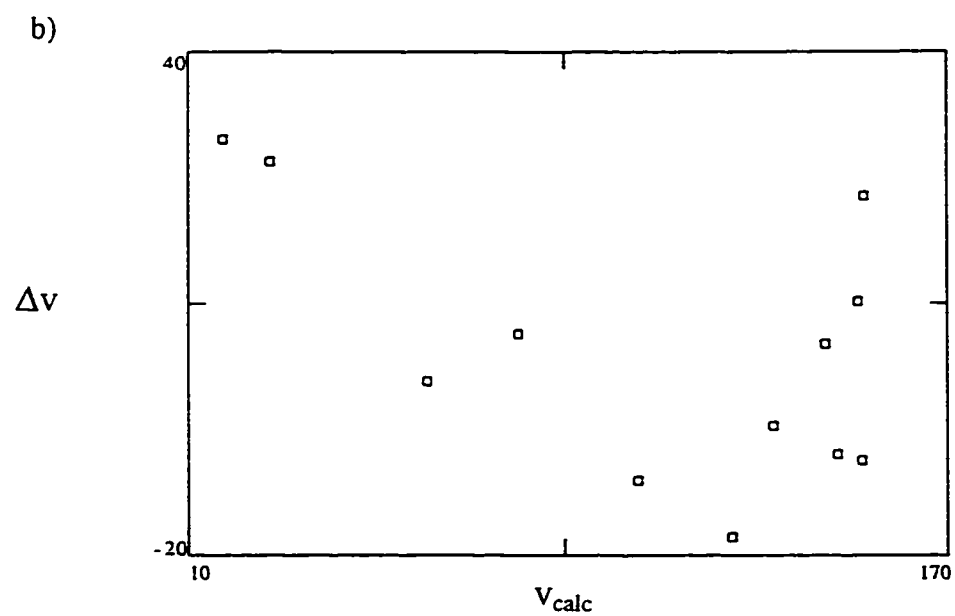
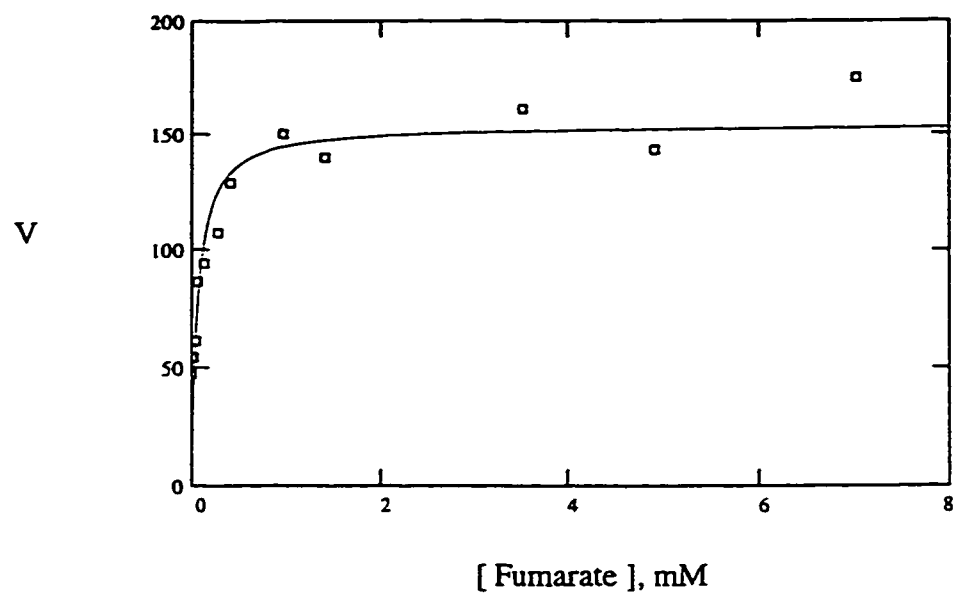


Figure 3-14. Fumarate reduction catalyzed by *E.coli* fumarate reductase with AMNQH₂ as electron donor. a) The plot of the reaction rate (in $\mu\text{mole AMNQH}_2/\text{min per mg protein}$) vs. fumarate concentration; b) the residual plot.

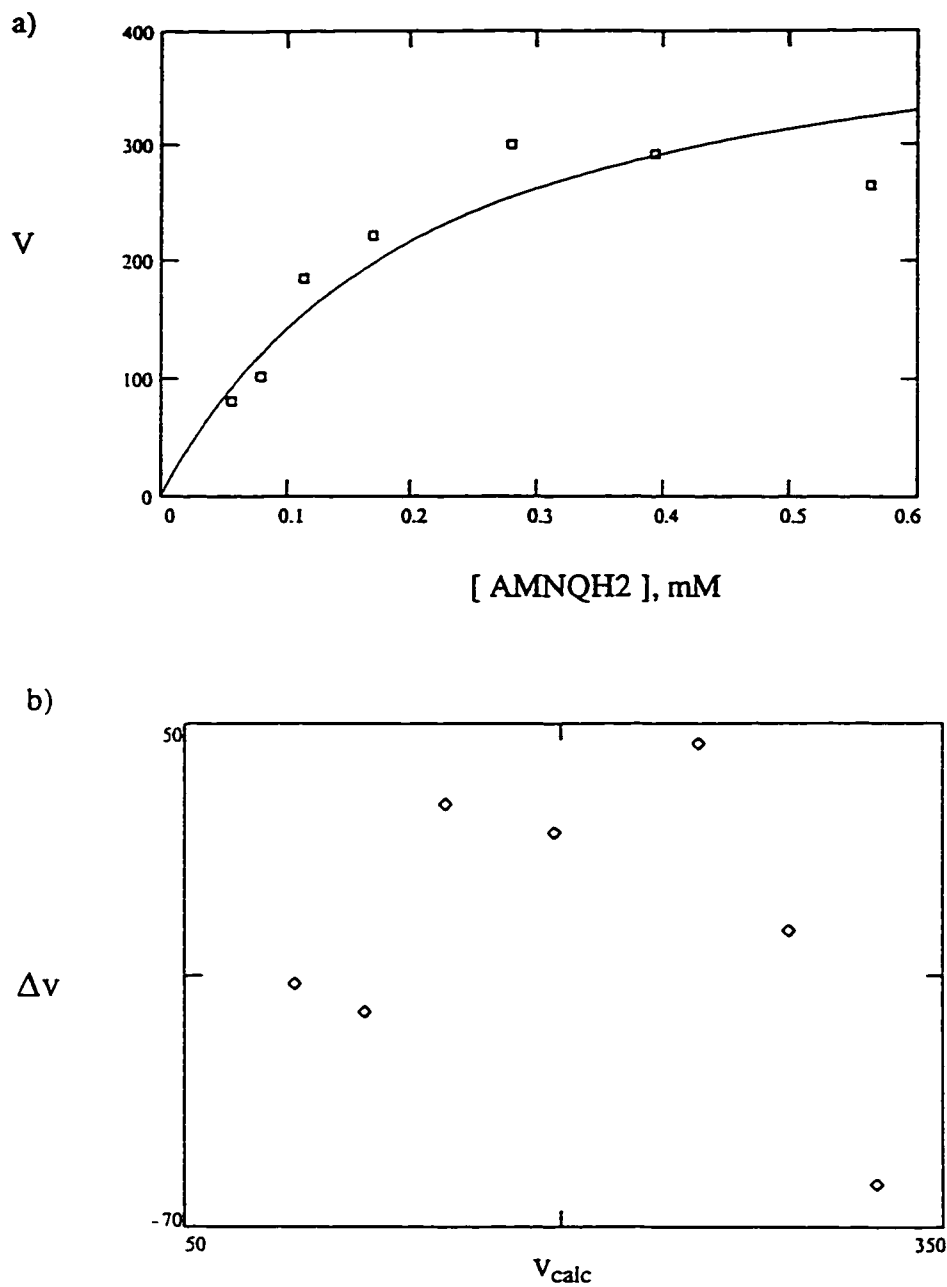


Figure 3-15. The oxidation of AMNQH₂ catalyzed by *E.coli* fumarate reductase at the enzyme-saturating concentration of fumarate. a) The plot of the reaction rate (in $\mu\text{mole AMNQH}_2/\text{min per mg protein}$) vs. quinone concentration; b) the residual plot.

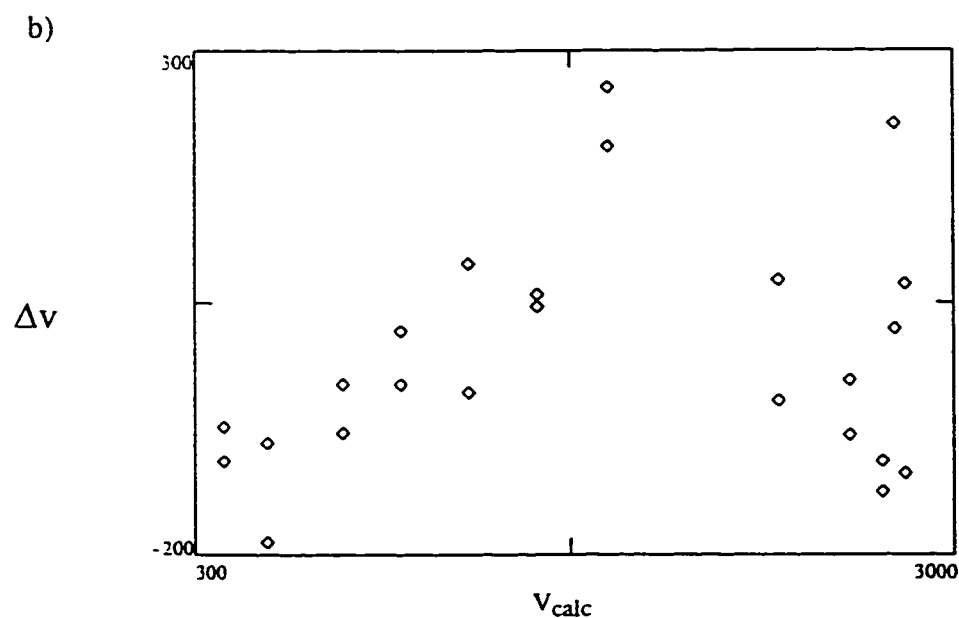
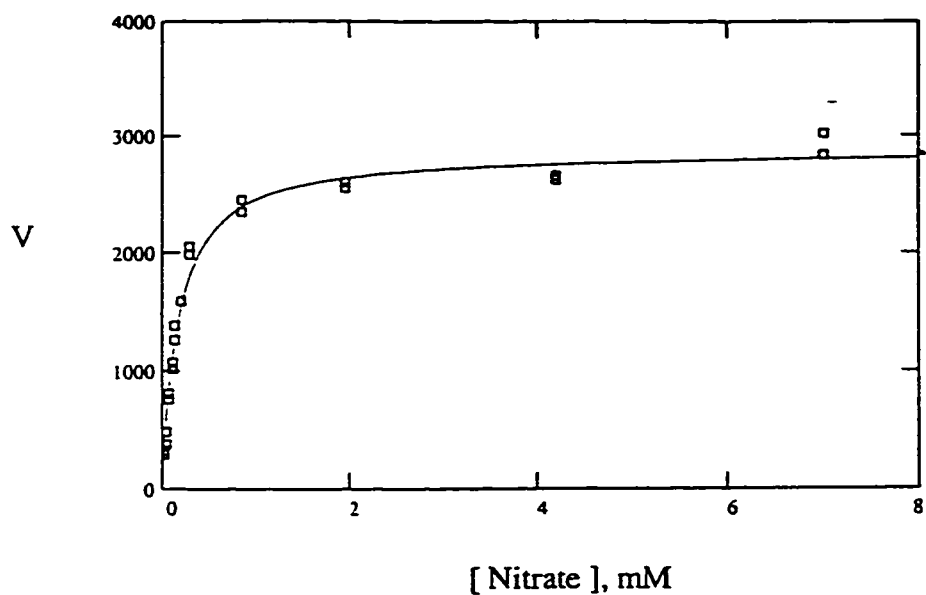


Figure 3-16. Nitrate reduction catalyzed by *E.coli* nitrate reductase A with reduced benzyl viologen as electron donor. a) The plot of enzyme activity (in $\mu\text{mole BV}_{\text{red}}/\text{min}$ per mg protein) vs. nitrate concentration; b) the residual plot.
Points of highest concentrations are omitted from both plots for clarity.

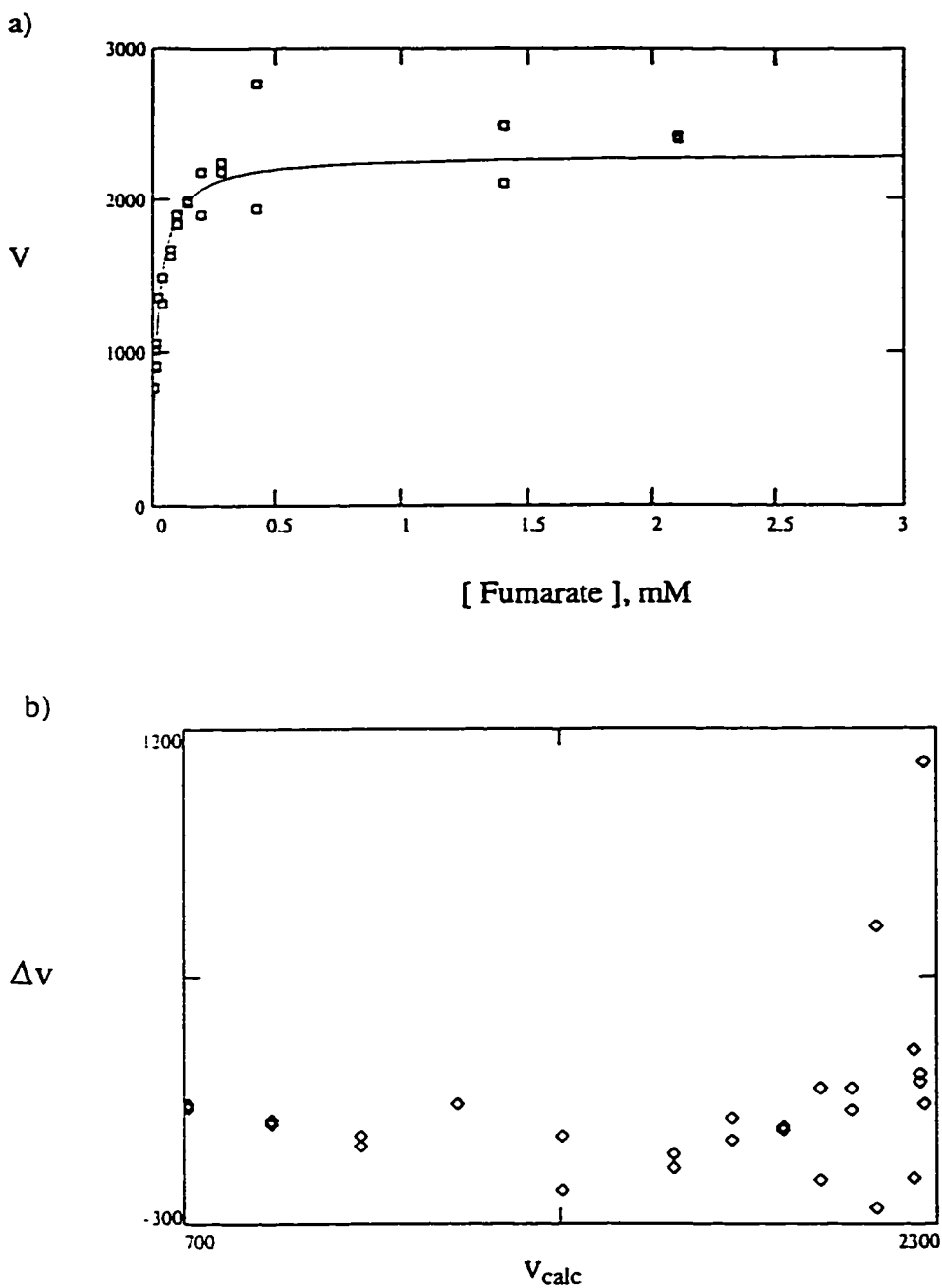


Figure 3-17. Fumarate reduction catalyzed by *E.coli* fumarate reductase with reduced benzyl viologen as electron donor. a) The plot of enzyme activity (in $\mu\text{mole BV}_{red}/\text{min per mg protein}$) vs. the substrate concentration; b) the residual plot. Points of highest concentrations are omitted from both plots to make the picture more illustrative.

Table 3-3. Michaelis constants for the substrates of nitrate reductase and fumarate reductase in BV and RQ assays

Substrate	K _m , μ M
AMNQH ₂ with nitrate as electron acceptor	250 \pm 30
Nitrate with AMNQH ₂ as electron donor	73 \pm 6
Nitrate with BV _{red} as electron donor	170 \pm 10
AMNQH ₂ with fumarate as electron acceptor	185 \pm 33
Fumarate with AMNQH ₂ as electron donor	65 \pm 9
Fumarate with BV _{red} as electron donor	21.6 \pm 1.2

Comparative behavior of DMSO reductase mutants in RQ and BV assays

In the recent years, a number of DMSO reductase mutants with defects in electron transfer were prepared (Rothery and Weiner, 1996). The mutant DmsABC^{H65R} is defective in quinol oxidation while DMSO reduction with BV_{red} as electron donor is not affected. In DmsAB^{C102S}C mutant the [4Fe-4S] cluster with the highest potential (-50 mV) is replaced with the +260 mV [3Fe-4S] cluster. Analogous change occurs in the DmsAB^{C102W}C mutant. This substitution also blocks quinol oxidation activity of DMSO reductase, and both DmsAB^{C102}C mutants do not support anaerobic growth on DMSO.

The mutant DmsABC^{C59X} has a truncated non-functional membrane subunit (Sambasivarao and Weiner, 1991) so that DMSO reductase dimer DmsAB is accumulated in the cytoplasm. This mutant is also defective in quinol oxidation while its BV_{red}-oxidizing activity is high.

These four mutants were used to characterize electron-transfer pathways in DMSO reductase and mechanisms of donating electrons to DMSO reductase by AMNQH₂ and BV_{red}. Plasmids with mutations in the DMSO reductase operon DmsABC^{H65R}, DmsAB^{C102S}C and DmsAB^{C102W}C were transformed into *E.coli* HB101 while for the mutant DmsABC^{C59X} the *E.coli* strain DSS401 was the host.

Cells were grown anaerobically and everted (inside-out) membrane vesicles were prepared using the standard protocol. According to the current topological model of DMSO reductase (Weiner *et al.*, 1992), subunits A and B are located on the cytoplasmic surface of the bacterial plasma membrane and, therefore, are exposed to the chemical agents when everted vesicles are analyzed. Use of everted vesicles allows to study the enzyme in its native state and avoid problems related to the substrate transport across the plasma membrane.

For the mutant DmsABC^{C59X}, both the membrane fraction and the supernatant containing soluble DmsAB dimer were used for tests of enzymatic activity.

Protein contents of membrane and cytoplasmic fractions was estimated by the modified Lowry procedure, and enzyme activity was expressed in units per mg protein. Since the mutants varied greatly in the protein level expression, no direct comparison of the mutant proteins was made. Instead, each mutant DMSO reductase was characterized by its AMNQH₂- and BV_{red}-oxidizing activity, and these two activities were compared for each mutant (Table 3-4). Each reported value was average of three measurements; standard error did not exceed 6%.

Other potential substrates and inhibitors of DMSO reductase

Among synthetic quinonoid compounds available commercially, indigo carmine (Fig. 3-18b) resembles naphthoquinone very closely, structurally and electrochemically. Its remarkable spectral properties (transition in visible region at 608 nm upon reduction with $\Delta\epsilon$ of about 10,000), ease of reduction (glucose in aqueous alkali at elevated temperature, thus avoiding the need of using dithionite (Davidson *et al.*, 1932)) and high solubility of both oxidized and reduced forms could make it a convenient assay reagent for redox proteins.

Reduced form of indigo carmine was tested for support of DMSO reduction using the assay analogous to BV assay, and the substance appeared not to be a substrate for DMSO reductase.

One of the intermediates of MNNQ synthesis, 2-methyl-1,4-hydroxynaphthalene diacetate (Fig. 3-18a), is similar in structure to menaquinones but its hydroxyl groups are blocked

Table 3-4. Comparative behavior of wild-type and some DMSO reductase mutants in RQ- and BV-assays

Mutant	Cellular fraction ^a	V _{BV} ^b	V _{RQ} ^c	V _{BV} /V _{RQ}	(V _{BV} /V _{RQ}) ^d
WT DmsABC	m	71±4	1.4±0.03	51	1
DmsAB ^{C102S} C	m	23±1.5	0.081±0.005	287	6
DmsABC ^{H65R}	m	11±0.4	0.013±0.0002	874	17
WT DmsABC	c	16±1	0.018±0.001	909	18
DmsAB ^{C102W} C	m	52±2	0.024±0.002	2220	44
DmsABC ^{C59X}	c	10±0.3	0.003±0.0001	3328	66

^a m, membrane; c, cytoplasmic

^b Specific activity in BV assay, $\mu\text{mole BV}_{\text{red}}/\text{min}$ per mg protein

^c Specific activity in RQ assay, $\mu\text{mole AMNQH}_2/\text{min}$ per mg protein

^d Activity ratio normalized to the wild-type enzyme, membrane fraction

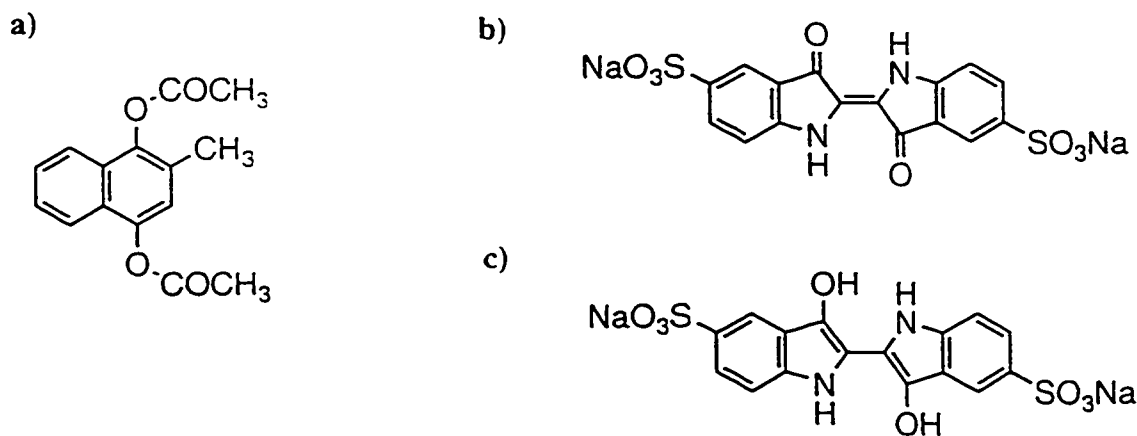


Figure 3-18. Chemical structure of indigo carmine and 2-methyl-1,4-dihydroxynaphthalene diacetate. a) 2-Methyl-1,4-dihydroxynaphthalene diacetate; b) indigo carmine, oxidized form; c) indigo carmine, reduced form.

by acetylation thus preventing it from redox transitions. Potential inhibitory properties of this compound were tested in RQ assay analogously to HOQNO. The presence of 1 mM 2-methyl-1,4-hydroxynaphthalene diacetate in the reaction did not affect AMNQH₂ oxidation (data not shown).

Discussion

One of the most convenient reporter groups for spectroscopic determination is the nitro group. Compounds such as *p*-nitrophenyl phosphate are widely used for enzymatic assays. Introduction of the nitro group into 2-methyl-1,4-naphthoquinone (menadione) was supposed to increase the difference in the UV- or visible absorption between quinone and quinol forms of the compound and increase their solubility in water.

Unfortunately, MNNQ appeared to be unsuitable for the task. Very low water solubility of the oxidized form and the ease of reduction of the nitro group prevented the use of MNNQ as a possible substrate for DMSO reductase. Problems with the selective reduction of MNNQ were pointed out in the study of Vladimirtsev and Stromberg (Vladimirtsev and Stromberg, 1957). Reducing nitronaphthoquinones polarographically, at the dropping mercury electrode, they found that the reaction mechanism depended on the position of the substituent nitro group. If the nitro group was attached to the phenyl ring of 1,4-naphthoquinone, it was reduced at lower electrode potentials than the quinone carbonyls. If the nitro group was in the quinone ring, reduction of the carbonyls and the nitro group occurred simultaneously. This finding explains why the hydroquinone of MNNQ was not isolated in our study: reduction of carbonyl groups of MNNQ coincided with the reduction of the nitro group, and the resulting AMNQH₂ was quickly reoxidized to AMNQ by air.

AMNQH₂ generated by reduction of MMNQ or by other means possesses a number of physical and chemical properties that can make it a very useful potential substrate for DMSO reductase. The structure of the molecule closely resembles that of natural menaquinone. Its oxidized form can be easily measured by visible spectroscopy. The solubility of both forms in water is high enough for enzymatic assays while high

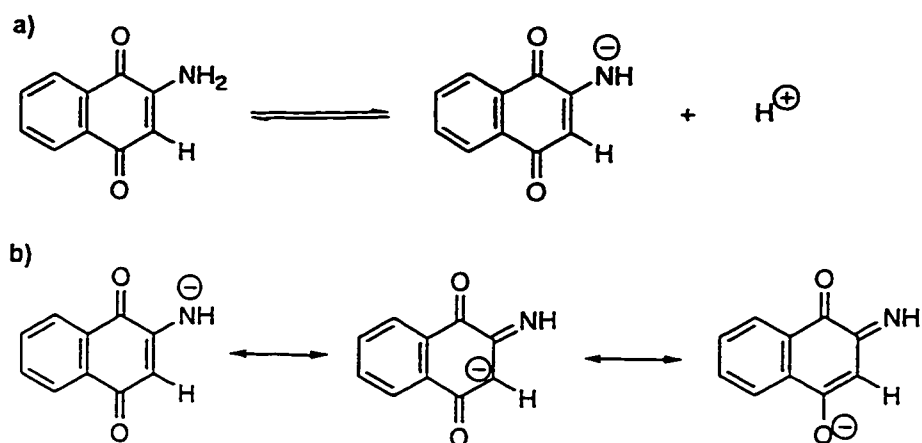


Figure 3-19. Dissociation of the amino group in 2-amino-1,4-naphthoquinone.
 a) Dissociation equilibrium; b) resonance hybrids of the anion showing the distribution of the negative charge between nitrogen, oxygen and carbon atoms.

solubility in organic solvents allows for the preparation of concentrated stock solutions and provides access to micelles or bacterial membrane particles containing the enzyme. Electron-withdrawing effect of the quinonoid ring causes great decrease in the basicity and nucleophilicity of the amino group in AMNQ. The formation of the corresponding hydrochloride was not observed even in concentrated hydrochloric acid, and this observation is in agreement with the literature data: the redox titration of the AMNQ homologue, 2-amino-1,4-naphthoquinone, did not reveal its protonation even at pH 0.33 (Fieser and Fieser, 1934). On the opposite, the amino group in the latter compound is capable of dissociating with pK_a of 9.96 (Table 3-5). The strong electron-withdrawing effect of the quinonoid ring reduces the electron density on the negatively charged nitrogen atom stabilizing the anion (Fig. 3-19).

In fact, the amino group in AMNQ under neutral pH is more similar to a methyl group in its charge distribution and lack of reactivity than to a regular amino group attached to aromatic ring or aliphatic carbon. Polarographic studies of Vladimirtsev and Stromberg (Vladimirtsev and Stromberg, 1957) demonstrated that the reduction of 2-aminonaphthoquinone and its numerous derivatives occurs exclusively as reversible reduction of carbonyl groups of the quinones with the formation of hydroquinone. Only two derivatives, 1,4-naphthoquinone 2,3-oxide and 2-(N-pyridyl)-1,4-naphthoquinone,

showed anomalous behavior. In both cases, reduction of another functional group was observed, and in both cases these side reactions were irreversible.

Reduction of AMNQ by sodium dithionite or sodium borohydride in aqueous solution observed in this study was completely reversible. The reduced form of AMNQ is rapidly reoxidized upon contact with air, so that isolation of AMNQH₂ proved to be very difficult. As a result, the hydroquinone was not obtained in pure form, and the reduction of AMNQ to AMNQH₂ for enzyme assays was carried out *in situ*, by addition of the aqueous solution of sodium dithionite.

This inertness of the amino group in AMNQ highly contrasts the behavior of the hydroxyl group in some commercially available naphthoquinones such as phthiocol (2-hydroxy-3-methyl-1,4-naphthoquinone), lapachol (2-hydroxy-3-(3-methylbuten-2-yl)-1,4-naphthoquinone) and especially lawsone (2-hydroxy-1,4-naphthoquinone) (Fig. 3-20). In these compounds the electron-withdrawing effect of the quinonoid ring also stabilizes the anionic form of the quinone, and they all have considerable acidic properties and reduced affinity for hydrophobic environment. In fact, lawsone is insoluble in ether and benzene but is very soluble in water and ethanol. pK_a values of 2-hydroxyl-substituted 1,4-naphthoquinones are low (Table 3-5), and under physiologic conditions these molecules are completely ionized. In fact, lawsone is an even stronger acid than acetic acid (pK_a 4.75) while phthiocol and lapachol have only slightly weaker acidic properties.

Use of these anionic quinones may introduce additional confusion in the interpretation of experimental data. Undoubtedly, quinol-binding sites of enzymes are designed to bind polar quinols and release the highly hydrophobic products, oxidized quinone species. With hydroxyl-substituted quinones, the enzymes bind polar quinol, but the product is an anionic molecule. Although this may be interesting to observe for special purpose, it is not reasonable to assume that interaction of 2-hydroxyl-substituted quinones with redox enzymes represents a realistic model for the interaction of naturally occurring quinones with the enzymes.

UV/visible spectra of anionic quinones, unlike those of neutral molecules, are greatly affected by conditions such as pH, ionic strength, presence of hydrogen bond donors (glycerol), detergents, *etc.* As a result, these compounds are much less suitable for

enzymatic assays than neutral quinones because their detection would require frequent recalibration.

AMNQH₂ is a substrate for DMSO reductase, fumarate reductase and nitrate reductase A from *E.coli*. Its oxidation follows Michaelis-Menten mechanism with all of these enzymes. Although its high Michaelis constant with DMSO reductase does not allow easy

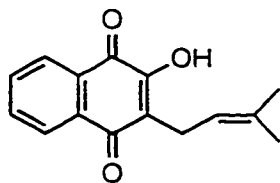
Table 3-5. Dissociation constants for some naphthoquinones and their corresponding quinols

Compound	Oxidized form	Reduced form		Reference
	pK _a	pK _{a1}	pK _{a2}	
2-Amino-1,4-naphthoquinone	9.96 ^{a)}	9.57	11.27	b)
Lawsone	3.98	8.68	10.71	b)
Phthiocol	5.02	8.74	11.84	(Ball, 1936)
Lapachol	5.06	8.68	11.70	(Ball, 1936)

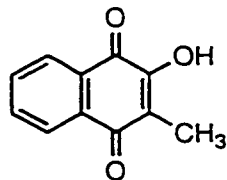
^{a)} pK_a of dissociation of 2-amino group

^{b)} (L.F. Fieser and M.Fieser, 1934)

a)



b)



c)

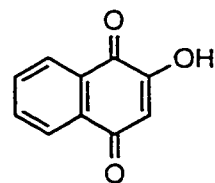


Figure 3-20. Chemical structure of 2-hydroxyl-substituted naphthoquinones.

a) lapachol; b) phthiocol; c) lawsone.

determination of kinetic parameters for N- and S-oxides because of impossibility to achieve the enzyme-saturating concentration of AMNQH₂, this feature did allow us to establish unequivocally that the reaction between pyridine N-oxide with AMNQH₂ catalyzed by DMSO reductase has a substituted-enzyme (ping-pong) mechanism. Michaelis constants of AMNQ with fumarate reductase and nitrate reductase are lower (200-300 μM) and can be measured directly. K_m values for more hydrophobic quinone analogs reported for formate dehydrogenase were much lower (6 μM for DMNQ, 14 μM for menadione, 18 μM for quoroquinone) (Kröger *et al.*, 1979). Although direct comparison is not possible because of differences in reaction conditions, substrates and the complexity of kinetic mechanisms, it is possible that lower Michaelis constants of hydrophobic quinone analogs better reflect the nature of the interaction between a redox enzyme and its quinol substrates. On the other hand, such low K_m values for quinones make measurements very difficult, and reaction mechanism in the cited paper was analyzed with BV_{red} (K_m 530 μM) as an electron donor rather than with one of the quinones. It is also possible that the Michaelis constant of AMNQH₂ with DMSO reductase is so high because the actual reacting species is semiquinone. As we saw previously, the enzyme is capable of reacting with structurally different quinols such as a naphthoquinone derivative DMNQ and a benzoquinone derivative duroquinone while *in vivo* it accepts electrons from menaquinol and not ubiquinone. The two-electron redox potentials of DMNQ and duroquinone are similar to those of their parent compounds. The only apparent feature that relates DMNQ and duroquinone is their one-electron redox potentials from semiquinone to quinone. It is possible that DMSO reductase from *E.coli* reacts preferentially with semiquinone rather than quinol. This hypothesis may explain much lower activity of the enzyme when quinols are used as electron donors (reaction rates are about two orders of magnitude lower with AMNQH₂ than with BV_{red}): quinones and quinols are more stable molecules than semiquinone, and the equilibrium of the disproportionation ($2 Q^{\cdot -} \rightleftharpoons Q + Q^{2-}$) is unfavorable for semiquinone. As a result, the reactive semiquinone is always present in the reaction mixture at very low concentration. The rate-limiting step in the reaction becomes the generation of semiquinone from quinol and quinone, and the reaction rate depends very little on the nature of sulfoxide and

amine oxide. This is consistent with our finding that the rates of reduction of DMSO, TMAO and pyridine N-oxide are very similar (about 1-2 micromoles/min per mg protein) while with another electron donor, BV_{red}, these rates differ by more than an order of magnitude.

Certainly, this is not the only explanation of lower activity of DMSO reductase with quinols in comparison with BV_{red}. Another possibility is that electron transfer from the quinol-binding site in the subunit C to iron-sulfur cluster(s) in the subunit B is a very slow process that limits the overall reaction rate.

Oxidation of AMNQH₂ by DMSO reductase closely resembles that of natural menaquinols. It requires the presence of functional membrane anchor subunit and is inhibited by HOQNO. The strong inhibition of DMSO reductase by HOQNO suggests that the structure of HOQNO closely resembles the structure of the reaction transition state.

The difference in BV_{red}/AMNQH₂-oxidizing activity can be used for characterization of DMSO reductase mutants. Among the mutants tested, DmsAB^{C102S}C has the highest rate of AMNQH₂ oxidation relative to BV_{red} oxidation and, respectively, the least impaired quinol-oxidizing activity. Another similar mutant, DmsAB^{C102W}C, has greatly decreased quinol oxidizing activity relative to the rate of BV_{red} oxidation. The reason may be that serine is still capable of forming a bond to the iron-sulfur cluster which is weaker than that of cysteine but capable of preserving the structural integrity of this protein domain. This bond may be too weak for the growth support in anaerobic conditions but is detectable in an artificial assay. Tryptophane, on the other hand, destroys the structure and disrupts the normal electron flow through DmsB subunit. Stronger suppression of quinol-oxidizing activity relative to BV_{red}-oxidizing activity in the DmsAB^{C102W}C mutant allows to suggest that electron transfer from DmsC to DmsA subunit requires close interaction between all three subunits of DMSO reductase.

The structure and electrochemical properties of AMNQ also closely resemble that of its natural derivative, rhodoquinone, which was found in some eucaryotic and procaryotic organisms to serve as electron carrier under anaerobic conditions and, in some gram-positive bacteria, even under aerobic conditions.

The high aqueous solubility of AMNQ and its remarkable spectral and substrate properties can make it one of the most convenient assay reagents for many redox enzymes.

Bibliography

Baker, B.R., T.H. Davies, L. McElroy and G.H. Carlson (1942). The antihemorrhagic activity of sulfonated derivatives of 2-methylnaphthalene. *J. Amer. Chem. Soc.* **64**, 1096-1101.

Cleland, W.W. (1963). The kinetics of enzyme-catalyzed reactions with two or more substrates or products. *Biochim. Biophys. Acta* **67**, 104-137.

Cole, S.T., C. Condon, B.D. Lemire and J.H. Weiner (1985). Molecular biology, biochemistry and bioenergetics of fumarate reductase, a complex membrane-bound iron-sulfur flavoenzyme of *Escherichia coli*. *Biochim. Biophys. Acta* **811**, 381-403.

Cornforth, J.W. and A.T. James (1956). Structure of a naturally occurring antagonist of dihydrostreptomycin. *Biochem. J.* **63**, 124-130.

Crawford, M. (1935). The reaction between 2,3-dimethyl-1,4-naphthoquinone and phenylmagnesium bromide. *J. Amer. Chem. Soc.* **57**, 2000-2004.

Davidson, A., A.J. Hailwood, F. Henesey and A. Shepherdson. (1932). Production and manufacture of stable leuco-indigo preparations. *U.S.A. Patent* 1,861,382.

Estornell, E., S. Di Bernardo, F. Pallotti, G. Parenti Castelli and G. Lenaz (1996). Steady-state kinetics of the reduction of coenzyme Q analogs by complex I (NADH:ubiquinone oxidoreductase) in bovine heart mitochondria and submitochondrial particles. *Biochemistry* **35**, 2705-2716.

Fieser, L.F. and M. Fieser (1934). The tautomerism of aminonaphthoquinones. *J. Amer. Chem. Soc.* **56**, 1565-1578.

Fieser, L.F. and J.L. Hartwell (1935). The reaction of hydrazoic acid with the naphthoquinones. *J. Amer. Chem. Soc.* **57**, 1482.

Fieser, L.F. and R.B. Turner (1947). The addition of sulfhydryl derivatives to 2-methyl-1,4-naphthoquinone. *J. Amer. Chem. Soc.* **69**, 2335-2338.

- Fujita, S. and K. Sano (1975). N,N-Diethylhydroxylamine. A versatile reagent for reducing quinones to quinols. *Tetrahedron Letters* **21**, 1695-1696.
- Ilan, Y.A., G. Czapski and D. Meisel (1976). The one-electron transfer redox potentials of free radicals. I. The oxygen-superoxide system. *Biochem. Biophys. Acta* **430**, 209-224.
- Jones, R.W. and P.B. Garland. (1982). The function of ubiquinone and menaquinone in the respiratory chain of *Escherichia coli*. In Function of quinones in energy conserving systems, B. L. Trumpover, ed. (London: Academic Press), pp. 465-476.
- Kröger, A., E. Winkler, A. Innerhofer, H. Hackenberg and H. Schagger (1979). The formate dehydrogenase involved in electron transport from formate to fumarate in *Vibrio succinogenes*. *Eur. J. Biochem.* **94**, 465-475.
- Lemma, E., C. Hagerhall, V. Geisler, U. Brandt, G. von Jagow and A. Kröger (1991). Reactivity of the *Bacillus subtilis* succinate dehydrogenase complex with quinones. *Biochim. Biophys. Acta* **1059**, 281-285.
- Lorenzen, J., S. Steinwachs and G. Uden (1994). DMSO respiration by the anaerobic rumen bacterium *Wolinella succinogenes*. *Arch. Microbiol.* **162**.
- Marcinkeviciene, J.A. and J.S. Blanchard (1995). Quinone reductase reaction catalyzed by *Streptococcus faecalis* NADH peroxidase. *Biochemistry* **34**, 6621-6627.
- Meisel, D. and G. Czapski (1975). One-electron transfer equilibria and redox potentials of radicals studied by pulse radiolysis. *J. Phys. Chem.* **79**, 1503.
- Patel, K.B. and R.L. Willson (1973). Semiquinone free radicals and oxygen. Pulse radiolysis study of one electron transfer equilibria. *J. Chem. Soc. Faraday Trans. I* **69**, 814-825.
- Ramasarma, T. (1985). Natural occurrence and distribution of coenzyme Q. In Coenzyme Q, G. Lenaz, ed. (New York: Wiley), pp. 67-82.
- Rich, P.R. and R. Harper (1990). Partition coefficients of quinones and hydroquinones and their relation to biochemical reactivity. *FEBS Lett.* **269**, 139-144.
- Rothery, R.A. and J.H. Weiner (1996). Interaction of an engineered [3Fe-4S] cluster with a menaquinol binding site of *Escherichia coli* DMSO reductase. *Biochemistry* **35**, 3247-3257.

- Sambasivarao, D. and J.H. Weiner (1991). Dimethyl sulfoxide reductase of *Escherichia coli*: an investigation of function and assembly by use of in vivo complementation. *J. Bacteriol.* **173**, 5935-5943.
- Simala-Grant, J.L. and J.H. Weiner (1996). Kinetic analysis and substrate specificity of *Escherichia coli* dimethyl sulfoxide reductase. *Microbiology* **142**, 3231-3239.
- Unden, G. and J. Bongaerts (1997). Alternative respiratory pathways of *Escherichia coli*: energetics and transcriptional regulation in response to electron acceptors. *Biochim. Biophys. Acta* **1320**, 217-234.
- Vladimirtsev, I.F. and A.G. Stromberg (1957) Polarographic study of 2,3-derivatives of 1,4-naphthoquinone. *J. General Chem. of the USSR* **27**, 1110-1123.
- Weiner, J.H., R. Cammack, S.T. Cole, C. Condon, N. Honore, B.D. Lemire and G. Shaw (1986). A mutant of *Escherichia coli* fumarate reductase decoupled from electron transport. *Proc. Natl. Acad. Sci. USA* **83**, 2056-2060.
- Weiner, J.H., R.A. Rothery, D. Sambasivarao and C.A. Trieber (1992). Molecular analysis of dimethylsulfoxide reductase: a complex iron-sulfur molybdoenzyme of *Escherichia coli*. *Biochim. Biophys. Acta* **1102**, 1-18.

Chapter 4. Amine oxides and sulfoxides

Introduction

The chemistry of sulfoxides

The nature of the double bond in sulfoxides is quite complicated, and the overall molecular structure of a sulfoxide represents a resonance hybrid of several structures. The most important contribution is made by the structure with separated charges (positive on the sulfur, negative on the oxygen) shown on Fig. 4-1a,b. The sulfur-oxygen bond in sulfoxides is polar and it withdraws the electron density from adjacent carbon atoms, so that their hydrogen atoms possess increased acidity and can be easily substituted. The ability to form enantiomers and comparatively high reaction activity makes sulfoxides valuable building blocks for asymmetric synthesis (Andersen, 1988). Unfortunately, chemical separation of enantiomers of sulfoxides is very difficult in most cases reported. The probability of using enzymes for this purpose would greatly increase the possibilities of asymmetric organic synthesis in producing new complex biologically active molecules that have been impossible to synthesize by other means.

In sulfoxides, the sulfur atom sits in the center of tetragonal pyramid formed by two alkyl or aryl substituents, the oxygen atom and the lone pair of electrons (Fig. 4-1a,b). Due to this type of symmetry, sulfoxides with different substituents are chiral and can be (at least, theoretically) separated into enantiomers. Optical separation of sulfoxides, though, proved to be a very complicated task when the substituent groups have no active functional groups. Very few such compounds are available in pure enantiomeric form, and they tend to be very expensive. One of these compounds, methyl *p*-tolyl sulfoxide was used in this work to determine the stereospecificity of sulfoxide reduction catalyzed by DMSO reductase from *E.coli*.

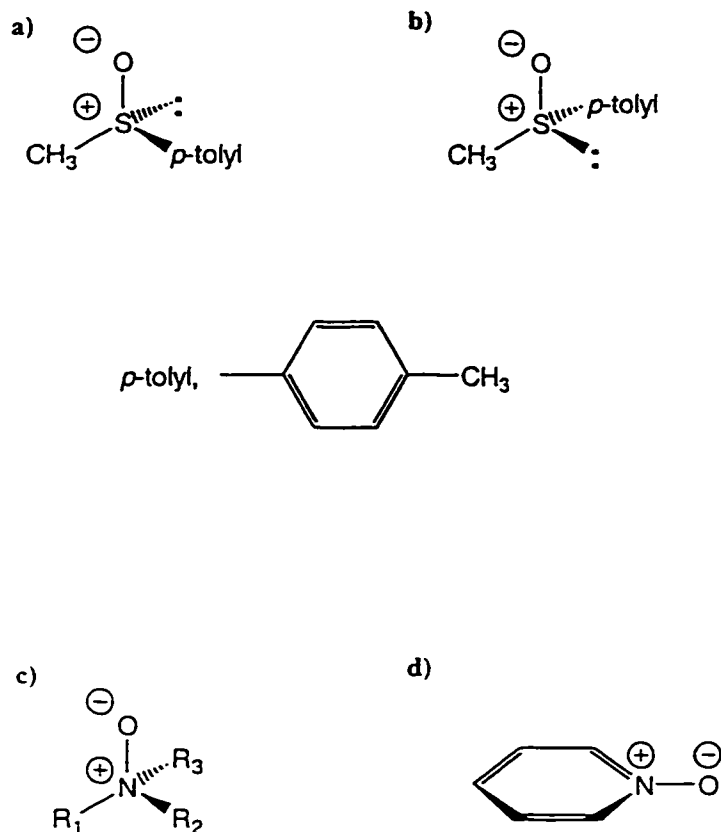


Figure 4-1. Stereochemistry of sulfoxides and amine oxides. a) (*R*)-methyl *p*-tolyl sulfoxide; b) (*S*)-methyl *p*-tolyl sulfoxide; c) aliphatic amine oxide; d) aromatic amine oxide.

Most sulfoxides are stable under normal conditions, and dimethyl sulfoxide (DMSO) is widely used in labs and industry as an aprotic polar solvent. Despite their stability, sulfoxides can be reduced to sulfides by relatively mild reductants such as zinc/hydrochloric acid and metal hydrides. Reduction of sulfoxides to sulfides is widespread in nature. Along with bacterial respiration which was discussed above, many eucaryotic organisms contain unrelated enzymes that reduce DMSO to DMS. The reverse reaction, oxidation of DMS to DMSO also occurs in some organisms, *e.g.* yeast.

The chemistry and biochemistry of amine N-oxides

In amine oxides the lone-pair electrons of the nitrogen atom of the tertiary amine occupy a vacant orbital of the oxygen atom forming a single bond. Based on the nature of the tertiary amine, there are two main classes of amine oxides, aliphatic and aromatic N-oxides. In the former, the nitrogen atom has three substituent groups. In the latter compounds, nitrogen is a part of an aromatic heterocycle and thus have only two substituents. The two types of amine oxides differ in physical and chemical properties, molecular structure and other properties.

Oxygen and three ligands in aliphatic amines take up a more or less symmetric position around the nitrogen atom (Fig. 4-1a). The symmetry of this structure resembles that of tetravalent carbon, and aliphatic N-oxides with three different alkyl substituents can be resolved into enantiomers. In aromatic amine oxides, the nitrogen atom is a part of a flat ring, and the oxygen atom connected to it lies in the plane of the ring (Fig. 4-1b). The structure has a plane of symmetry, and the nitrogen cannot be chiral.

Amine oxides are very polar compounds highly soluble in water and insoluble in hydrophobic solvents. Most aliphatic N-oxides are very hygroscopic; aromatic amine oxides are mostly not, and some of them are easily soluble in ether and benzene in the absence of water. Polarity of amine oxides is lower than that of their parental amines, and their basicity is lower as well (pKa values for amine oxide/corresponding amine: TMAO 9.74 / 4.65, PyNO 5.29 / 0.79). Polarity and basicity of aliphatic amine oxides is higher than those of aromatic N-oxides, and protonation of TMAO and related compounds at pH

5-6 and below should be taken into account. Pyridine N-oxide, on the other hand, is a neutral molecule at pH above 2-3.

The bond between nitrogen and oxygen is unstable because of the high electronegativity of both elements. This bond can be more or less easily broken either by reduction or by heating. There is a huge difference in stability of aliphatic and aromatic N-oxides. Even mild reducing agents such as sulfurous acid (H_2SO_3) reduce aliphatic amine oxides. Heating leads to their decomposition into an aldehyde and a secondary amine (*Cope reaction* (Cope and Ciganec, 1963)). Aromatic amine oxides are much more resistant to reduction and thermal decomposition because electrons on the oxygen atom are tightly involved in resonance interactions with the aromatic system that makes the whole structure energetically more stable.

Stereochemistry of aliphatic amine oxides predicts the existence of enantiomers which can react with enzymes differently. Unfortunately, this propensity is difficult to exploit because the resulting tertiary amine is also optically active and undergoes racemization by the pyramidal inversion (Fig. 4-2). The rate of racemization is greatly affected by reaction conditions and the structure of the amine.

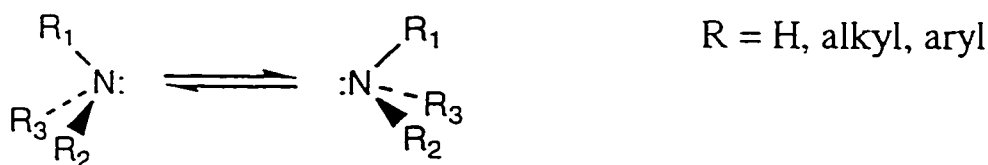


Figure 4-2. Pyramidal inversion in amines.

Pyridine N-oxide and other aromatic amine oxides are valuable precursors in organic synthesis. Significance of aliphatic amine oxides is not so high, although they have several useful applications as mild oxidants or intermediates in the synthesis of alkenes.

Amine oxides are widely distributed in nature. The most abundant is TMAO that has been found in muscles of a shark as long ago as 1909. Since then, the important role of this compound as an osmolyte and cryoprotector in marine species has been well

established (Groninger, 1959). It preserves the native structure of proteins in unfavorable conditions such as low temperature and high concentration of salt. Apparently, TMAO has the ability to form hydrogen bonds with proteins and stabilize them when extremal conditions lead to their unfolding.

Amine oxides also compose numerous alkaloids, antibiotic aspergillic acid and related compounds. The regulatory role of aliphatic and aromatic amine oxides in the formation of disulfide bond *in vivo* has been proposed (Brzezinski and Zundel, 1994). Commercially available supply of amine oxides is limited to a number of pyridine N-oxide derivatives; only few aliphatic N-oxides are available.

The diversity in the structure of sulfoxides and, especially, amine oxides may be used to reveal some structural and chemical features of the DMSO reductase substrate-reduction active site.

Results

Synthesis of aliphatic amine oxides

Chemical synthesis of aliphatic N-oxides proved to be a serious task because of problems with isolation of the compounds. Aliphatic N-oxides are very hygroscopic substances highly soluble in water and easily form non-crystallizing syrups when attempts are made to precipitate them. They decompose at high temperatures and cannot be distilled, unlike their aromatic counterparts.

Specific conditions found for each of the synthesized N-oxides allowed their precipitation in pure form (pages 41-43). The composition of the molecules was determined by elemental analysis. IR analysis of triethylamine N-oxide hydrochloride ($\text{Et}_3\text{NO}\cdot\text{HCl}$) showed the presence of N-O bond (moderate absorption peak at 945 cm^{-1}) and O-H bond (broad peak at 3395 cm^{-1}). None of these bands is present in IR spectra of triethylamine or triethylamine hydrochloride. Proton magnetic resonance spectrum of this compound confirmed its structure and high purity.

The following amine oxides were obtained in pure form: triethylamine N-oxide hydrochloride, *N,N*-dimethylaniline N-oxide, *N,N*-dimethylbenzylamine N-oxide

monohydrate, 4-ethylmorpholine N-oxide hydrochloride, and 1-dimethylamino-2-propanol N-oxide.

Reduction of sulfoxides and N-oxides catalyzed by DMSO reductase with reduced benzyl viologen as electron donor

Kinetic parameters of various sulfoxides and N-oxides were determined using the standard BV assay. For several substrates including triethylamine N-oxide, 4-ethylmorpholine N-oxide, *N,N*-dimethylbenzylamine N-oxide, and *N,N*-dimethylaniline N-oxide Michaelis constant and maximal rate could not be determined because the rate depends linearly on the substrate concentration in all concentration range tested. Propyl sulfoxide and (*S*)-methyl-*p*-tolyl sulfoxide are not reduced by DMSO reductase.

Kinetic analysis of the data for the other substrates showed that the electron donor (BV_{red}) as well as all sulfoxides and PyNO follow the Michaelis-Menten equation while most of the aliphatic N-oxides including TMAO do not. The deviations from the Michaelis-Menten kinetics are reflected by the appearance of a clear pattern on the residual plot of activity vs. the substrate concentration (*v* vs. *s*), deviation of the reaction-rate curve from the rectangular hyperbola calculated from the experimental data, and non-linearity of reciprocal plots such as Eadie-Hofstee (*v* vs. *v/s*) and double-reciprocal plot (*1/v* vs. *1/s*). Michaelis constants and maximal rates of the tested DMSO reductase substrates are summarized in Table 4-1. The kinetic curves for DMSO, pyridine N-oxide and aliphatic amine oxides are presented in Fig. 4-3 - 4-6. The kinetic parameters of the electron donor, BV_{red}, was measured with 1M TMAO (Fig. 4-8).

To verify the possibility that deviation from the Michaelis-Menten kinetics is caused by the disturbances in the enzyme structure during the solubilization procedure, the kinetic parameters of TMAO were also determined with overexpressed DMSO reductase in the bacterial membrane. The principal character of the kinetic curve was the same as for the purified enzyme (Fig. 4-7a). The Eadie-Hofstee plot presented on Fig. 4-7b shows a hyperbolic relationship between the reaction rate and *v/s* ratio rather than linear dependence characteristic for the true Michaelis-Menten kinetics.

Table 4-1. Kinetic parameters of sulfoxide and amine oxide substrates of DMSO reductase

Compound	K_m	V_{max} ($\mu\text{mole BV}_{red}/\text{min.}$ per mg enzyme)
Reduced benzyl viologen (BV_{red}) ^{a)}	$15 \pm 1 \mu\text{M}$	673 ± 11
Pyridine N-oxide (PyNO)	$90 \pm 7 \mu\text{M}$	112 ± 2
Dimethyl sulfoxide (DMSO)	$13.5 \pm 1.1 \mu\text{M}$	35 ± 6
Diethyl sulfoxide	$32 \pm 3 \mu\text{M}$	14 ± 1
Dipropyl sulfoxide	ND ^{b)}	0
Methyl phenyl sulfoxide	$150 \pm 13 \mu\text{M}$	20 ± 1.6
Ethyl phenyl sulfoxide	$232 \pm 29 \mu\text{M}$	13 ± 0.8
Methyl benzyl sulfoxide	$113 \pm 11 \mu\text{M}$	17 ± 1.6
Ethyl benzyl sulfoxide	ND	0
(<i>R</i>)-Methyl <i>p</i> -tolyl sulfoxide (RMPTSO)	$40 \pm 7 \mu\text{M}$	52 ± 2
(<i>S</i>)-Methyl <i>p</i> -tolyl sulfoxide (SMPTSO)	ND	0
Trimethylamine N-oxide (TMAO)	- ^{c)}	-
Triethylamine N-oxide	- ^{d)}	-
Dimethylaniline N-oxide	- ^{d)}	-
Dimethylbenzylamine N-oxide	- ^{d)}	-
4-Methylmorpholine N-oxide	- ^{c)}	-
4-Ethylmorpholine N-oxide	$6.8 \pm 0.5 \text{ mM}$	517 ± 15
1-Dimethylamino-2-propanol N-oxide	- ^{c)}	-

a) With 1M TMAO as electron acceptor

b) Not determined

c) The substrate does not follow the Michaelis-Menten kinetics

d) The kinetic parameters were not determined because no saturation was observed at all substrate concentrations tested

To further test the influence of the reaction conditions on the reduction of TMAO with BV_{red} as an electron donor, a series of experiments was done in which some chemical compounds were added to the reaction mixture, and the kinetics of TMAO reduction was measured. Under all conditions tested (20% glycerol, 10% polyethylene glycol 8000, 0.1% and 1% Triton X-100, 1 mg/ml bovine serum albumin, 120 mM sodium chloride), the reduction of TMAO did not follow the Michaelis-Menten kinetics and remained basically unaffected (data not shown).

The inhibitory properties of substrates that are not reduced by DMSO reductase were tested. The presence of 20 mM dipropyl sulfoxide or (*S*)-methyl *p*-tolyl sulfoxide did not affect the rate of reduction of DMSO and (*R*)-methyl *p*-tolyl sulfoxide, respectively (data not shown).

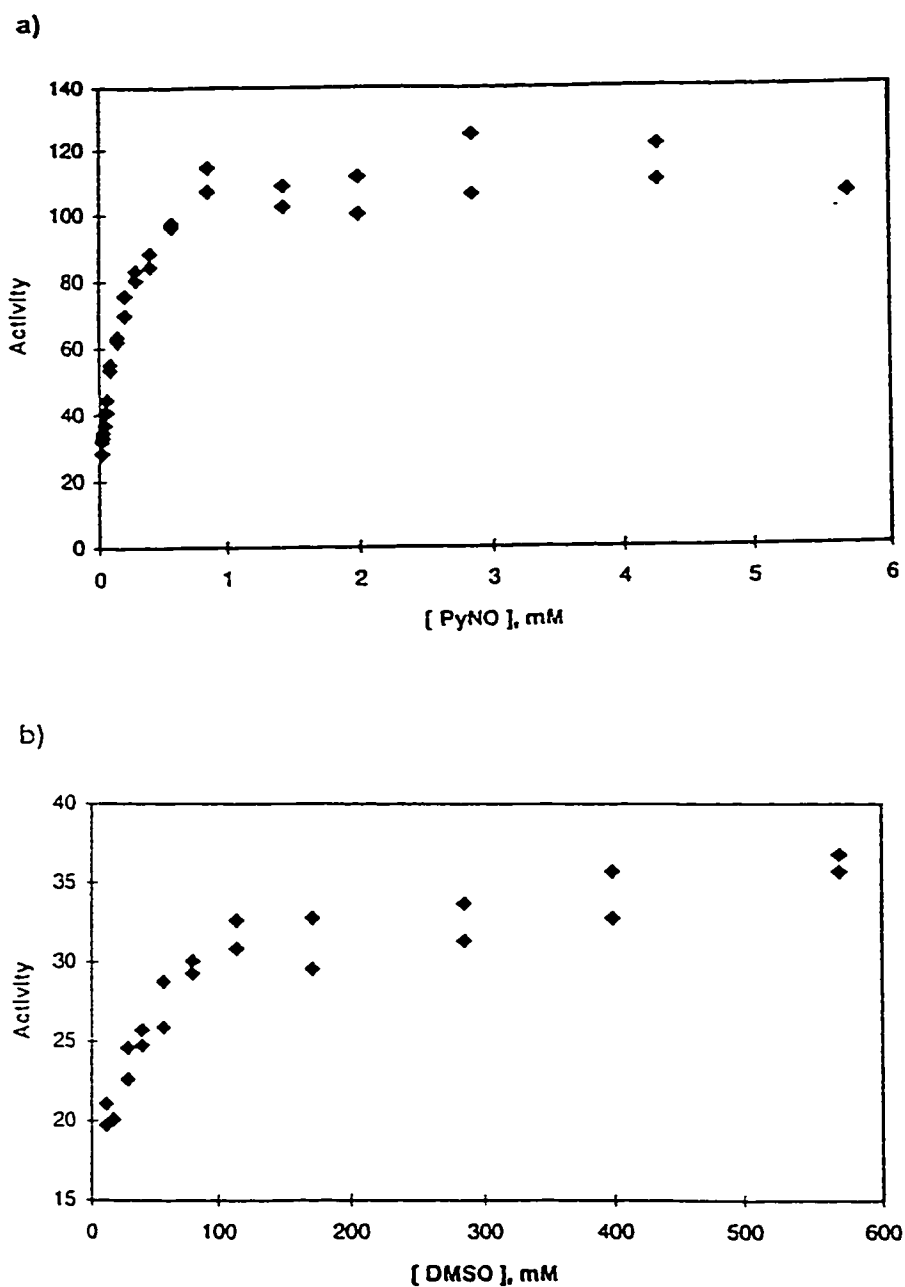


Figure 4-3. The reduction of pyridine N-oxide and dimethyl sulfoxide with reduced benzyl viologen as electron donor catalyzed by DMSO reductase from *E.coli*. a) The plot of activity vs. pyridine N-oxide concentration; b) the plot of activity vs. dimethyl sulfoxide concentration.

The enzyme activity is measured in $\mu\text{mole BV}_{\text{red}}/\text{min}$ per mg protein

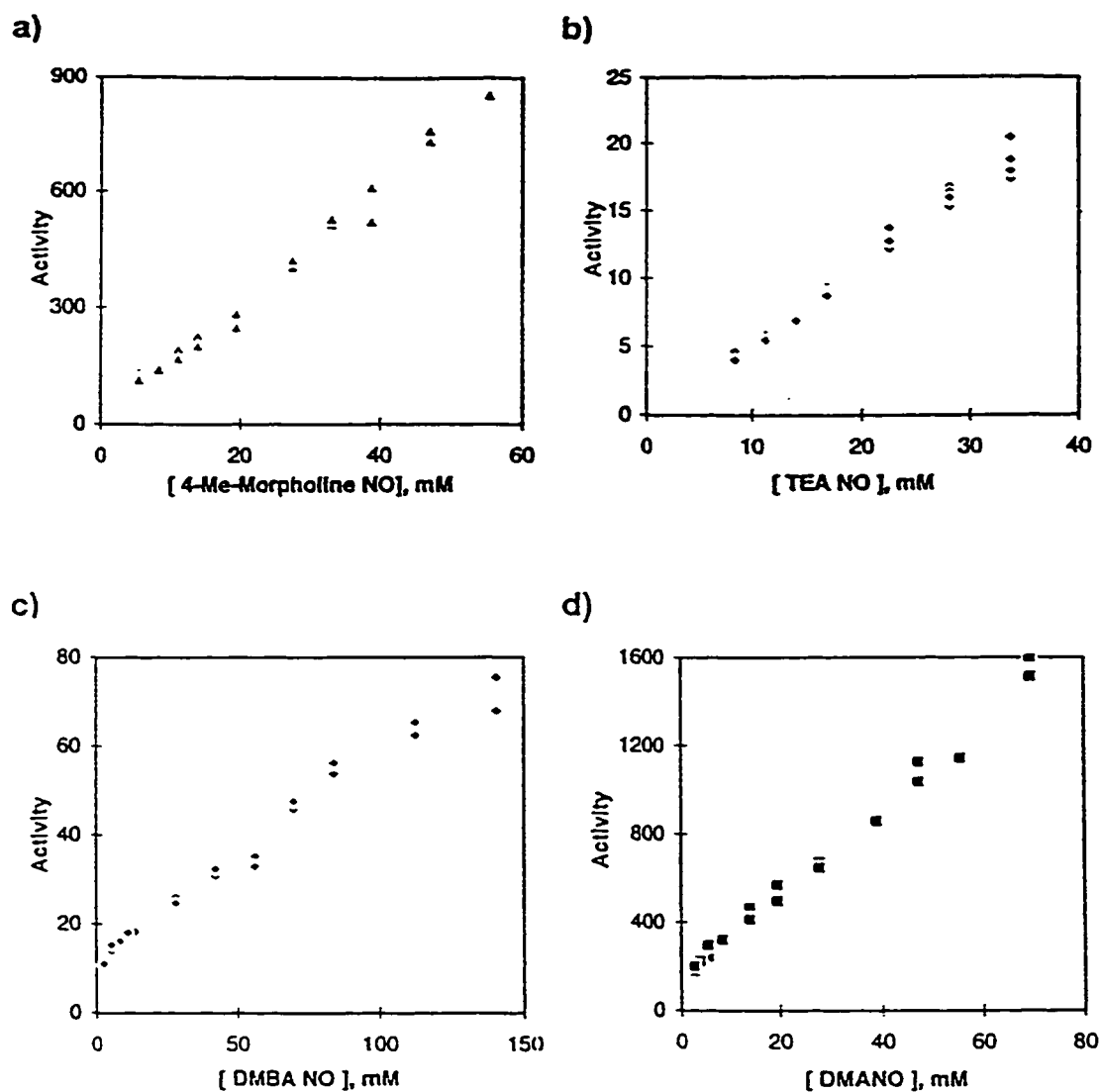


Figure 4-4. The rate of reduction of some aliphatic amine oxides with reduced benzyl viologen as electron donor catalyzed by DMSO reductase from *E.coli* is not saturable even at physiologically high concentrations. The plot of the reaction rate (in $\mu\text{mole BV}_{\text{red}}/\text{min}$ per mg protein) vs. the substrate concentration for: a) 4-methylmorpholine N-oxide; b) triethylamine N-oxide; c) *N,N*-dimethylbenzylamine N-oxide; d) *N,N*-dimethylaniline N-oxide.

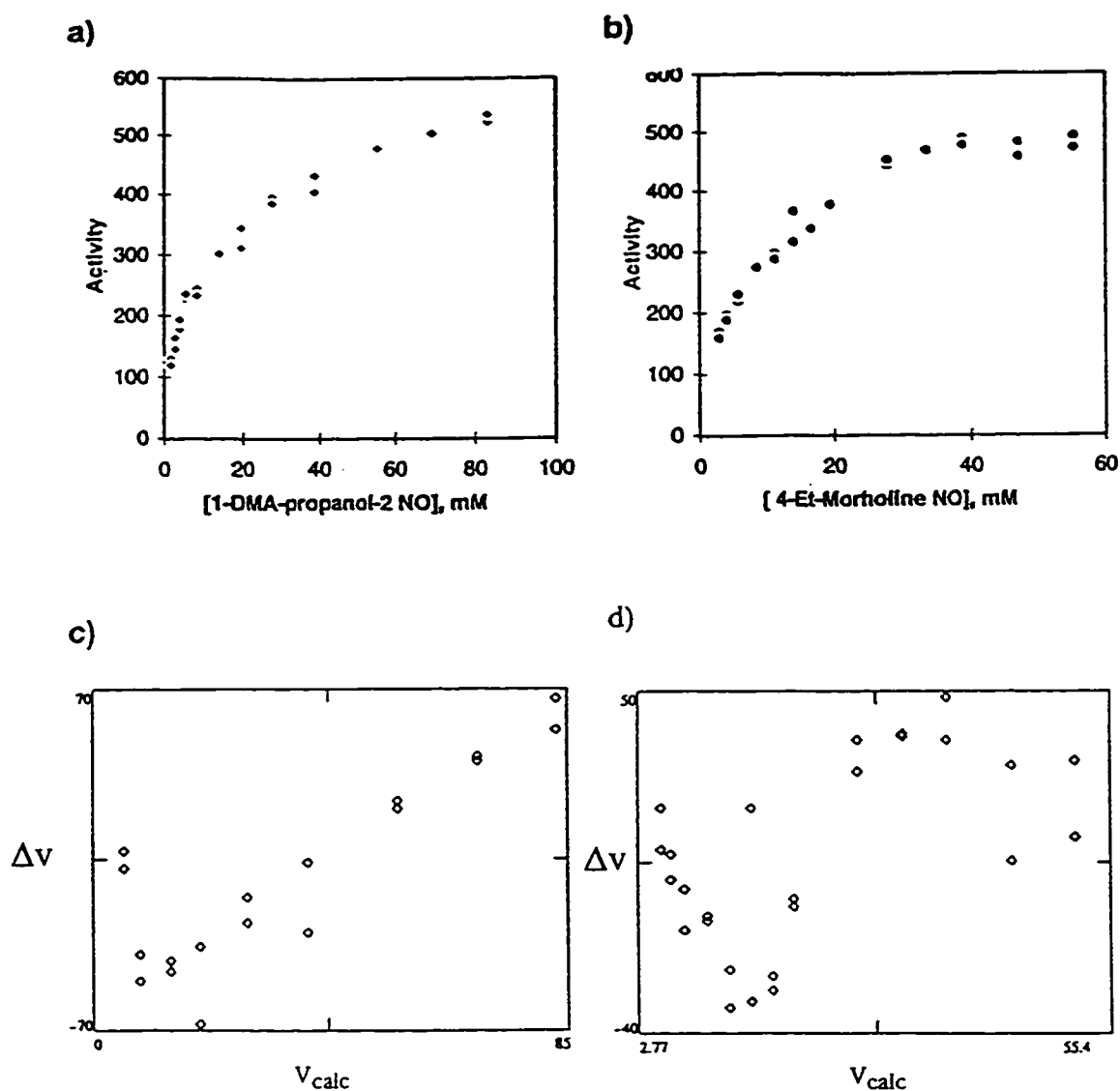
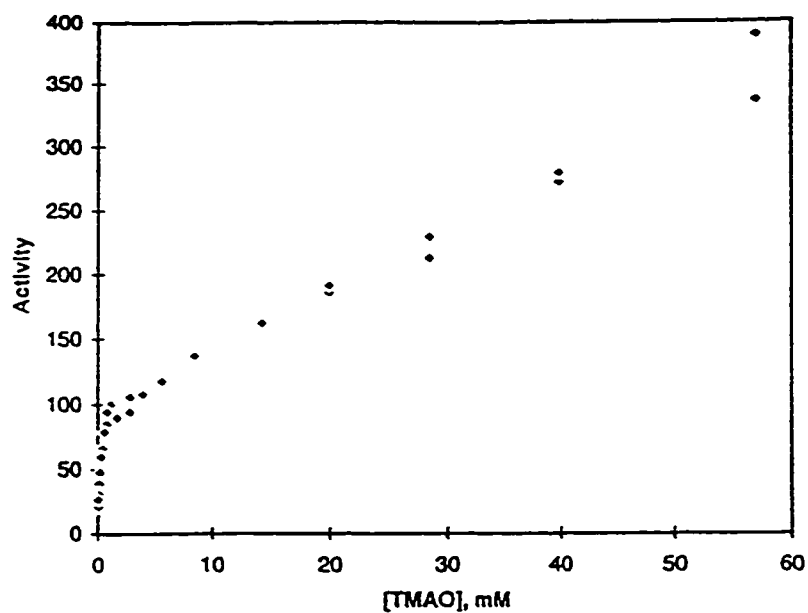


Figure 4-5. The reduction of 4-ethylmorpholine N-oxide and 1-dimethylaminopropanol-2 N-oxide with reduced benzyl viologen as electron donor catalyzed by DMSO reductase from *E.coli*. a) and b) The plot of the reaction rate (in $\mu\text{mole BV}_{red}/\text{min per mg protein}$) vs. the substrate concentration for 4-ethylmorpholine N-oxide and 1-dimethylaminopropanol-2 N-oxide, respectively; c) and d) the residual plots.

a)



b)

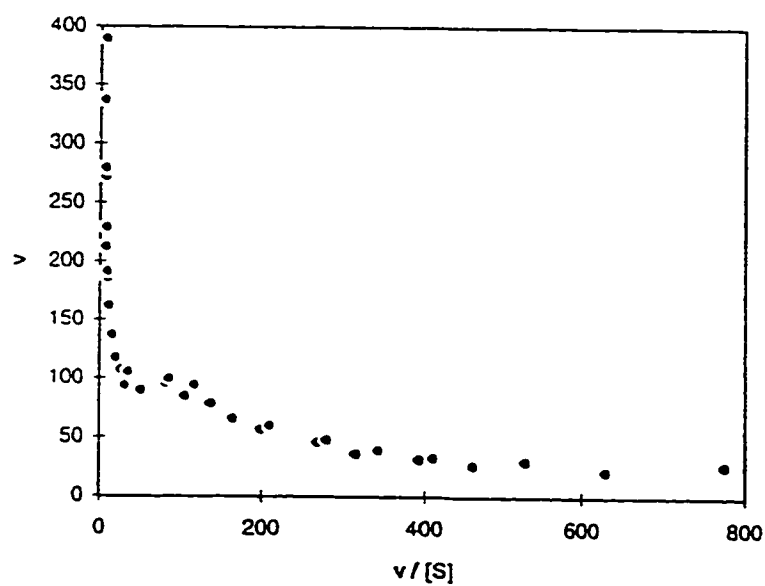


Figure 4-6. The reduction of TMAO with reduced benzyl viologen as electron donor catalyzed by solubilized *E.coli* DMSO reductase. a) The dependence of the initial reaction rate (in $\mu\text{mole BV}_{\text{red}}/\text{min}$ per mg protein) on the substrate concentration; b) the Eadie-Hofstee plot.

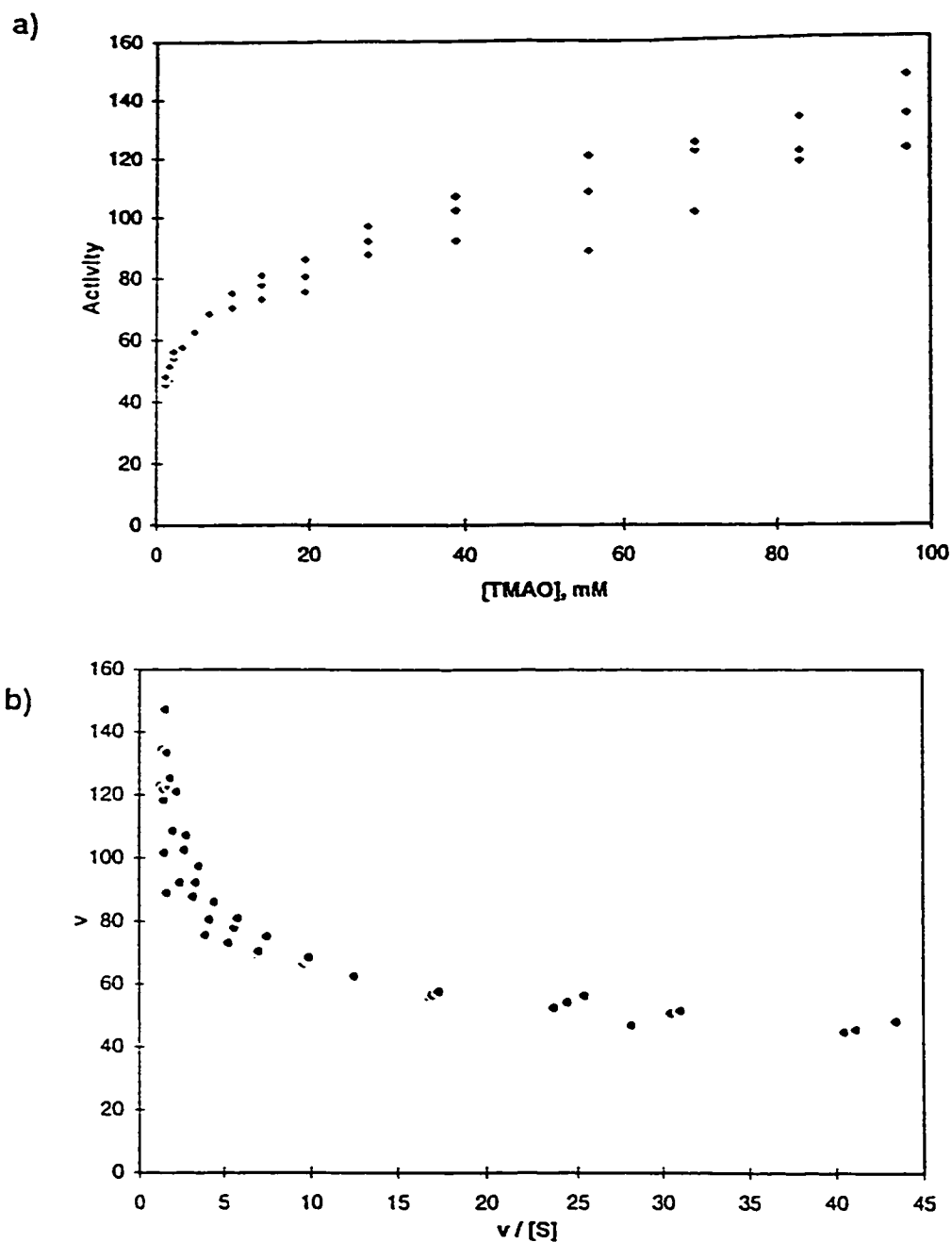


Figure 4-7. The reduction of TMAO with reduced benzyl viologen as electron donor catalyzed by *E.coli* membranes containing overexpressed DMSO reductase. a) The dependence of the initial reaction rate (in $\mu\text{mole BV}_{\text{red}}/\text{min}$ per mg protein) on the substrate concentration; b) the Eadie-Hofstee plot.

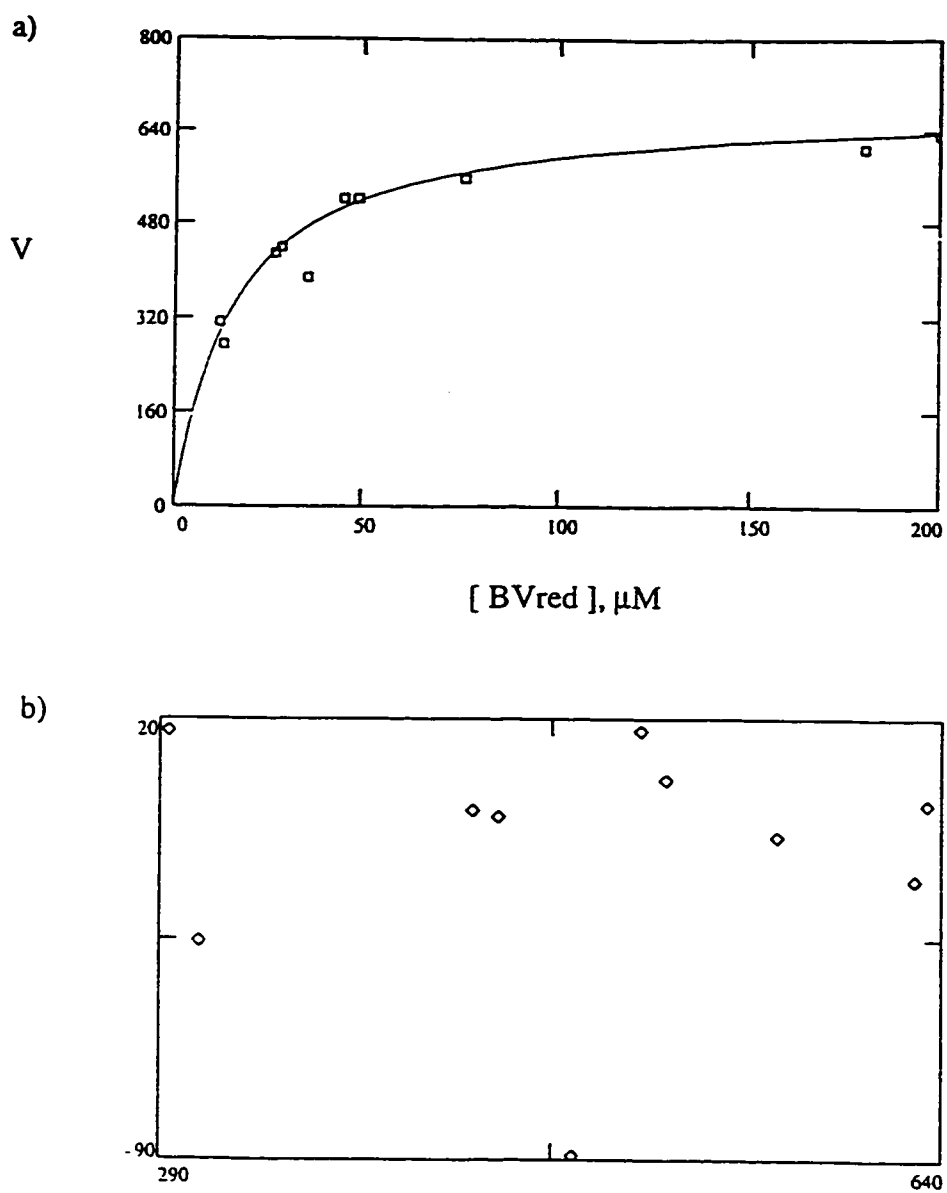


Figure 4-8. The oxidation of benzyl viologen catalyzed by *E.coli* DMSO reductase with TMAO as electron donor. The real initial concentration of BV_{red} was determined spectrophotometrically. TMAO was added to the reaction buffer at 1M concentration. The reaction rate is measured in $\mu\text{mole BV}_{\text{red}}/\text{min}$ per mg protein.

Discussion

The enzyme DMSO reductase from *E.coli* has a very broad range of substrate specificity. It is capable of reducing various sulfoxides, aromatic and aliphatic N-oxides and some other substances. Because of the apparent difficulties with studying three-dimensional structure of this unstable membrane protein, other methods, such as the investigation of DMSO reductase specificity, may shed some light on the nature of the enzyme active sites. The number of commercially available substrates for DMSO reductase is quite limited, and most of them belong to a one particular class, aromatic N-oxides. There are only a few sulfoxides and aliphatic N-oxides. Thorough investigation of interaction of these substrates with DMSO reductase was necessary because DMSO and TMAO, a sulfoxide and an N-oxide, are the most commonly used substrates for enzyme assays. Besides, structural features of these two classes of DMSO reductase substrates can provide structural information that is unavailable with aromatic N-oxides.

An attempt to synthesize a number of amine oxide substrates for DMSO reductase partially succeeded. Some N-oxides were obtained in pure form while others appeared to be extremely hygroscopic and resistant to all attempts to dry and crystallize them. This might be the reason why compounds of this class, with only a few exceptions, are not commercially available.

Kinetic analysis showed the big differences between aromatic amine oxides and sulfoxides on one hand and aliphatic amine oxides, on the other. The former have low Michaelis constants and maximal reaction rates while aliphatic N-oxides have high apparent K_m and V_{max} values (Fig. 4-3 vs. Fig. 4-4 - 4-7). Determination of kinetic parameters was carried out in such a way that the measurements were taken in the substrate concentration range surrounding its apparent K_m value calculated from preliminary experiments as the concentration where reaction rate compose 50% of the maximal rate. For most aliphatic amine oxides, it appeared impossible to achieve the saturation rate, and the plateau on the kinetic curve is absent despite the steep initial increase. This behavior raised the question of whether these compounds follow the Michaelis-Menten equation. Analysis of linear plots (double reciprocal and Eadie-

Hofstee) revealed that these plots were not linear for all aliphatic amine oxides except 4-ethylmorpholine N-oxide. Residual plots of the reaction rate *versus* the substrate concentration demonstrates the clear pattern of increased positive rate deviation at higher substrate concentrations.

All this allows to suggest that reduction of aliphatic amine oxides with reduced benzyl viologen as electron donor catalyzed by DMSO reductase from *E.coli* does not follow the Michaelis-Menten kinetics.

It is a well-known fact that trimethylamine N-oxide greatly affects the protein conformation (Groninger, 1959). A possible explanation for unusual behavior of aliphatic N-oxides is that an increase in the concentration of TMAO and related compounds allosterically increases the activity of DMSO reductase. Certainly, the ability of TMAO to form hydrogen bonds with proteins and stabilize their three-dimensional structure allows this explanation, but the effect should be quite unspecific because it requires high concentrations of the substrate (0.1 M and higher).

To test this hypothesis, a series of experiments was carried out to determine the effect of variation in ionic strength, the presence of hydrogen bond donors in the reaction mixture, detergent concentration on the kinetic behavior of TMAO. Although such treatments slightly affected the calculated kinetic parameters, the main features of the kinetic behavior remained the same: non-linear reciprocal plots and the parabolic pattern on the residual plot. Besides, TMAO does not demonstrate any abnormalities at the same concentrations when reduced with AMNQH₂ as the electron donor. This raises the possibility that anomalous behavior of aliphatic N-oxides may be the artifact related to abnormal properties of the electron donor, reduced benzyl viologen. The non-natural mechanism of electron transfer from reduced benzyl viologen to DMSO reductase has been noticed a long time ago, it was discussed in the preceding chapters. It is possible that the interaction of benzyl viologen cation-radical with DmsA or DmsB subunit(s) leads to an unusual conformational change or formation of an abnormal transition state that can directly affect the reduction of aliphatic amine oxides. This mechanism may not work with sulfoxides or aromatic N-oxides because these compounds are much more resistant to reduction, and the rate of the side reaction is negligible.

Another noticeable trend in the kinetic properties of substrates is an increase in Michaelis constant with an increase of volume of the substituents in the substrate molecule. K_m of diethyl sulfoxide is considerably higher than that of dimethyl sulfoxide, and K_m of ethyl phenyl sulfoxide is higher than K_m of methyl phenyl sulfoxide. This feature has been noticed in another study of DMSO reductase with substituted pyridine N-oxides (Simala-Grant and Weiner, 1996). Although the interpretation of the Michaelis constant as a measure of affinity of a substrate to an enzyme is not completely correct, especially when applied to the complicated two-substrate reactions, a series of analogous substrates allows to propose that the substrate binding to DMSO reductase is somewhat decreased when one of methyl groups is replaced by ethyl group. The binding is greatly reduced when two substituents are ethyl groups, and it is absent when two substituents are bulkier propyl groups. This finding is consistent with the three-dimensional models for DMSO reductase from *Rhodobacter sphaeroides* (Schindelin *et al.*, 1996) where the atom of molybdenum participating in the electron transfer from the enzyme to DMSO is located on the bottom of narrow depression, far apart from the surface of the enzyme.

The most remarkable feature of DMSO reductase is its ability to react stereospecifically with (*S*)-isomers of methyl *p*-tolyl sulfoxide. Reduction of (*R*)-enantiomer was not detected. This specificity is opposite to the specificity of DMSO reductase from *Rh. sphaeroides* (Abo *et al.*, 1995).

The crystal structure of the latter enzyme at 3.5 Å resolution was published recently (Schindelin *et al.*, 1996). DMSO reductase from *Rh. sphaeroides*, a single-polypeptide soluble periplasmic protein, has only one prosthetic group, the molybdenum cofactor. Neither iron-sulfur clusters nor a quinol-binding site are present. The enzyme accepts electrons from a soluble cytochrome. The chemical mechanism of DMSO reduction was established using the isotope analysis (Schultz *et al.*, 1995). The enzyme can exist in two forms, oxidized and reduced. The reduced form binds the substrate, and two electrons are transferred from Mo(IV) to DMSO. The oxygen atom of the substrate is transferred to the metal as an oxo ligand generating the reaction product DMS and oxidized form of the enzyme containing Mo(VI). In the second half-cycle, two protons and two electrons are donated to the molybdenum center, producing a molecule of water and regenerating the

reduced form of the enzyme (Fig. 4-9b). This mechanism is consistent with the substituted-enzyme mechanism determined for *E.coli* DMSO reductase in this study.

The enzyme active site contains two molybdopterin guanine dinucleotide (MGD) molecules coordinating the molybdenum atom (Fig. 4-9a). The structure of the cofactor is not completely symmetrical. The pyran ring is tilted by less than 30° in the P pterin and by more than 40° in Q pterin, relative to the other two rings of the cofactor. As the model proposed by Schindelin *et al.* explains the substrate stereospecificity of the enzyme, the asymmetry in bending of the two MGD molecules around molybdenum center may be responsible for the stereospecificity of substrate reduction. If this is the case, the spatial orientation of the molybdenum cofactor in DMSO reductases from *Rhodobacter sphaeroides* and *Escherichia coli* is different.

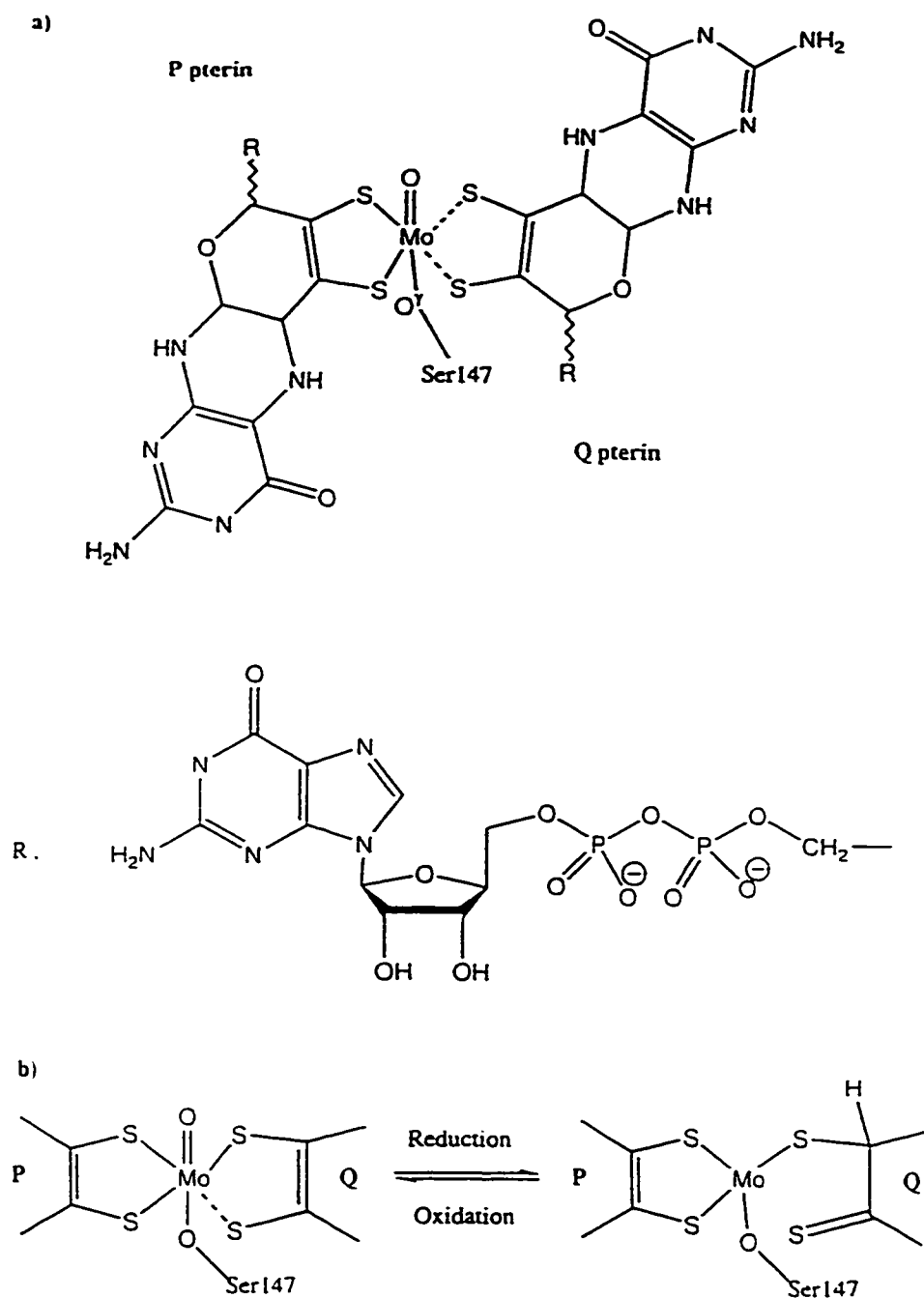


Figure 4-9. The structure of the molybdenum cofactor in the active site of DMSO reductase from *Rhodobacter sphaeroides*. a) The structure of the oxidized form of Moco; b) molybdenum cycles between the two major redox states, Mo(IV) and Mo(VI), upon oxidation/reduction. Unstable state Mo(V) is an intermediate.

Bibliography

- Abo, M., M. Tachibana, A. Okubo and S. Yamazaki (1995). Enantioselective deoxygenation of alkyl aryl sulfoxides by DMSO reductase from *Rhodobacter sphaeroides* f.s. *denitrificans*. *Bioorg. and Med. Chem.* **3**, 109-112.
- Andersen, K.K. (1988). Optically active sulfoxides. *In* The chemistry of sulfones and sulfoxides, S. Patai, Z. Rappoport and C. J. M. Stirling, eds. (New York: Wiley), pp. 55-94.
- Brzezinski, B. and G. Zundel (1994). Possible regulatory role in biology of trimethylamine N-oxide and aromatic N-oxides: formation of disulfide bonds. *J. Mol. Struct.* **303**, 141-147.
- Cope, A.C. and E. Ciganec (1963). Methylene cyclohexane and N,N-dimethylhydroxylamine hydrochloride. *Org. Syn., Coll. Vol.* **4**, 612-615.
- Gazdar, M. and S. Smiles (1908). *J. Chem. Soc.* **93**, 1833-1838.
- Groninger, H.S. (1959). The occurrence and significance of trimethylamine oxide in marine animals. *US Fish. Wildl. Serv. Sci. Rep. Fish* **333**, 1-22.
- Schindelin, H., C. Kisker, J. Hilton, K.V. Rajagopalan and D.C. Rees (1996). Crystal structure of DMSO reductase: redox-linked changes in molybdopterin coordination. *Science* **272**, 1615-1621.
- Schultz, B.E., R. Hille and R.H. Holm (1995). Direct oxygen atom transfer in the mechanism of action of *Rhodobacter sphaeroides* dimethyl sulfoxide reductase. *J. Amer. Chem. Soc.* **117**, 827-829.
- Simala-Grant, J.L and J.H. Weiner (1996). Kinetic analysis and substrate specificity of *Escherichia coli* dimethyl sulfoxide reductase. *Microbiology* **142**, 3231-3239.

Chapter 5. Conclusion

Although three-dimensional structures for two soluble bacterial DMSO reductases have been published, the probability of making crystals of *E.coli* DMSO reductase seems very low. The enzyme consists of three subunits combined by weak non-covalent interactions. The stability of this complex is quite low, and our understanding of how the enzyme works will long be based on physico-chemical studies of the wild-type protein and its mutants.

The determination of the kinetic mechanism of action of DMSO reductase in this study demonstrated its complexity. It is probable that the actual mechanism consists of several intermediate steps with the corresponding enzyme states only one of which can be determined kinetically. Detailed studies of the mechanism's complexity requires special instruments such as powerful inhibitors of the molybdenum active site. Such inhibitors are not available at the present time.

One source for such inhibitors may be organophosphorus compounds. Some of them, containing phosphorus-oxygen double bond, are similar to sulfoxides and amine oxides in the structure and charge distribution but may be much more resistant to reduction. Rich abilities of phosphorus to exist in several redox states and accept a wide range of substituents provide an opportunity to find a nonreducible analog of the transient state that can be a powerful inhibitor of sulfoxide reduction. The most promising candidates for this role include substituted phosphine oxides, phosphonates and methyl esters of substituted phosphinic acids. Unfortunately, not all of these compounds are available commercially, but the fact that DMSO reductase activity is inhibited by the phosphate buffer (Weiner *et al.*, 1992) encourages the investigation.

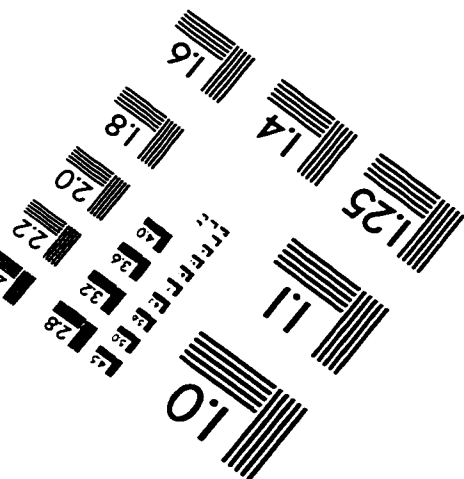
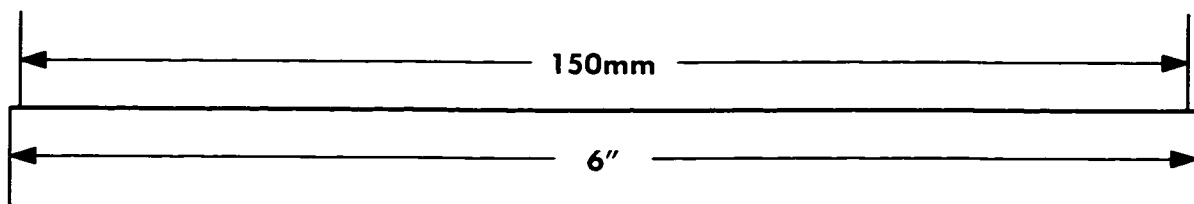
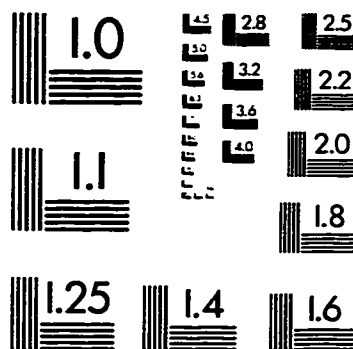
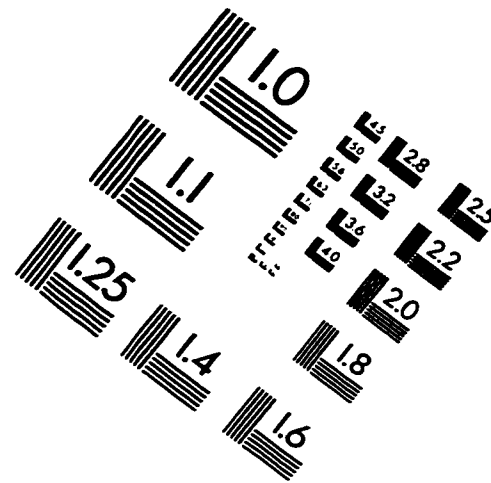
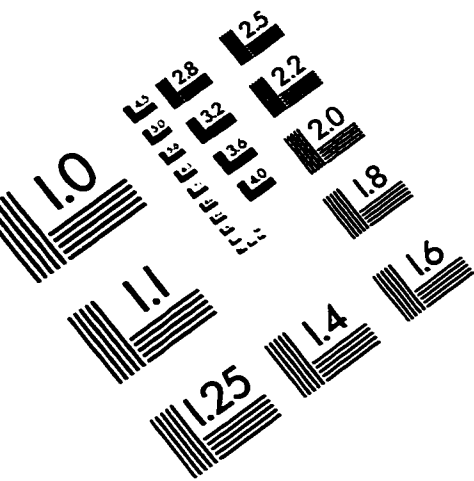
Another possible direction of future studies is determination of amino acid residues surrounding the enzyme quinone-binding site. So far, only histidine 65 in the DmsC subunit was proved to play an important role in the enzyme function. The fact that HOQNO inhibits quinol oxidation by DMSO reductase at nanomolar concentrations suggests a high-affinity binding of this compound to the quinone-binding site. A photoaffinity labeling of the protein by HOQNO derivative such as 3-azido-2-^[125]iodo-4-

hydroxyquinoline N-oxide may provide more information on other amino acid residues in the vicinity of the active site. Such derivative can be prepared comparatively easily from commercially available precursors.

Bibliography

Weiner, J.H., R.A. Rothery, D. Sambasivarao and C.A. Trieber (1992). Molecular analysis of dimethylsulfoxide reductase: a complex iron-sulfur molybdoenzyme of *Escherichia coli*. *Biochim. Biophys. Acta* **1102**, 1-18.

IMAGE EVALUATION TEST TARGET (QA-3)



APPLIED IMAGE, Inc.
1653 East Main Street
Rochester, NY 14609 USA
Phone: 716/482-0300
Fax: 716/288-5989

© 1993, Applied Image, Inc., All Rights Reserved

